UNIVERSITAT
POLITÈCNICA
DE VALÈNCIA

ESCUELA POLITECNICA SUPERIOR DE GANDIA

Departamento de Física Aplicada

Giuseppina Larosa

Design and Development of an acoustic positioning system for a cubic kilometre underwater neutrino telescope

Tesis Doctoral

Director de tesis:

Dr. Miguel Ardid Ramírez

Julio 2012

"Alla mia famiglia

&

a Demetrio"

Contents

4 Integration of the acoustic transceiver in Underwater Neutrino Telescopes 81

Conclusions 105

Acronyms 109

References 113

Acknowledgments 119

Summary

Context

Lately underwater neutrino telescopes have become very important since it is a new and unique method to observe the Universe. The neutrinos are uncharged particles and interact weakly with matter. They can escape from sources which have produced them and arrive to the Earth unperturbed by magnetic fields and without interaction with other particles. This means that neutrinos can bring us astrophysical information that other messengers cannot and, then they can open a potential new window on the Universe.

On the other hand, their low interaction cross section imposes to build very large detectors with dimensions of ~1 km^3. Therefore, it is necessary the instrumentation of large volumes of water (or ice) with several optical sensors in order to detect characteristic signatures of high energy neutrino interactions. One way to detect neutrino interactions can be afforded through the detection of the Cherenkov light emitted by the muon generated after a neutrino interaction. This particle travels across the detector at a speed greater than the speed of light in water, so generating a faint blue luminescence called Cherenkov radiation, which can be detected through an array of optical sensors (photomultipliers). The arrival times of the light collected by photomultipliers can be used to reconstruct the muon track, and consequently that of the neutrino, which has produced it. The accuracy of the reconstruction of the muon track depends on the precision in the measurement of the light arrival time and on precise knowledge of the positions of the optical detectors. For this reason, in an underwater telescope an acoustic positioning system (APS) able to monitoring the position of the optical sensors with an accuracy of ~10 cm is necessary (about the length of the photomultipliers diameter). The studies in this thesis have been developed within the framework of acoustic position calibration in two European collaborations for the design, building and operation of an underwater neutrino telescope in the Mediterranean Sea: ANTARES (in operation phase) and KM3NeT (in preparatory phase for the construction).

Summary

In this thesis the work and the results for designing, developing, testing and characterizing a prototype of acoustic transceiver to be used in the APS of the future KM3NeT neutrino telescope are presented.

Objectives

The goals of this thesis can be summarized in the following aspects:

- Design of the acoustic transceiver for the APS of KM3NeT.
- Development of the acoustic transceiver prototype.
- Characterization of the transceiver in the laboratory and in the sea.
- Adapting the prototype for its integration in ANTARES and NEMO sites for the in situ test.

Elements of the methodology to emphasize

We would like to remark that the work of the thesis has been developed within the international consortium KM3NeT, funded with European and National funds.

Due to the context and the nature of the activities done it has been necessary training in different fields: neutrino telescopes and astroparticles, but also in other field such as underwater acoustics or transducers. Moreover, different skills and abilities in different application fields have been developed: instrumentation, design and characterization of the acoustic system in water, data analysis, etc. Particularly, in order to design the transceiver, the acoustic transducer has been chosen according to the performance for the proposed application and afterwards specific electronics has been designed. Different configurations of the measurements have been set up to test and prove the prototype, the different measurements have been analyzed and the results and conclusions have been obtained. Finally, the tasks towards the integration in underwater neutrino telescopes have been done.

Results

Different studies for the development and testing of a prototype of transceiver for the proposed APS of KM3NeT have been done. The prototype consists of a transducer type Free Flooded Ring FFRSX30 with 20-40 kHz frequency range and an electronic board named SEB (Sound Emission Board), especially designed for it. The SEB is able to manage the emission and reception of different signals, as well as allowing the communication and configuration of the system. In a first step, the characterization of

the hydrophones has been done in order to study the sensitivity and its dependence at high pressure (up to 440 bars). In a second step, the whole system (FFRSX30 plus SEB) has been tested and characterized in different conditions (tank, water pool and harbour of Gandia) in order to integrate it in the ANTARES, NEMO and KM3NeT neutrino detectors. The proposed transducers have good characteristics for their application for the KM3NeT APS and they can also be used as receivers, but in this case a good parameterisation of the sensitivity as a function of the frequency and angle for each transducer will be needed.

The transducers have a very low intrinsic noise ~ -120 dB re V^2/Hz (~ ≤Sea State 1) and they are quite stable at different pressures, that is with depth. For simplicity and due to limitations to the integration in both detectors, it was decided to test the transceiver only as emitter. The receiver functionality will be tested successively in other tests. The changes performed in the transceiver in order to integrate it in the different detectors show that the system is versatile and adaptable to the different conditions. The system, with low power consumption, is able to have a transmitting power above 170 dB re 1µPa@1m that combined with signal processing techniques allow to deal with the large distances involved in a neutrino telescope.

In conclusion, the system has been integrated with success in ANTARES and NEMO neutrinos telescopes and, after being proved in situ, it will be implemented in the final configuration of the KM3NeT detector. Finally, we would like to remark that the acoustic system proposed is compatible with the different options for the receiver hydrophones proposed for KM3NeT and it is versatile, so in addition to the positioning functionality, it can be used for neutrino acoustic detection studies or for acoustic monitoring studies in deep-sea. Moreover, the transceiver (with slight modifications) may be used in other acoustic positioning systems or emitter-receiver systems, alone or combined with other marine systems, where the localization of the sensors is an issue. In that sense, the experience gained from this research can be of great use for other possible applications.

Resumen

Contexto.

En los últimos años los telescopios submarinos de neutrinos han cobrado una mayor importancia ya que consisten en un nuevo y único instrumento para observar el Universo. Los neutrinos son partículas sin carga e interactúan muy débilmente con la materia que les rodean, pueden escaparse fácilmente de la fuente que los ha producidos y llegar a La Tierra sin ser desviada por los campo magnético y sin interactuar con otras partículas. Esto implica que los neutrinos pueden traer informaciones astrofísicas que otros mensajeros no pueden aportar y abrir una potencial ventana hacia el Universo. Por otro lado, su baja interacción con la materia impone la necesidad de construir un detector de grandes dimensiones del orden de 1 km^3 utilizando volumen de agua o hielo y con muchos sensores ópticos para detectar esta interacción de neutrino de alta energía. Un método para detectar neutrinos es a través de la luz Cherenkov emitida por el muon generado después de una interacción de neutrino. Esta partícula, al atravesar el detector con una velocidad superior a la luz en el medio, genera una débil luz azulada llamada radiación de Cherenkov que es detectada por una red de sensores ópticos (fotomultiplicadores). El tiempo de llegada de la luz a los fotomultiplicadores puede ser utilizado para reconstruir la traza del muon y consecuentemente del neutrino que lo ha producido. La precisión en la reconstrucción de la traza del muon depende de la precisión en la medida del tiempo de llegada de la luz y en la precisión en de la posición de los sensores ópticos en el detector. Por esta razón, en telescopios submarinos es necesario un sistema de posicionamiento acústico (APS) capaz de monitorizar el movimiento de los sensores ópticos con una precisión de ~10 cm (prácticamente la longitud del diámetro del fotomultiplicador). Los estudios realizados están enmarcados dentro de las actividades de calibración de posicionamiento acústico en dos colaboraciones europeas para el diseño, construcción y operación de telescopios submarinos de neutrinos en el Mediterráneo: ANTARES (en fase de operación) y KM3NeT (en fase de preparación para la construcción).

Síntesis.

En esta tesis se presentan los trabajos y resultados para el diseño, desarrollo, test y caracterización de un prototipo de transceptor acústico para ser utilizado en el APS del futuro telescopio de neutrinos KM3NeT.

Objetivos.

Los objetivos de este trabajo pueden resumirse en los siguientes aspectos:

- Diseño del transceptor acústico para el APS de KM3NeT.
- Desarrollo del prototipo de transceptor acústico.
- Caracterización del transceptor en el laboratorio y en el mar.
- Adaptación del prototipo para su integración en ANTARES y NEMO sites para su validación in situ.

Elementos de la metodología a destacar.

Cabe destacar aquí que el trabajo se ha desarrollado en el marco del consorcio internacional KM3NeT, financiado con fondos europeos y nacionales. Por su contexto y el carácter de las actividades realizadas ha sido necesaria la formación en distintos campos: telescopios de neutrinos y astropartículas, pero también en otras áreas como la acústica submarina y los transductores. Además, se ha desarrollado diversas capacidades y destrezas en diversos ámbitos: en instrumentación, en diseño y caracterización de sistemas acústicos en agua, en análisis de datos, etc.

Más concretamente, para el diseño del transceptor se ha elegido el transductor acústico con mejores prestaciones para la aplicación propuesta y se ha diseñado la electrónica. También se ha realizado diferentes configuraciones de medidas para testear y validar el prototipo, se han analizado las diferentes medidas y se ha obtenido los resultados y conclusiones. Finalmente, se ha realizado las labores para su integración en telescopios de neutrinos submarinos.

Resultados logrados.

Se ha realizado el estudio, desarrollo y test de un prototipo de transceptor para el APS de KM3NeT propuesto. El prototipo es constituido por un transductor de tipo Free Flooded Ring FFRSX30 con rango de trabajo desde 20 kHz hasta 40 kHz y una tarjeta electrónica llamada SEB (Sound Emission Board) capaz de controlar la emisión y recepción de diferentes señales. En primer lugar, se ha caracterizado los transductores con el fin de estudiar su sensibilidad y su dependencia a elevada presión (hasta 440 bar). En segundo lugar se ha testeado y caracterizado el sistema entero (FFRSX30 más SEB) en diferentes condiciones ambientales (tanque, piscina y puerto de Gandia) con el

objetivo de integrarlo en los detectores de neutrinos ANTARES, NEMO y KM3NeT. Cabe destacar que los transductores propuestos presentan buenas características para su aplicación en el APS del detector KM3NeT e incluso se podrían utilizar como receptores, aunque se tendrían que considerar sus dependencias en sensibilidad para diferentes frecuencias y ángulos. Tienen un ruido intrínseco muy bajo ~ -120 dB re V^2/Hz (~ $\leq$ Sea State 1) y son bastantes estables al variar de la presión, es decir, con la profundidad. Por simplicidad y debido a las limitaciones por su integración en los detectores, se ha decidido de utilizar el sistema solo como emisor y la funcionalidad como receptor será testeada sucesivamente en otras configuraciones. Los cambios aportados por la integración en los diferentes detectores destacan que el sistema es muy versátil y capaz de adaptarse a las diferentes condiciones. El sistema tiene baja potencia de consumo y es capaz de obtener una potencia de trasmisión mayor que 170 dB re 1µPa @ 1 m que combinado con técnicas de procesado de señal permitiría llegar a las largas distancias implicadas en los telescopios de neutrinos.

En conclusión, el sistema se ha integrado positivamente en los telescopios de neutrinos ANTARES y NEMO y, tras su validación in situ, será implementado en la configuración final del detector KM3NeT. Además, se remarca que el sistema propuesto es compatible con las diferentes opciones para hidrófonos propuestos para KM3NeT y es versátil, con lo que puede ser utilizado también en el estudio de la detección de neutrinos o estudios de monitorización acústica en el mar. Asimismo, el sistema (con algunas modificaciones) puede ser utilizado en otros sistemas de posicionamiento acústico o sistemas de emisión-recepción, autónomos o combinado con otros sistemas marinos, y en donde la localización de los sensores es clave. En este sentido, la experiencia ganada a través de esta investigación puede ser de gran valía para otras posibles aplicaciones.

Resum

Context.

En els últims anys els telescopis submarins de neutrins han cobrat una major importància ja que consisteixen en un nou i únic instrument per observar l'Univers. Els neutrins són partícules sense càrrega i interactuen molt dèbilment amb la matèria que els envolten, poden escapar fàcilment de la font que els ha produït i arribar a La Terra sense ser desviats pels camps magnètics i sense interactuar amb altres partícules. Això implica que els neutrins poden portar informacions astrofísiques que altres missatgers no poden aportar i obrir una potencial nova finestra cap a l'Univers. D'altra banda, la seva baixa interacció amb la matèria imposa la necessitat de construir un detector de grans dimensions, de l'ordre d'1 km3, mitjançant un gran volum d'aigua o gel i amb molts sensors òptics per detectar aquesta interacció de neutrí d'alta energia. Un mètode per detectar neutrins és a través de la llum Cherenkov emesa pel muó generat després d'una interacció de neutrí. Aquesta partícula, en travessar el detector amb una velocitat superior a la llum en el medi, genera una feble llum blavosa anomenada radiació de Cherenkov que és detectada per una xarxa de sensors òptics (fotomultiplicadors). El temps d'arribada de la llum als fotomultiplicadors pot ser utilitzat per reconstruir la traça del muó i conseqüentment del neutrí que l'ha produït. La precisió en la reconstrucció de la traça del muó depèn de la precisió en la mesura del temps d'arribada de la llum i en la precisió de la posició dels sensors òptics en el detector. Per això, en telescopis submarins és necessari un Sistema de Posicionament Acústic (APS) capaç de monitoritzar el moviment dels sensors òptics amb una precisió de ~ 10 cm (pràcticament el diàmetre del fotomultiplicador). Els estudis realitzats estan emmarcats dins de les activitats de calibratge de posicionament acústic en dues col·laboracions europees per al disseny, construcció i operació de telescopis submarins de neutrins a la Mediterrània: ANTARES (en fase d'operació) i KM3NeT (en fase de preparació per a la construcció).

Síntesi.

En aquesta tesi es presenten els treballs i resultats per al disseny, desenvolupament, test i caracterització d'un prototip de transceptor acústic per ser utilitzat en l'APS del futur telescopi de neutrins KM3NeT.

Objectius.

Els objectius d'aquest treball es poden resumir en els següents punts:

- Disseny del transceptor acústic per a l'APS de KM3NeT.

- Desenvolupament del prototip de transceptor acústic.

- Caracterització del transceptor al laboratori i al mar.

- Adaptació del prototip per a la seva integració en ANTARES i NEMO *sites* per a la seva validació in situ.

Elements de la metodologia a destacar.

Cal destacar aquí que el treball s'ha desenvolupat en el marc del consorci internacional KM3NeT, finançat amb fons europeus i nacionals. Pel context i el caràcter de les activitats realitzades ha estat necessària la formació en diferents camps: telescopis de neutrins i astropartícules, però també en altres àrees com l'acústica submarina i els transductors. A més, s'ha desenvolupat diverses capacitats i destreses en diversos àmbits: en instrumentació, en disseny i caracterització de sistemes acústics en aigua, en anàlisi de dades, etc.

Més concretament, per al disseny del transceptor s'ha triat el transductor acústic amb millors prestacions per a l'aplicació proposta i s'ha dissenyat l'electrònica. També s'han realitzat diferents configuracions de mesures per testejar i validar el prototip, s'han analitzat les diferents mesures i s'han obtingut els resultats i conclusions. Finalment, s'han realitzat les tasques per a la seva integració en telescopis de neutrins submarins.

Resultats assolits.

S'ha realitzat l'estudi, desenvolupament i test d'un prototip de transceptor per a l'APS de KM3NeT proposat. El prototip és constituït per un transductor de tipus *Free Flooded Ring* FFRSX30 amb rang de treball des de 20 kHz fins a 40 kHz i una targeta electrònica anomenada SEB (*Sound Emission Board*) capaç de controlar l'emissió i recepció de diferents senyals. En primer lloc, s'ha caracteritzat els transductors amb la finalitat d'estudiar la seva sensibilitat i la seva dependència a elevada pressió (fins a 440 bar). En segon lloc s'ha testejat i caracteritzat el sistema sencer (FFRSX30 més SEB) i s'ha provat el sistema en diferents condicions ambientals (tanc, piscina i port de Gandia) amb l'objectiu d'integrar-lo en els detectors de neutrins ANTARES, NEMO i KM3NeT. Cal destacar que els transductors proposats presenten bones característiques per a la

seva aplicació en l'APS del detector KM3NeT i fins i tot es podrien utilitzar com a receptors, encara que s'haurien de considerar les seves dependències en sensibilitat per a diferents freqüències i angle. Tenen un soroll intrínsec molt baix ~ -120 dB re V^2/Hz (~ ≤ *Sea State* 1) i són bastant estables en variar la pressió, és a dir, amb la profunditat. Per simplicitat i a causa de les limitacions per la seva integració en els detectors, s'ha decidit d'utilitzar el sistema només com a emissor i la funcionalitat com a receptor serà testada successivament en altres configuracions. Els canvis aportats per a la integració en els diferents detectors destaquen que el sistema és molt versàtil i capaç d'adaptar-se a les diferents condicions. El sistema té baixa potència de consum i és capaç d'obtenir una potència de transmissió major que 170 dB re 1μPa @ 1 m que combinat amb tècniques de processament del senyal permetria arribar a les llargues distàncies implicades en els telescopis de neutrins.

En conclusió, el sistema s'ha integrat positivament en els telescopis de neutrins ANTARES i NEMO i, després de la seva validació in situ, serà implementat a configuració final del detector KM3NeT. A més, es remarca que el sistema proposat és compatible amb les diferents opcions d'hidròfons proposats per KM3NeT, i és versàtil, amb la qual cosa podria ser utilitzat també en l'estudi de la detecció de neutrins o estudis de monitorització acústica al mar. Així mateix, el sistema (amb algunes modificacions) podría ser utilitzat en altres sistemes de posicionament acústic o sistemes d'emissió-recepció, autònoms o combinats amb altres sistemes marins, on la localització dels sensors és clau. En aquest sentit, l'experiència guanyada a través d'aquesta investigació pot ser de gran interés per a altres possibles aplicacions.

Introduction

The seas and oceans comprise more than 70% of the Earth's surface, and as a natural resource of raw materials, fuel and food, they have never been as important as today. The deep sea is mostly dark, optically opaque and does not allow for propagation of electromagnetic waves since salt water exhibits a strong conductivity, and is therefore highly dissipative. Contrarily, the water is acoustically transparent and is a natural medium for the effective transmission of acoustic waves, carrying information underwater. In this thesis underwater acoustics is applied for the position calibration systems of deep-sea neutrino telescopes. Recently, neutrino telescopes have become an important tool of astroparticle physics, providing a new and unique method to observe the Universe. Neutrinos are uncharged particles and interact weakly with matter. They can escape from the sources which have produced them and arrive at the Earth unperturbed by magnetic fields and without interaction with other particles. This means that neutrinos can bring us astrophysical information that other particles cannot and, opening a potential new window to the Universe. The studies done in this thesis have been developed within the framework of the design and prototyping for the acoustic position calibration of the future KM3NeT deep-sea neutrino telescope. The outline of the thesis is as follows.

In Chapter 1 the history of applications of underwater acoustics will be overviewed as well as the use of underwater transducers, either as acoustic sources or as underwater acoustic receivers. Moreover a brief sketch on the military and civilian application will be described. Particularly, the application of the acoustic positioning, nucleus of this thesis, will be deeply described.

Since the main aim of this work is the acoustic positioning system in underwater neutrino telescopes, Chapter 2 focuses on the description of underwater neutrino telescopes and of the different detector developed that are in operation and in construction. In particular, we will pay attention to their acoustic positioning systems in order to describe the basis for the new acoustic positioning system proposed for the new and bigger KM3NeT underwater detector.

Chapter 3 presents the experiments and tests which have been carried out to design, develop and characterise the acoustic transceiver for the KM3NeT positioning system.

The transducers and electronics used and the tests done on them are described in detail, as well as the tests of the whole system in different environments (tank, pool and harbour) in order to prove the system in different conditions. The results of these tests are also discussed.

Finally, the activities for the integration of the acoustic transceiver prototype in the ANTARES and NEMO neutrino detectors are detailed in Chapter 4. The expected behavior of the transducer as well as the expected pressure and signals obtained by the ANTARES/AMADEUS and NEMO hydrophones are presented. A data analysis of the latest tests realized with this prototype and the results are also described and discussed.

Chapter 1

Principles and Applications to Underwater Acoustics

1.1 History of the applications to underwater acoustics

The oceans are a vast, complex, mostly dark, optically opaque but acoustically transparent world that has been only thinly sampled by today's limited technology and means of science. Underwater acousticians and acoustical oceanographers use sound as the premier tool to determine the detailed characteristics of physical and biological bodies and processes at sea. Myriad components of the ocean world are being discovered, identified, characterized, and imaged by their interactions with sound [MED05]. In fact, the possibility of using sound to detect distant ships, by simply listening to the noise they radiate into the water, has apparently been known for a very long time. Leonardo da Vinci is often mentioned as the first to propose this. But practical applications have been more recent, and the first underwater acoustic devices used efficiently were the passive detection systems developed by the Allies during World War I, to counter the then new threat of German submarines. The idea that obstacles to navigation and targets in warfare could be detected by *active acoustic systems* has been studied from the beginning of the 20th century, in particular, after the steamship *Titanic* struck an iceberg in 1912. Within a month of the disaster, a patent application was filed by L.R. Richardson in the United Kingdom (10 May 1912) for "detecting the presence of large objects under water by means of the echo of compressional waves (directed in a beam) by a projector". The basic idea was that a precise knowledge of the speed of sound in water, and the travel time of the sound from source to scattered and back to the source/receiver, permits the calculation of the distance to the scattering body. This was to be the beginning of the use of underwater sound projectors and receivers. They were to be called "SONARs" i.e., devices for Sound Navigation and Ranging [MED05]. But, a major breakthrough came from Paul Langevin, a French physicist, where during groundbreaking experiments on the River Seine and at sea, between 1915 and 1918, he demonstrated that it was possible to transmit signals, and to actively detect submarines, giving both their angles and

distances from the receiver. His decisive innovation consisted in using a *piezoelectric transducer* to replace capacitive transducer. With Langevin's invention more efficient sandwich transducer bore. Although these developments came too late to be of much use against submarines in World War I, numerous technical improvements and commercial applications followed rapidly [DAV02].

Between the two world wars, sonar technology improved considerably. It benefited from the emergence of first-generation electronics and from progress in the newborn radio industry. At the beginning of World War II, the technology of active sonar was advanced enough to be used on a large scale by the Allied navies (these were the famed ASDIC systems of the Royal Navy). In particular, the USA entered the war in 1941 and made a huge effort in sonar research and development. This greatly improved the performance of active sonar systems, as well as the understanding of underwater acoustic propagation, or the theories associated with detection and measurement of signals buried in noise.

After the war had ended in 1945, the "Cold War" between the Western and Eastern blocks resulted in continued efforts in scientific and technological research would continue. In the following years, in the West and in the Soviet Union, large programmes of research and experimentation were started. At the end of the 1950s, a new impulse was given by the appearance of nuclear submarines capable of launching strategic missiles, followed swiftly by the production of attack nuclear submarines. This led to a complete review of underwater warfare strategies since until then, the sonar was used locally to monitor ship convoys or shipping corridors. Now, it had to be able to monitor vast areas of the oceans. In the 1960s, priority was thus given to the study of passive detection techniques, capable of achieving much larger ranges than active acoustics. A technological revolution occurred at the end of the 1960s, with the introduction of digital signal processing. This led to the increase in capabilities and versatility of sonar systems. The extreme degree of sophistication reached at this time by passive sonar was, however, countered by progress in reducing acoustic noise radiated by submarines. So the trend was again reversed in the 1990s, with a return of active sonar techniques, extended to lower frequencies (to reach larger ranges). Those studies at the end of the 20$^{\text{th}}$ century confirmed the importance of mastering sonar techniques to counter the treats of attack submarines or of mines.

In parallel with military developments, oceanography and industry were able to profit from the development of underwater acoustics. *Acoustic sounders* quickly replaced the

traditional lead line to measure the water depth below a ship or to detect obstacles. It became widely used between the two world wars and today these systems are both scientific instruments and indispensable navigation tools. These same systems began to be used to detect fish shoals early in the 1920s; underwater acoustics has progressively become one of the main elements of sea fishing and scientific monitoring of the biomass. The use of *sidescan sonars* to obtain "acoustic images" from the seabed became one of the major tools of marine geology after their invention in the early 1960s. The efficiency of seabed acoustic mapping increased dramatically with the emergence in the 1970s of *multibeam echosounders,* allowing multiplication of the number of simultaneous soundings. Merged with sidescan imagery at the end of the 1980s, this concept today allows for the collection of maps of remarkable quality, which measure both the topography of the seabed and its *acoustic reflectivity* (i.e., yielding insights into its nature). The offshore oil and underwater industries were also concerned with acoustic mapping developments. They initiated the development of specific acoustic techniques for the *positioning* of ships or underwater vehicles, or for data *transmission*. In the domain of physical oceanography, the propagation of acoustic waves has been used since the 1970s to measure hydrological perturbations locally (*acoustic Doppler current profiling*) or on a medium scale (*ocean acoustic tomography*). Techniques of acoustic monitoring have even been suggested to monitor the evolution of the average temperature of large ocean basins on a permanent basis, as part of global climate studies.

Therefore, the number and type of applications has grown and underwater acoustics today plays in the ocean the same essential role played by radar and radio waves in the atmosphere and in space [LUR 02].

1.2 Underwater Electro-Acoustic Transducers

During the years, underwater electro-acoustic transducers have been instrumental for the transmission and reception of underwater acoustic signals. They convert acoustic energy into electric energy and vice versa. Underwater acoustic sources are called *projectors*. The reception transducers are called *hydrophones*. Extended transducers are named *antennas*, or *arrays*. The latter expression is usually reserved for structures made up of several elementary transducers. A *transmitter* is made up of a projector and its

associated electronics. Similarly, a receiver is made up of a hydrophone array and its associated low-level electronics (preamplifier and filters).

Underwater acoustic transducers use several physical processes to generate or receive sound waves. Presumably, 90%-95% of underwater acoustic transducers use the *piezoelectric* properties of some crystals, natural or artificial (*ceramics*). An electric field applied to these materials causes a deformation related to electrical excitation. These mechanical deformations in turn create acoustic waves (Fig.1.1). The opposite effects are used in reception: a piezoelectric material stressed by sound waves will generate an electric potential between its sides.
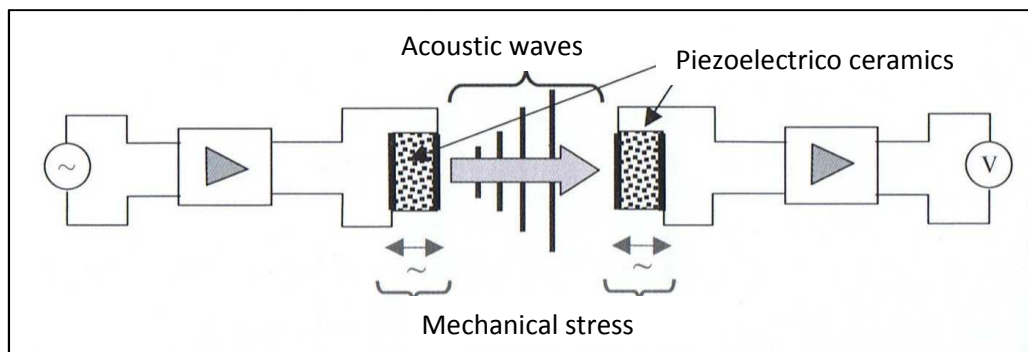

Figure 1.1: Piezoelectric effect: (left) transmission: applying an electric signal to a piece of piezoelectric material induces a mechanical deformation, generating an acoustic wave; (right) reception: the mechanical stress caused by the acoustic wave is transformed by the piezoelectric material into an electric voltage [LUR02].

Natural piezoelectric crystals, such as quartz or Seignette salt, were used in the early days of underwater acoustics. Such crystals are now replaced by synthetic ceramics. They are produced by mixing components under high temperature and high pressure (*sintering*). The resulting material is then machined to the dimensions required and coated with metal. The ceramics produced is not spontaneously polarized; this is created artificially by applying a very intense electric field to induce a *remnant polarisation*. The piezoelectric effect will be linear and reversible around this remnant polarisation.

The fundamental equations of piezoelectricity link together the mechanical, electrical and piezoelectrical values of ceramics. As a simple case, we mention here that the thickness a of a ceramic plate, submitted to a voltage V between its sides (assumed perpendicular to the direction of polarisation, see Fig. 1.2), will vary proportionally to the amplitude of the excitation:

$$\Delta a = d_{33}V \qquad\qquad (1.1)$$

where d_{33} is the *piezoelectric constant* of the ceramic in the direction of polarisation. The resulting mechanical displacement are very small, due to the typical values of d_{33}, e.g., $d_{33} \approx 40 - 750 \cdot 10^{-12} \, m/V$ for PZT (lead and titanium zirconate). Ceramics used to transmit high powers show a typical value of $d_{33} \approx 300 \cdot 10^{-12} \, m/V$; thus, a voltage of 1,000V will yield a thickness variation $\Delta a \approx 0.30 \mu m$. The mechanical effect can be amplified by stacking several piezoelectric ceramic plates, to which electric excitations will be applied in parallel, hence cumulating small displacements. On reception, a ceramic plate of thickness a and surface S undergoing a compression F parallel to its direction of polarisation will generate a voltage:

$$V = g_{33} a \frac{F}{S} \qquad (1.2)$$

The constant g_{33} equals ca. $15 - 30 \cdot 10^{-3} \, V \, m/N$ for PZT (for comparison, a natural quartz piezoelectric crystal has characteristic values of $d_{33} \approx 2 \cdot 10^{-12} \, m/V$ and $g_{33} \approx 50 \cdot 10^{-3} \, Vm/N$).
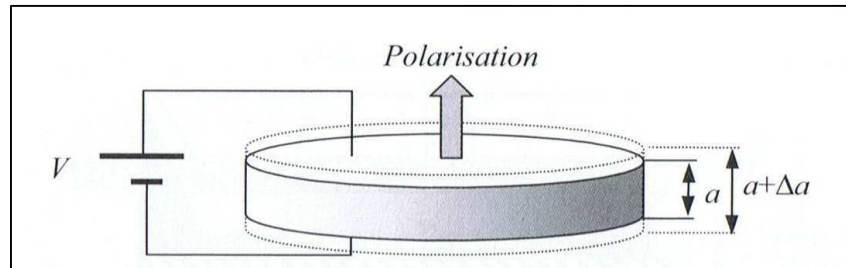

Figure 1.2: Deformation of a piezoelectric ceramic disk submitted to an electrical tension [LUR02].

In general, underwater transducer (when transmitting) work around their resonant frequency to yield the best output level achievable. But it is often possible to look for a compromise with a bandwidth broad enough to pass several close frequencies, or a wide-spectrum modulated signal. The receiving transducers used in sonars generally work around their resonance regime. Hydrophones that are used for laboratory measurement are wideband devices.

Finally, directional transducers are sometimes preferred, as specific directions of transmission and/or reception can be achieved and controlled. The *directivity pattern* of an antenna can be obtained either from the transducer geometry or processing the signal emitted by the elements of array. This study permits to control both the signal-to-noise

ratio of the measurement (via the directivity index) and the target angle estimation, essential in many sonar systems [LUR02].

1.2.1 Underwater acoustic sources and hydrophones

1.2.1.1 Tonpilz transducers

Tonpilz technology is the most frequently used in underwater acoustic transducers. Piezoelectric ceramic plates are separated by electrodes (Fig. 1.3) and stacked under strong static pressure imposed by a *prestressing rod.* This stack is interdependent by the radiating *headmass* (balanced by a *tailmass* at the other end). It transmits to the surrounding water the vibrations induced by a driving electric field applied along the electrodes of the stack of piezoelectric disks. The entire system, covered with a polymer coating, is packaged inside a waterproof housing, filled with air to limit backward radiation of the headmass. This air filling precludes the use of Tonpilz transducers at large depths, since the housing risks being crushed by high hydrostatic pressures. Filling it with oil increases the depth achievable, at the expense or lower sensitivity.

The size of the piezoelectric ceramics that are in the transducer determines the resonance frequency, the transmission level and the electrical impedance. The diameter and the thickness of the headmass, acting as a transformer adapting the active ceramics to the propagation medium, influence both the resonance frequency and the transmission level. The use of a sufficiently light metal (e.g., aluminum or magnesium) makes it possible to broaden the bandwidth. The role or the tailmass is to limit backward acoustic radiation, and to tune the resonance frequency. To be effective, it must be made of a dense enough material (e.g., steel or bronze).

Tonpilz transducers are based on a resonance concept. They can achieve high transmission levels with good power efficiency, but they only allow for limited bandwidths. Quality factors as low as 2 or 3 can be obtained (this means that that bandwidth is $\frac{1}{2}$ or $\frac{1}{3}$ of the resonant frequency). Because of their simple design, Tonpilz transducers are very successful in the majority of applications at frequencies typically between 2 kHz and 50 kHz. At frequency around 1 kHz and below, their size and their weight make them too cumbersome for practical applications. Conversely, at higher

frequencies, their dimensions are so small that they become difficult to build, and other simpler solutions are then preferred [LUR02].
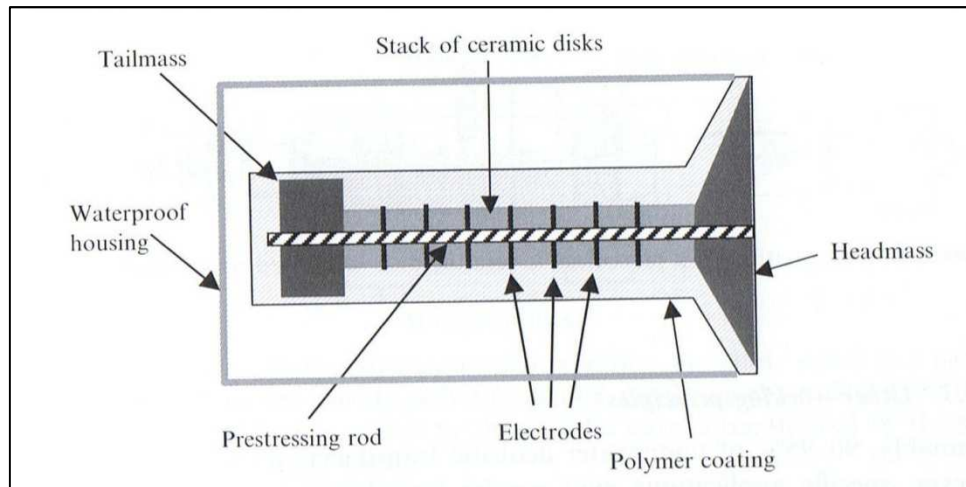

Figure 1.3: Transverse section of a typical Tonpilz transducer [LUR02].

1.2.1.2   High-frequency transducer

At high frequencies, where Tonpilz technology can no longer be used, one uses blocks of piezoelectric ceramics, electrically driven directly by surface electrodes. Many different shapes can be built: rods or parallelepipeds, rectangular or round plates, and rings. They work best at the resonant frequency of the constitutive ceramics, determined by its thickness, equal to the nominal half-wavelength. This type of transducer is used at frequencies typically larger than 100 kHz, but lower frequency dimensioning is achievable down to 50 kHz. These transducers are strongly resonant, and their bandwidth (with a typical quality factor between 5 and 10) is less advantageous than that of Tonpilz transducers.

If the dimensions of an elementary ceramic block are not large enough, several of them are built into the antenna by fixing on a rigid backing structure (Fig. 1.4). The most common shapes are rectangles or rings, depending on the type of directivity sought. The mechanical behaviour of the backing (material and dimensions) is very important, as it limits backward acoustic radiation, which should be as small as possible.

To ensure good acoustic radiation from the ceramics into the water, the entire set is either moulded in an elastomer matrix, or embedded in an acoustically transparent fluid-

21

filled housing (most commonly castor oil). This type of equipressure packaging makes these transducers particularly well suited to large depths.

At high frequencies, another possibility is the *composite ceramic* technology. Piezoelectric sticks are grouped to form a given projector shape, and embedded in a polymer matrix ensuring mechanical rigidity. This makes it possible to manufacture transducers of varied shapes with a relatively good performance, both in efficiency and in bandwidth [LUR02].
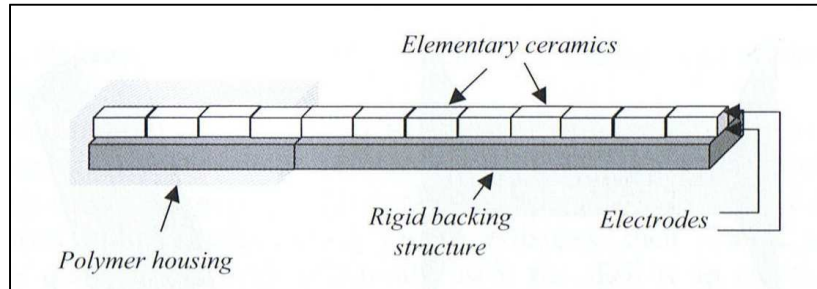
Figure 1.4: High-frequency linear transducer based on monolithic ceramics [LUR02].

1.2.1.3   Low-frequency transducer

At very low frequencies (below 1 kHz), acoustic source technology encounters serious limitations. The transducer must be capable of withstanding at the large amplitudes emitted; and they are very heavy and big.

Several solutions have been proposed (Fig. 1.5) each one being generally adapted to solve a particular problem. Among them, one can cite:

- The extension of Tonpilz technology to low frequencies with some modifications. For example, the *Janus* concept equips the Tonpilz transducer with two opposing projectors (Fig. 1.5a). This type of solution is particularly well suited when high transmission levels are required.
- Sources based on the *Helmholtz resonator* technology. These are commonly used by oceanographers for acoustic tomography experiments. An open metal tube is excited at one end by a piezoelectric driver (Fig. 1.5b). The entire structure resonates at a frequency given by $L=\lambda/4$, where L is the length of the tube. Initially designed for frequencies between 400 Hz and 250Hz, this solution is simple, robust, low-cost and insensitive to hydrostatic pressure.

Unfortunately, it shows poor efficiency, limited power and very narrow frequency bandwidths.

− A Helmholtz resonator can be coupled with a Janus transducer, leading to the *Janus-Helmholtz concept* (Fig. 1.5c). Coupling the resonance of the transducer with that of the Helmholtz resonator yields a wide bandwidth and is efficient at the same time. This means that the elasticity inside the resonator cavity must be increased, using either compliant tubes or a compressible fluid. Initially designed for military low-frequency active sonars, and usable at great depths, this concept has been extended to sources used in physical oceanography and marine seismology.

− *Flextensional* transducers are also an appealing solution for high-power applications such as military sonars. They consist of an elastic shell, in which an electro-acoustic driver is inserted. This is the piezoelectric stack, whose longitudinal vibrations induce deformations in the radiating shell. The Class IV type (Fig.1.5d) is the most commonly used: the shell is an elliptical cylinder, and the ceramic bar is inserted along its main radial axis. These transducers have a high efficiency at low frequencies, with compact dimensions. However, they cannot withstand high pressure, as the static deformation of the shell decouples it from the piezoelectric driver.

− *Hydraulic* technology has been used for acoustic thermometry experiments requiring large, broadband transmissions around 60Hz. A hydraulic block, electrically controlled, moves radiating shells trough a piston. Well suited to very low frequencies, this transducer concept requires high electric power and specific cooling devices; it is therefore ill-adapted to autonomous sources.

− *Electrodynamic* sources similar to aerial loudspeakers can be used to transmit broadband low-frequency signals. But the levels available are very limited because of mediocre efficiencies, and it is very difficult to compensate for hydrostatic pressure below a few metres [LUR02].
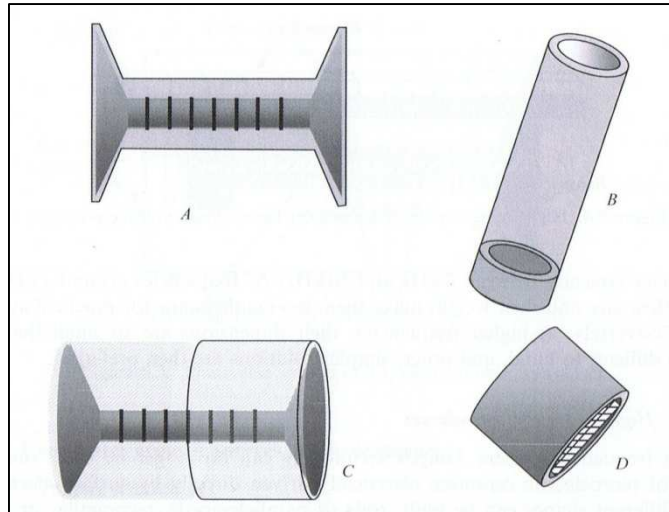
Figure 1.5: Examples of low-frequency acoustic transducers: Janus Tonpilz (A); Helmholtz resonator (B); Janus-Helmholtz (C); Class IV flextensional (D) [LUR02].

1.2.1.4   Hydrophones

Hydrophones are receiving transducers, designed to convert the acoustic pressures into electrical signals. They usually are piezoelectric devices, most often made of PZT (Lead Zirconate Titanate), featuring good sensitivity and low internal noise levels. *Lithium sulphate* is reserved for high-frequency measurement hydrophones. Physically large hydrophones (e.g., submarine flank arrays) are sometimes made in PVDF (*polyvinylidene bifluoride*), a versatile material which can be tailored into very large plates, easily fitted on curved surfaces. Finally, as with projectors, *piezo-composite materials* are increasingly used: they are made of ceramic elements embedded in a polymer matrix.

Contrary to projectors, hydrophones are often capable of working over a wide frequency band. This is because they do not actually need to be tuned to a particular resonance frequency. Their sensitivity (ratio of the output electric power to the input acoustic power) is usually not problematic, as the electric signal can always be amplified. But it is imperative that low acoustic signals can be detected amidst the internal noise of the receiver (combination of the internal noise of the ceramics and the self-noise of the amplifier). Measurement hydrophones are usually small compared with acoustic wavelengths, and their frequency resonance is rejected beyond the upper limit of the flat part of the frequency response (Fig. 1.6). A required directivity pattern can be obtained by combining several hydrophones into a large array.

The same transducer is often used for transmission and reception in many sonar systems, e.g., single-beam echo sounders, acoustic Doppler current profilers (ADCPs), sidescan sonars.
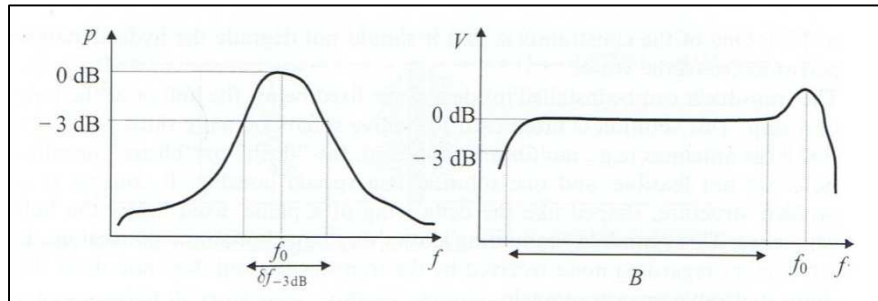

Figure 1.6: (Left) Frequency response curve and bandwidth δf_{-3dB} of a transducer. (Right) Frequency response curve of a hydrophone: the resonance frequency f_0 is rejected beyond the effective bandwidth B [LUR02].

1.3 Underwater Acoustics Applications

The use of underwater sounds is a recent technological development and it is now part of most human activities at sea. Its technology is applied in the oceans, scientifically, militarily or industrially. The number and type of applications has grown considerably, and in general, they are used underwater to:

a. "detect" and "locate" obstacles and target; this is the primary function of sonar systems, mostly for military applications such as anti-submarine warfare and minehunting, but also used in fisheries;

b. "measure" either the characteristics of the marine environment (seafloor topography, living organisms, currents and hydrological structures, etc.) or the location and velocity of an object moving underwater;

c. "transmit" signals, which may be data acquired by underwater scientific instrumentation, messages between submarines and surface vessels, or commands to remotely operated systems.

These systems are for the most part *active systems*, that is, they transmit a characteristic signal, and this signal will be reflected on a target or transmitted directly to a receiver. But there are also *passive systems*, designed to intercept and exploit underwater sounds coming from the target itself [LUR02].

In the following, the main modern applications of underwater acoustics divided in military and civil applications will be shown briefly.

1.3.1 Military applications

As known, most of the research and industrialization effort in underwater acoustics was largely linked to military applications. These systems are therefore mostly aimed at detecting, locating and identifying two types of target namely submarines and mines. Military sonars are classified into two main categories, depending on their mode of operation (Fig.1.7): *active sonars* and *passive sonars*.

Active sonars transmit a signal and receive echoes from a target (usually a submerged submarine). The measured time delay is used to estimate the distance between the sonar and its target, and receiving the signal on a suitable antenna completes the measurement with a determination of the angle of arrival of the signal. Further analysis of the echo allows identification of more characteristics of the target. A type of active sonar with very high resolution is the *minehunting* sonar. It is designed to detect and identify mines laid (or buried) on the seabed in coastal areas. *Passive sonars* are designed to intercept noises (and possible active sonar signals) radiated by a target vessel. In principle they can be used on submarines as well as on the ships hunting them. Acquiring the target-radiated noise allows not only for the detection of the target, but also its localization and its identification by analyzing the spatial structure of the acoustic field received on a sufficiently long antenna and its acoustic signature respectively [LUR 02].
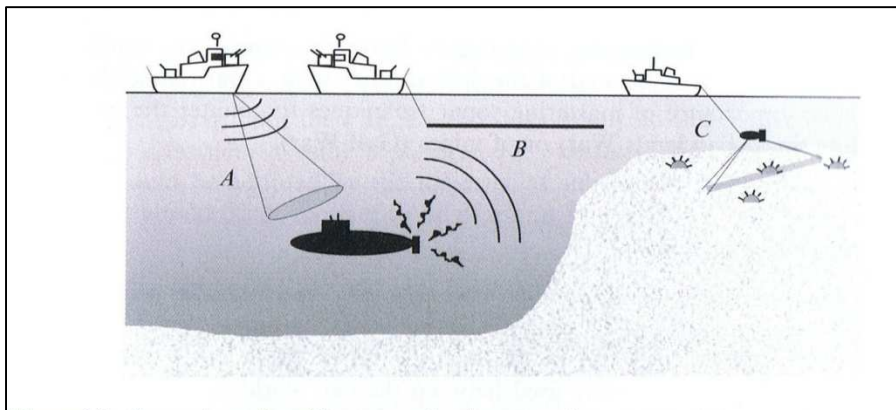

Figure 1.7: Examples of military applications: (A) active sonar; (B) passive sonar; (C) minehunting active sonar [LUR02].

1.3.2 Civilian applications

Civilian underwater acoustics is a more modest sector of industrial and scientific activity, but it is highly diverse and growing. It has been, specially, invigorated by the needs for scientific instrumentation raised by large scientific programmes of environment study and monitoring, as well as developments in offshore engineering and industrial fishing. The main categories of systems are: *bathymetric sounders*, *fishery sounders, sidescan sonars, multibeam sounders, sediment profilers, acoustic communication systems, acoustic Doppler systems, acoustic tomography networks and positioning systems (fig.1.8)* [LUR 02].

The *bathymetric sounders* are sonars specialized in the measurement of water depth. They transmit a signal downward, vertically, inside a narrow beam. They measure the time delay of the seabed echo. These sounders are now very well distributed and are universally used, from professional navigation to leisure yachting. Similar to these sounders there are the *fishery sounders* that are designed for the detection and localization of fish shoals. But they, in contrast to the other ones, support additional tools to detect and process the echoes coming from the entire water column. For the acoustic imaging of the seabed *sidescan sonars* are used. They allow high-accuracy observations. Placed on a platform towed close to the bottom, the sonar transmits, in a direction very close to the horizontal, a short pulse that sweeps the bottom. The signal, reverberated as a function of time, yields an image of the irregularities, obstacles and changes in structures. These systems are used in marine geology, or for the detection of mines and shipwrecks. To map the seafloor *multibeam sounders* are used. They are installed aboard oceanographic or industrial survey vessels to map the topography of the seabed accurately. A fan of elementary beams, transmitting athwartship, rapidly sweeps a large swathe of the seabed and measures its relief. If the angular aperture is large enough, the sounder can also provide acoustic images, like sidescan sonars. Then, to study the stratified internal structures of the seabed *sediment profilers* are used. These are single-beam sounders, similar to those used in bathymetry. Their frequency is much lower, enabling penetration of tens and even hundreds of metres into the sea floor, depending on the type of seafloor. In the same domain, *seismic* systems use explosive or percussive sources and long receiving antennas. They are able to explore the seabed down to several kilometres of depth, and are widely used in oil and gas exploration, and in geophysics. Other systems, like *acoustic communication systems* (e.g., underwater

telephone), beyond their primary use as a phone link, are also used for the transmission of digital data (e.g., remote control commands, images, results from measurements). Their performance is limited by the small bandwidths available, and by the difficulties inherent to underwater propagation. Rates of several kilobits per second are, however, achievable at distance of several kilometres. To measure the speed of the sonar relative to a fixed medium or the speed of water relative to a fixed medium instrument using the frequency shift of echoes *acoustic Doppler systems* are employed. Instead *acoustic tomography networks,* which use fixed transmitters and receivers, are employed to measure propagation times or amplitude fluctuations to assess the structure of hydrological perturbations, using speed variations estimates. Last, and very important for the study developed in this thesis, there are *positioning systems.* They are used, for example, for the dynamic anchoring of oil drilling vessels or the tracking of submersibles or towed platforms. The mobile target is often located by measuring the time delays for signals coming from several fixed transmitters placed on the bottom [LUR02]. Different geometries are in fact achievable. In the next section the different types of this system will be described.
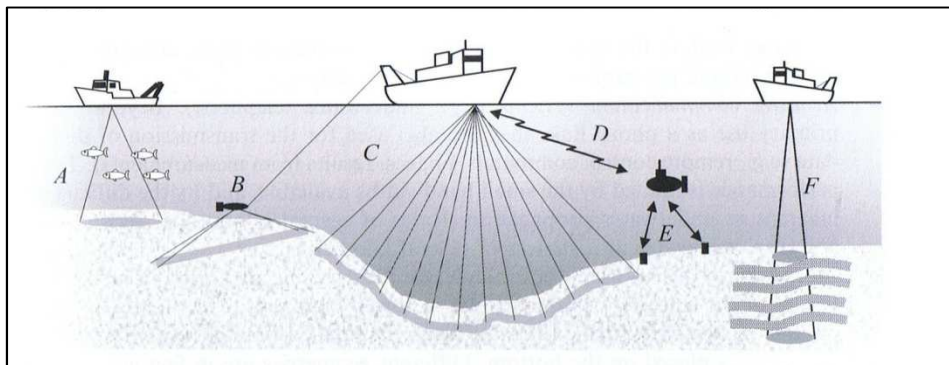

Figure 1.8: Examples of civil applications: (A) bathymetry or fishery sounder; (B) sidescan sonar; (C) multibeam sounder; (D) data transmission system; (E) acoustic positioning system; (F) sediment profiler [LUR02].

1.4 Acoustic Positioning

The means available for direct intervention in increasingly deeper waters have steadily progressed during the last 50 years. The scientific community interested in the deep ocean wanted dedicated instrumentation that could be used at depths of several kilometres, and the development of appropriate deployment tools. At the same time, the

offshore industry increasingly looked at the possibility of deepwater hydrocarbon exploitation and shipwreck investigation. All these applications, some of which have important economic implications, led to the development of the original underwater acoustic techniques, for the local positioning of ships and submersibles on the one part, and for the transmission of data on the other. But in this section only the positioning systems will be delineated.

The positioning systems are divided in three types of system corresponding to different types of measurement. They are the *long-baseline systems, short-baseline systems and ultra-short-baseline systems.* The *long-baseline systems* (LBLs) use a network of acoustic beacons (at least three not coplanar), widely spaced over the area to be covered (Fig. 1.9(a)). Their position must be accurately determined prior to using the system. The position of the moving object (e.g., submersible or torpedo) that needs to be located is deduced from the travel times of the signals received from each beacon. Measurement of the absolute durations requires the use of clocks that are synchronous with the moving object and the beacons, or a system of interrogation of the beacons (transponders) by the moving object. After calibration, long-baseline systems can yield localization accuracies of the order of a metre over kilometres. A recent interesting variant consists in installing the acoustic beacons below drifting buoys whose positions can be tracked by GPS. While the *short-baseline systems,* denoted with the acronym SBLs, are easier to use than long-baseline systems, their accuracies are not as good. They use a single transmitter and a series of receivers placed close to each other (Fig. 1.9(b)). The relative position is determined by time differences between the paths received at different points on the antenna. Conceptually similar to SBLs are the *ultra-short-baseline systems* denoted USBLs. They use a single receiver featuring a small array. Measuring the phase differences between the different points on the array determines the direction of arrival of the acoustic waves from the transmitter placed on the moving object. Depth in the sea can be measured using a pressure sensor, and transmitted acoustically; alternatively, it can be assessed acoustically if the receiver has access to absolute travel times. The most modern USBLs have positioning accuracies of around 10 metres in deep water [LUR 02].
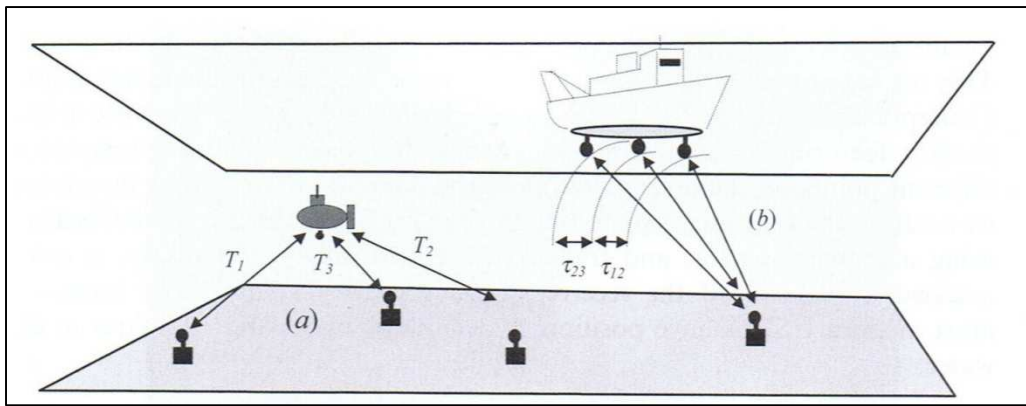
Figure 1.9: Acoustic positioning systems. (a) Long-baseline: the travel times between the three beacons and the mobile are used to determine its position at the intersection of the three spheres of radii $R_i=cT$; (b) SBL: the differences τ_{ij} of the travel times are used to determine the position of the bottom of the ship relative to the reference beacon [LUR02].

Chapter 2

Acoustic Positioning System in Underwater Neutrino Telescopes

2.1 Underwater Neutrino Telescopes

Lately underwater neutrino telescopes have become important tools of astroparticle physics since they allow for a new and unique method to observe the Universe. Neutrinos are stable neutral particles that interact only via the weak force. They can escape from sources surrounded with dense matter or radiation fields and can traverse cosmological distances without being absorbed or scattered. This implies that neutrinos can bring us astrophysical information that other messengers cannot and, open a potential new window on the Universe [AGE11] This property contrasts to that of other particles, such as gammas, protons, cosmic rays, etc. that can be absorbed by the cosmic dust, by the radiation or deviated by the galactic and intergalactic magnetic fields and then they cannot bring us information about their originating place. On the other hand, the low interaction cross section of the neutrinos imposes a great challenge for their detection: only a tiny fraction of incident neutrinos can be observed. To compensate for this it is necessary to build very large detectors. One way to detect neutrino interactions can be afforded through the detection of the Cherenkov light emitted by the muon generated after a neutrino interaction. This particle travels across the detector at speed greater than the speed of light in water, so generating a faint blue luminescence called Cherenkov radiation. As said, it is necessary the instrumentation of large volumes of water (or ice) with several optical sensors in order to detect characteristic signatures of high energy neutrino interactions. The main elements of a neutrino telescope are therefore the sensitive optical detectors, usually photomultiplier tubes (PMTs) hosted to the inner surfaces of pressure-resistant glass spheres named optical modules (OMs), which collect the light and transforms it into electric signals. The arrival times of the light collected by optical detectors distributed over a three dimensional array can be used to reconstruct the muon trajectory, and consequently that of the neutrino, which at sufficiently high energies are collinear (see Fig. 2.1). The accuracy of reconstruction of

the muon track depends on the precision in measuring the light arrival time and on the precise knowledge of the positions of the optical detectors. Good time and position calibration of the detector is therefore of utmost importance to achieve a good angular resolution. The measurement of the amount of collected light can be effectively used to eliminate background events, to improve the muon track reconstruction quality and to estimate the neutrino energy [BIG09].
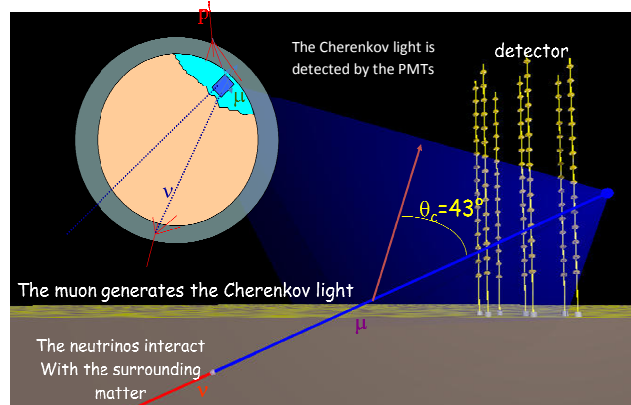

Figure 2.1: Principle of detection of high energy neutrinos (~TeV) in a deep-sea neutrino telescope.

In the deep sea the semi rigid structures containing the OMs are anchored on the seabed and maintained vertical by a buoy, and then the top part of the structures can move under the effect of currents. Since the accuracy required for the position of the OMs to effectively reconstruct the muon track is ~10 cm, an Acoustic Positioning System (APS) is needed to monitor the OM positions continuously. In particular, the APS is a sub-system of the detector that must provide the position of the telescope's mechanical structures both during the deployment and the operating phases of the telescope (monitoring of the OMs positions) [CDR08]. The possibility of reconstructing the detector position in real time, during the deployment phase, will support safe naval and remotely operating vehicle (ROV) operations; during this phase the accuracy needed is of the order of 1 m. This capability will also be fundamental in measuring the telescope, absolute position and pointing direction, allowing for the reconstruction of the astrophysical source position in the sky. A deep-sea APS is composed of the following two main items: (1) a so called *Long Baseline* (LBL) of acoustic transceivers, anchored on the seabed in known positions and (2) an array of acoustic receivers (hydrophones) rigidly connected to the mechanical structures of the telescope. The positions of the

hydrophones are evaluated by measuring the difference between the emission time from sources of known position (LBL acoustic transceivers) and the arrival time at hydrophones of unknown position; it is possible to reconstruct their tridimensional location using triangulation techniques [SIM12].

Moreover the acoustic data can be used to monitor ocean noise and to study the acoustic neutrino detection. It will also allow monitoring of the environment around the detector and Earth and Sea Science studies: biology, geophysics and oceanography. In fact, other way to detect a high energy neutrino interaction is through acoustic detection. The basic idea is that, when the neutrino interacts in water a large amount of the neutrino energy can be deposited in a small volume of water. This instantaneous water heating produces a bipolar acoustic pulse, following the second time derivative of the temperature of the excited medium. The frequency spectrum of the signal is a function of the transverse spread of the shower, with typical maximum amplitude in the range of few tens kHz. The acoustic technique could be extremely fruitful because the sound absorption length is, in this frequency range, of the order of km [RIC04].

The first generations of neutrino telescopes were AMANDA at the South Pole [SPI05], ANTARES in the Mediterranean Sea [BRU10] and Baikal [AYN06] in the homonymous Siberian Lake. The target volume of these installations is typically of the order of $0.01 km^3$, but over the last decade it has been evident that larger detectors are needed to exploit the scientific potential of neutrino astronomy. For this reason, the international scientific community has aimed at the construction of km^3 scale detectors. A first km^3-size detector is IceCube [HUL11], installed at the South Pole. A new km^3-size detector planned in the Mediterranean Sea is the KM3NeT neutrino telescope [KM3Nw]. It will surpass IceCube in sensitivity by a substantial factor and complement it in its field of view. In particular, its field of view will cover the Galactic Center and a large fraction of the Galactic plane that are hardly visible to IceCube [KAT11].

In the next sections the ANTARES and NEMO detectors will be described and in particular their APS, since the proposed innovative APS of KM3Net is based on the experience achieved with these experiments. Moreover the study and development of the innovative APS of KM3NeT is the main aim of this thesis.

2.2 Acoustic Positioning System of the ANTARES detectors

ANTARES (Astronomy with a Neutrino Telescope and Abyss environmental RESearch) is currently the biggest underwater neutrino telescope in the world and is in operation in the Northern Hemisphere. The main aim of the detector is the search for high-energy neutrinos of astrophysical origin [AGU11b, ADR11].

The detector is located in the Mediterranean Sea, about 40 km from Toulon, off the French coast, at a mooring depth of about 2475 m and has a surface area of ~0.1km^2. It consists of 12 lines, anchored to the sea floor by an anchor called a '*bottom string socket*' (BSS) at distances of about 60-70 m from each other and kept vertical by buoys. The lines are equipped with altogether 885 10-inch PMTs, model R7081-20 from Hamamatsu [AGU11]. The PMTs are arranged in 25 three dimensional arrays, each one comprising three PMTs, directed at an angle of 45º towards the sea bed and sustained by titanium frames that also support titanium containers for the electronic components named Local Control Module (LCM). All this constitutes the storeys of the detector, see Figure 2.2. The cables between the storeys serve both as mechanical structure and as an electro-optical connection. The total length of each line is 480 m. The lowest storey of each line is located 100 m above the sea bed. The distance between consecutive storeys is 14.5 m. The PMTs [AGU05] are coupled with optical gel to the inner surfaces of pressure-resistant glass spheres (optical modules, OMs). A μ-metal cage inside the OM shields the PMT from the Earth's magnetic field [AGU11].
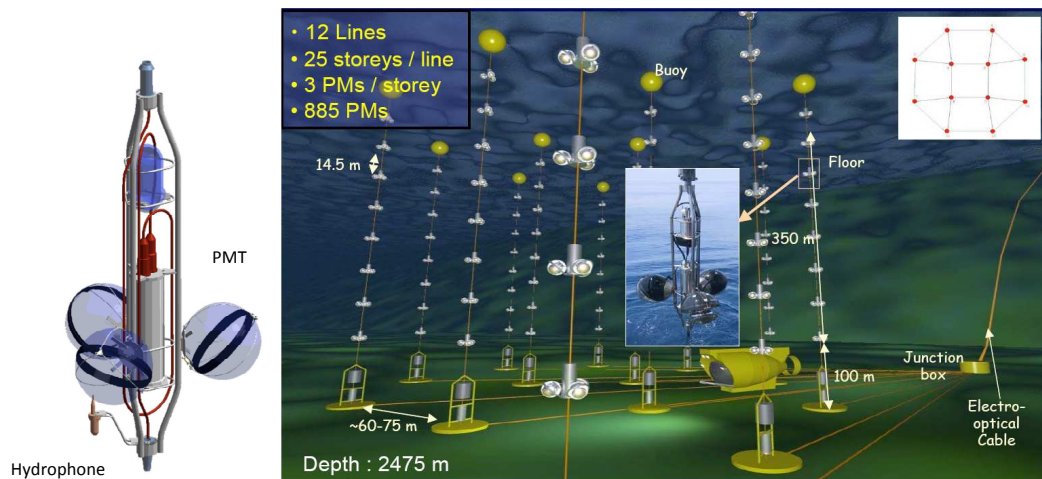
Figure 2.2: Left: schematic diagram of an ANTARES storey carrying three optical modules, an electronics container (LCM) and a positioning hydrophone fixed off-axis. Right: artistic view of the 0.1km^2 of the ANTARES neutrino telescope.

The lines are linked through submersible cables to the *Junction Box* (JB) that acts as a fan-out between the main electro-optical cable to shore and the lines.

The detector is complemented by an *Instrumentation Line (IL)* [AGE11] holding devices for measurements of environmental parameters as well as tools used by other scientific communities, including a seismometer. In addition, it includes three acoustic storeys, which are modified standard storeys replacing the PMTs by acoustic sensors with custom-designed electronics for signal processing. These three storeys together with three additional acoustic storeys on Detection Line 12 form the AMADEUS system that is a basic acoustic system to do long-term studies to check the feasibility of acoustic ultra-high-energy [1] neutrino detection [LAH12]. The R&D studies for the construction of the neutrino telescope started in 1996, with the first lines deployed and connected in 2006. The telescope was completed in May 2008 with the deployment and connection of the 12*th Detection Line* [ANTAw].

The telescope also contains timing and position calibration systems, which employ optical beacons and acoustic transducers installed in each line. The lines are not rigid structures, so deep-sea currents (typically around 5 cm/s) cause a displacement of the lines by several metres from vertical position and a rotation of the storeys around their line axis. Therefore, real time positioning of each line and of all OMs are needed to ensure optimal track reconstruction with accuracy better than 10 cm (corresponding to an uncertainty in the travel time of light in water of 0.5 ns). Moreover, the reconstruction of the muon trajectory and the determination of its energy also require the knowledge of the OM orientation with a precision of a few degrees. In addition, a precise absolute orientation of the whole detector has to be achieved in order to find potential neutrino point-sources in the sky and correlate them with sources of other messenger particles. To achieve this positioning accuracy during data taking, two independent systems are incorporated in the detector: an acoustic positioning system and tiltmeter-compass sensors in each storey.

The acoustic positioning system consists of four elements (Fig. 2.3):

- An emitter-receiver acoustic module (AM) located on the ship during the deployment operation.
- Five autonomous battery-powered transponders located on the sea floor around the detector area at distances of about 1100-1600 m [ADR12].

---

[1] In the context of neutrino physics typically it refers to neutrinos in excess of 10^18 eV.

- Transceivers (RxTx module) anchored on a rod of each BSS of the line mounted about one metre off-axis with respect to the line.

- Receiver hydrophones (Rx modules) located on five storeys of each line (storeys 1, 8, 14, 20 and 25, counted from the bottom upwards), with storeys 1 and 25 being the bottom and top storey, respectively. The other modules are distributed in a manner such that a larger density of hydrophones is obtained in the top third part of the string, where the maximum curvature of the line shape is expected.
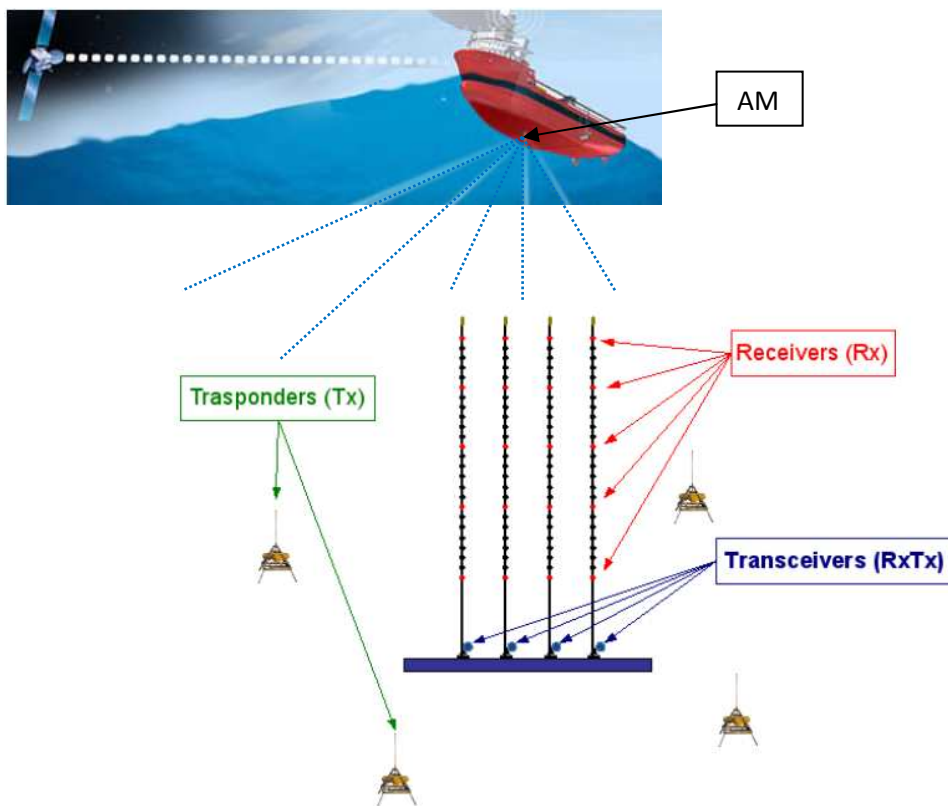
Figure 2.3: Schematic view of the acoustic positioning system of the ANTARES detector.

Moreover, these four elements compose two subsystems of the APS of the ANTARES detector [ADR12]: 1) the low frequency long baseline positioning system (LFLBL) used to connect the local frame of the detector to the geodetic reference frame, allowing for the determination of the absolute position and orientation of the detector; 2) the high frequency long baseline positioning system (HFLBL) used to measure the relative positions of the OMs with high accuracy.

The LFLBL acoustic positioning system is a commercial set of devices provided by the IXSEA Company [IXSEw]. It is able to measure the travel time of controlled acoustic pulse between the AM and the autonomous transponders and use the 8-16 kHz frequency range. The AM is operated on ship and is linked to a time counting electronic system. The use of acoustic signals at these frequencies allows for long propagation distances to be measured and for this reason it is suited to determine the position of ANTARES structures by triangulation from a ship on the sea surface [ADR12].

In the first step, the absolute geodetic positions of the autonomous transponder were individually determined with an accuracy of better than 1 m before the deployment of the detector. This result was obtained through several hundred triangulations of the LFLBL system from a ship positioned by Differential GPS (DGPS). The sound-velocity profile from the sea surface to the sea floor necessary for this calculation has been derived from the Chen-Millero formula [CHE77] using sets of temperature and salinity profiles measured at the ANTARES site.

In the second step, in order to monitor the position of the BSS in real time during the line deployment, the triangulation of the acoustic travel time measurements between the transponders on the BSS, the autonomous reference transponders and the AM on the ship was calculated. The latter is determined with accuracy of a few metres, whereas the accuracy of the final position of the BSS on the sea bed is about 1 m.

With respect to have a good knowledge of the absolute orientation of the detector, it is necessary to determine with good accuracy the BSS orientation and depth. The orientation of the BSS is determined using the compass of a submarine vehicle during an undersea line connection with an accuracy of about 5°.

The depth of the sea bed at the position of each BSS is measured by a pressure sensor on the submarine with a precision of about 10 cm. Moreover, the relative positions of the line anchors are obtained measuring all distances between different transceivers of the BSSs, which form an auto-calibrated positioning system.

Once the positions of the BSSs are known it is possible to determine the absolute orientation of the detector using the triangulation between transceivers and hydrophones, considering that the line remains almost vertical for small speeds of the sea current (smaller than 2 cm/s).

In summary, the absolute orientation of the neutrino telescope with respect to the sky, needed for neutrino astronomy, is obtained using both the absolute positions of the different line anchors and the BSS to BSS relative positions [ADR12].

The HFLBL acoustic positioning system was developed and constructed by the company GENISEA/ECA [ECAw] for the relative positioning of the detector strings. The method used is to measure the travel time of 40-60 kHz acoustic pulses between receiving hydrophones placed along the string and emitters fixed at the bottom of each line [KEL07]. Electronic boards manage the settings of the system, for emission, detection, filtering and recording. The 3D position of each hydrophone is then obtained by triangulation from the travel times between the hydrophone and each fixed emitter knowing the sound velocity profile. In fact, there are several sound velocity profilers located throughout the ANTARES detector, which measure the sound velocity profile continuously. The positions of all hydrophones and transducers are then computed from distances using triangulation principle based on a least-mean square minimization. Measurements for the line shape reconstruction are performed every 2 minutes, which is enough since the motion of the lines is due to slow counts.

The other independent system incorporated in the detector, as mentioned above, is the Tiltmeter-Compass System (TCS). It consists of a commercial TCM2 board, manufactured by PNI Sensor Corporation [PNICw, ADR12], that measures the inclination of the storey with respect to the horizontal plane in two perpendicular axes (pitch and roll). It is installed in the electronics module of each storey and it is based on the movement of a fluid in the sensors due to the inclination of the storey. The absolute orientation of the TCM2 (heading, i. e., rotation around line axis) also has to be measured. For this reason three flux tube magnetic sensors measure the Earth magnetic field in three perpendicular local directions (x, y, z) of the TCM2 frame [ADR12].

The range of measurement for the tiltmeters is ±20º on 2 perpendicular axes (roll and pitch), with an accuracy of 0.2º, while the compasses measure 360º of heading at a resolution of 1º. Data is read out from the TCM2 device every 2 minutes and is used in conjunction with the APS during the line fit [BRO09].

2.3 NEMO Acoustic Positioning System

The NEMO (NEutrino Mediterranean Observatory) Collaboration was set up in 1998 with the aim to carry out the necessary R&D towards a km^3 neutrino telescope in the

Mediterranean Sea. In the first step, the collaboration installed at the end of 2006, 25 km offshore the port of Catania (Sicily) at 2000 m depth in the Test Site, the NEMO Phase1detector: a technological demonstrator for a future km^3 Cherenkov neutrino telescope [MIG06, RIC09]. The site was equipped with an electro-optical cable connected to a shore station inside the Port of Catania. The project comprised the critical elements of the km^3 detector: the Junction Box (JB) and a prototype detection unit of reduced size called Mini-Tower with only four floors (rigid bar, Fig. 2.4) and a total of 16 OMs. Positions of the optical sensors in the Mini-Tower were reconstructed through an acoustic positioning system with a high level of accuracy. The NEMO prototype detector i.e., ''NEMO Phase-1'', has been successfully operated from December 2006 to May 2007 [MAR06, AMO09].

The acoustic positioning system in NEMO Phase-1 was composed of a Long Base Line (LBL) of acoustic beacons and an array of 10 hydrophones on the tower. The acoustic LBL had an emission frequency of 32 kHz and a transmitting power of 180 dB re @ 1 m and comprised three stand-alone battery-powered acoustic beacons placed on the seabed at about 400 m horizontal distance from the tower base and one additional beacon located on the tower base. The last one was connected with the NEMO power and data transmission system. The transmission system was synchronized through a signal PPS (Pulse Per Second, 1 Hz) provided by GPS, named Master Clock. Eight hydrophones (labeled H0 and H1) were installed at the end-points of each tower-floor, close to the optical modules (Fig. 2.4(left)). Two further hydrophones, defined as "*monitoring station*", were installed at the tower base (see Fig.2.4 (right)). The acoustic positioning system was based on the measurements of times of flight of acoustic signals between the beacons and the target hydrophones. Measurements were performed at regular intervals of ~ 1 second. Time of flight (TOF) was defined as the difference between the time of arrival (TOA) of the acoustic signal on the hydrophone and the time of emission on the beacon (TOE) [AMO08]. Hydrophone positions are calculated by converting time of flight into distances (knowing the sound velocity profile in the water column) and applying a triangulation method.
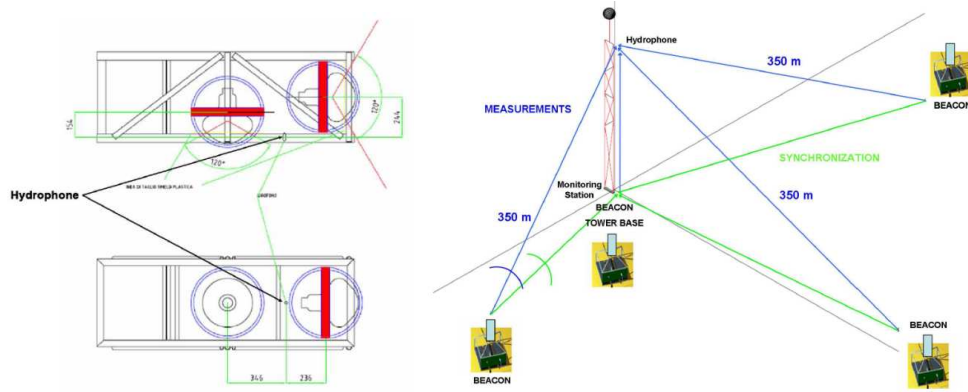
Figure 2.4: Left: Side and top view of floor ending part: position of the hydrophone and OMs in the Mini-Tower is shown. Right: Schematic view of Acoustic Positioning System (APS) and of the Long-Base-Line (LBL) configuration.

The beacon absolute positions and relative distances were determined, acoustically, during the detector deployment operations using a ROV equipped with a 32 kHz pinger, GPS time synchronized, and a high accuracy pressure sensor. The ROV hydrophone was positioned near at the monitoring station and the distance between the ROV and external beacon and monitoring station and external beacon were calculated. The error in the measurement of the distance between the beacons and the monitoring station was evaluated to be about 10 cm. The sound velocity in the site was evaluated using pressure, temperature and salinity values measured with the CTD installed on the first floor.

In order to calculate the absolute position of each hydrophone, it was also necessary to define the LBL coordinate system. The origin of the coordinate system was taken at the position of the beacon installed on the tower base. In this system x and y axis correspond respectively with absolute Easting and Northing directions. The knowledge of the correct orientation of the reference system was important not only for the acoustic positioning system but also to determine the tower position and orientation, in order to evaluate the absolute direction of the reconstructed muon tracks.

Since the beacon had a single frequency of emission, it was necessary to know which beacon emits the pulse. For this reason a technique called Time Spectral Spread Codes (TSSC) was adopted. A TSSC family of codes is based on pseudo-random sequence of acoustic pulses that form an orthogonal base in the time domain. These sequences have a period of 6 s, i.e. a pattern of 6 pseudo-random pulses (spaced by ~ 1 s) that is different from the others. In this way a typical beacon pulse sequence could be

recognized without ambiguity. Each pulse length was 5 ms and the sequence of pulses was built in such a way to avoid overlap between two consecutive pulses. This technique has the advantage that all beacons can be identical except for the software configuration that defines the pulse sequence, and receivers can be sensitive to only one acoustic channel. Acoustic pulses detected by the hydrophones were converted in an electric signal and identified by the APS Board in situ. The latter was able to recognize the signals emitted by the beacon through dedicated software. The TOA measured in the reference Master Clock time, was then transmitted to shore, where other dedicated software decodes hydrophone data to calculate the position of the hydrophone as a function of time. In order to estimate the accuracy of the positioning system, distances between hydrophones H0 and H1 on the same floor were calculated. Figure 2.5 shows the distance H0-H1 calculated for floor 2, using APS data. Each point represents the average distance calculated over a period of 300 s. The mean value of the measured distance is 14.24 ± 0.06 m (dashed green line) in agreement with the distance H0-H1 measured on-shore, during tower integration that is equal to 14.25 ± 0.01 m (dashed blue line) [AMO08].
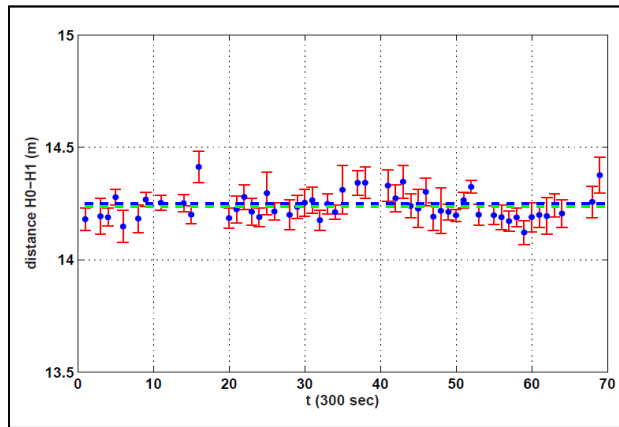
Figure 2.5: Distance of the hydrophone H0-H1 of floor 2 of the mini-tower of NEMO Phase-1, calculated with APS data and experimental statistical error. Each point represents the average distance over a period of 300 s. For comparison the distance measured on-shore during the integration phase (d = 14.25 ±0.01 m, dashed blue line) is shown.

This APS used in NEMO Phase-1 works accurately but it is not scalable to the dimension of a km^3 detector. The use of the autonomous beacons with a single frequency is not suitable at the dimension of a large detector. The calibration of the LBL is time consuming and is the main cause of error in the reconstruction of the hydrophone position. Moreover the use of APS Board in situ increases the cost, the dimension and the power consumption on the electronics off shore. In addition, it does

not allow for changes of the analysis data system after the deployment. For this reason the Collaboration NEMO has developed a new APS that will be described in the following.

As the next step, the collaboration will install, in 2012, the NEMO Phase II demonstrator off-shore Capo Passero (Sourth-East Sicily) at a depth of 3500 m. It is a prototype of a detection unit of a neutrino telescope consisting in a semi-rigid vertical structure called towers. The towers are composed of 8 horizontal 8 m-long frames (named floors) made of marine grade aluminum tensioned by a system of ropes. The prototype will be about 420 m high and will be anchored on the sea bed and kept vertical by buoy on the top. The distance between floors is 40 m, while that between the anchor and the lowermost floor is about 100 m. Each floor has two optical modules at either end, (resulting in a total of 32 optical modules in the tower), one looking vertically downwards and the other horizontally outwards. Each floor furthermore hosts instrumentation for positioning and environmental parameter monitoring. The positioning of the detector is provided by a 3D array of 18 acoustic sensors installed at both ends of each floor and at the base of the detector (monitoring station). In addition, four autonomous acoustic beacons will be anchored on the sea bed at distance of about 500 m from the base of the tower and one powered beacon will be located at the base of the tower (Fig. 2.6). The beacons, which are manufactured by ACSA [ACSAw], emit known packets of sinusoidal signals of 32 kHz, 5ms duration, 180 dB re 1 μPa at 1 m transmitting power. Moreover, they constitute the basic points to define a Cartesian reference system of orthogonal axes related to the so-called long baseline (LBL) that will permit to calculate the position of each hydrophone [SIM11].
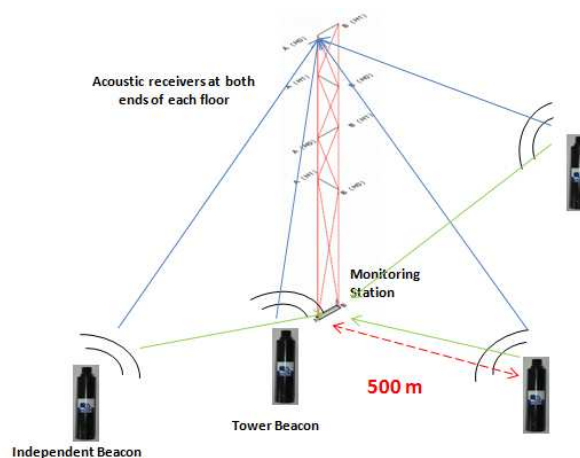
Figure 2.6: Schematic view of the acoustic positioning system of the NEMO Phase II detector. The positioning of the detector is based on the measurement of the time of flight of acoustic

signals between beacons of a long baseline acoustic system, anchored on the sea-floor, and acoustic receivers acting as targets, rigidly connected to the mechanical structures of the detector.

The receiver array is composed of: 14 high sensitivity and broadband (10 Hz-70 kHz) hydrophones SMID, provided by INFN (Italy); 2 free flooded rings (FFR) hydrophones Sensor Techonolgy Ltd SX-30, provided by UPV (Spain) in collaboration with CPPM-CNRS (France)-proposed for possible use in the KM3NeT long-baseline- that will be described in the next chapters and is the main subject of this thesis; 2 custom piezo-sensors developed by ECAP (Germany), that will be installed in special Opto-Acoustic Modules.

The acoustic beacons will be installed during the deployment of the detector. Their absolute positions and relative distances will be determined, acoustically, during the detector deployment operations using a ROV (remotely operated vehicle) equipped with a USBL (ultrashort baseline) positioning system [VIO12].

The hydrophone positions will be calculated by accurate TDoA (Time Difference of Arrival) measurement between beacon signal emission (start-time) and hydrophone signal reception (stop-time) with an expected accuracy better than 10 cm [SIM11].

Additionally, there will be in the anchor of the tower the prototype of a transceiver, acting as emitter, consisting of a free flooded ring (FFR) transducer and the associated electronics, the Sound Emission Board (SEB). This prototype will be fully explained in the next chapters.

Naturally, the NEMO Phase II tower will be equipped as well with data acquisition and transmission electronics, power supply and electro-optical cabling and environmental probes (2 CTDs, Conductivity-Depth-Temperature, 1 current meter, 1 light transmission meter).

Contrarily to previous acoustic positioning systems developed, for NEMO Phase I [AMO09] or ANTARES [ARD09] detectors, in NEMO Phase II the sensors' data acquisition system is fully integrated with the detector data transport system and is based on the "all data to shore" philosophy. Furthermore the structure design permits assembly and deployment in a compact configuration, and unfurling on the sea bottom under the pull provided by the buoy. In Figure 2.7 the mechanical scheme of the NEMO tower and a view of the NEMO Phase-2 site are shown. Differently from the one-dimensional strings of OMs (e.g., ANTARES [ANTAw]), the tower allows for

disentangling the reconstruction of the muon azimuthal direction even with data from only one single structure [SIM11].

NEMO Phase II will be a step towards the KM3NeT neutrino telescope in general, and with respect of the acoustic system in particular. In the next section, the KM3NeT case is introduced.
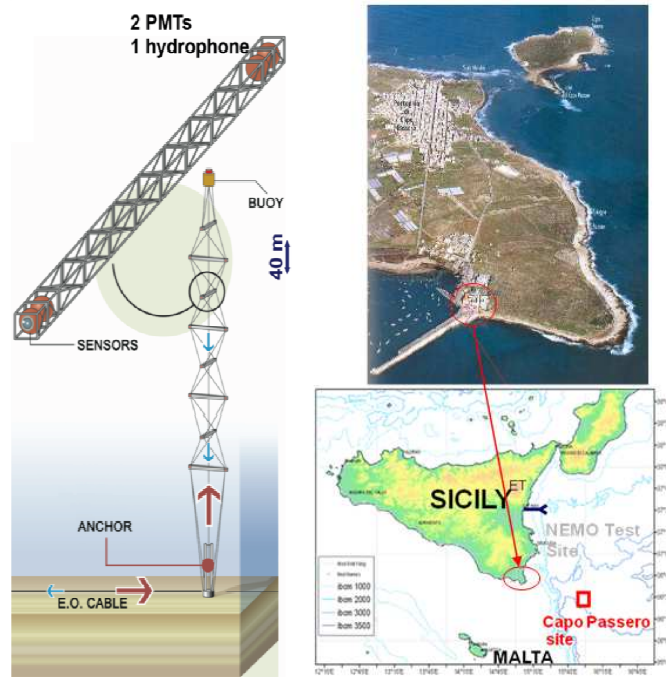

Figure 2.7: Mechanical scheme of the NEMO tower: the tower is anchored on the sea bed and consists of rigid arms connected to each other by ropes and kept vertical by a buoy (left). View of the site of the NEMO Phase-2 neutrino telescope (right).

2.4 KM3NeT detector and the proposed Acoustic Positioning System

KM3NeT is the acronym for km^3 Neutrino Telescope, a project aiming to build a deep-sea research infrastructure in the Mediterranean Sea hosting a km^3-scale neutrino telescope and dedicated instruments for long-term and continuous measurements in Earth and Sea sciences. The project is pursued by a Consortium of institutes from 10 European countries and builds upon the experience acquired with the ANTARES [ANTAw], NESTOR [NESTw] and NEMO [NEMOw] pilot projects. The first phase of the KM3NeT project has been the Design Study, funded by the 6th EU Framework Program for the period February 2006–October 2009.

This project has given rise to the publication, in April 2008, of the Conceptual Design Report (CDR) [CDR08] and has been concluded with issuing the Technical Design

Report (TDR) [TDR11], in March 2011. These two documents (CDR and TDR) describe the scientific objectives, and the concepts behind the design, construction, and operation of the KM3NeT Research Infrastructure and the technological solutions for the construction of a km^3 neutrino telescope in the Mediterranean Sea.

The next step has been the Preparatory Phase (March 2008–February 2012), funded by the EU 7th Framework Program. The primary objective of the KM3NeT Preparatory Phase has been to pave the path to political and scientific convergence on the legal, governance, financial engineering and siting aspects of the infrastructure and to prepare rapid and efficient construction. The current phase is of prototyping and construction called Pre-Production Model (PPM). In Figure 2.8 the projected KM3NeT time lines towards construction and operation is shown [KAT11].
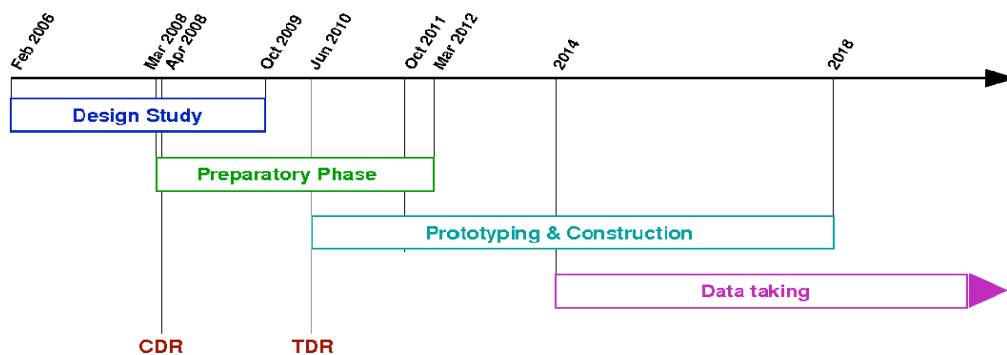
Figure 2.8: Time line of the KM3Net project development towards construction and operation [KAT11].

According to [TDR11] the neutrino telescope will consist of a three-dimensional array of optical sensors supported by 320 vertical structures named detection unit (DU) anchored on the seafloor and connected to shore through an electro-optical submarine cable network for transferring electrical power, control and data transmission. Sea bottom connections between the detection units and the cable network are carried out through the use of deep-sea remotely operated vehicles (ROVs). Each DU will consist of 20 horizontal bars (storeys) of 6 m length, with a vertical separation of 40 m between storeys. They will be located at a distance of 180 m from each other. Two DOMs (digital optical modules) are mounted in each storey. Each DOM will consist of 31 3-inch photomultipliers housed on a 17" glass sphere which also hosts read-out and data transmission electronics [KAL11].

Simulation studies have demonstrated the convenience of having a horizontal distance of a few meters between DOMs in local storeys in order to increase the reconstruction quality of muon tracks and thus the sensitivity of the telescope. Simulations also show that arranging photomultipliers in local clusters, as done in the DOMs is optimal to obtain the large photocathode area required to obtain the planned sensitivity in a cost-effective way. Moreover, optimization based on cost, physics sensitivity and reliability has led to the consideration of modular mechanical structures that facilitate production, transport and deployment procedures. For deployment it is planned to transport detection units in a compact package which is easy to handle and which will allow the detection unit to unfurl once it is placed on the seafloor [TDR11]. In Figure 2.9 and 2.10 a scheme of the KM3NeT detector, DOM, DU structure and Storey with buoyancy NEMO Deployment method are shown, respectively.
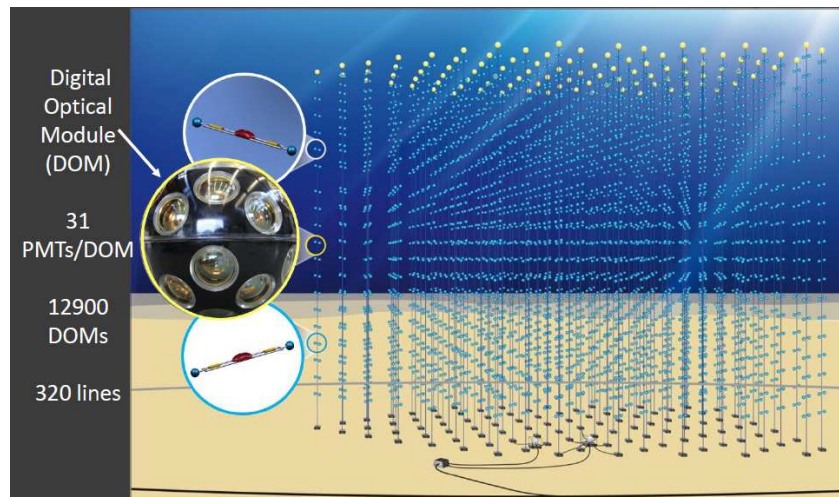
Figure 2.9: Scheme of the KM3NeT detector and the DOM.
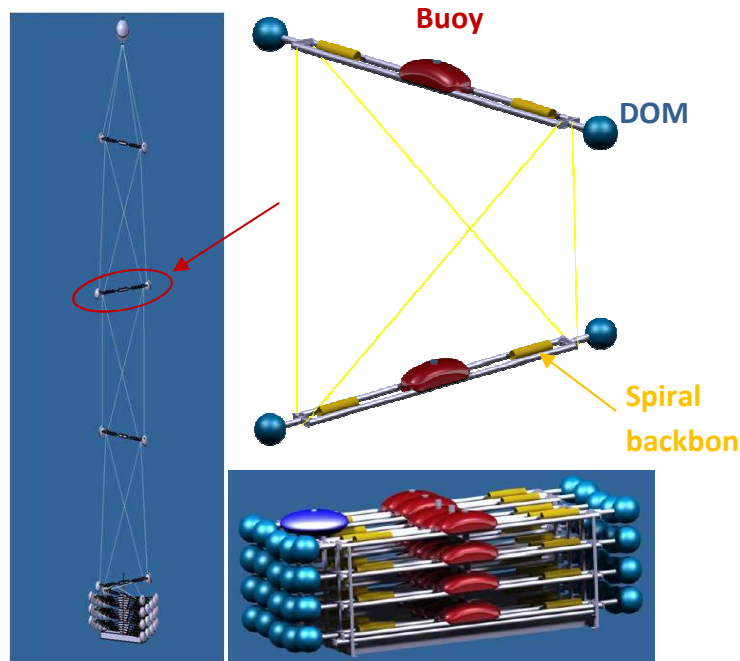
Figure 2.10: Scheme of the DU structure based on NEMO Deployment method. The DUs are in a compact package and will allow the detection unit to unfurl once it is placed on the seafloor.

The overall power consumption of the telescope will be approximately 125 kW and the expected data rate will be roughly 25GBytes/s. This large data stream to shore is carried on a point-to-point fibre optic network (using current telecom DWDM (dense wavelength division multiplexed) technology) which transfers all the optical module data to the shore. A shore station will house the power supplies, the lasers that will drive the fibre optic network, and will also host the data acquisition system that will implement data filtering, recording and distribution. Since event reconstruction is based on the PMT hit time, a common timing reference must be available to front end boards, to allow for detector wide synchronization. In order to facilitate the clock distribution a synchronous protocol will be used: the clock information is embedded in the slow control data by an on-shore transmitter in a unique bit stream. The receiver, at the storey, is able to recover the clock information and to extract the data. In this way, all the receivers will be synchronized by design to the on-shore time reference, which is derived from a GPS station [TDR11].

As already mentioned, another key element in the detector is the positioning system that must supply information for both the installation and operation phases of the detector. During the deployment of the detector, the positioning system must provide the position of the telescope's mechanical structures, in a geo-referenced coordinate system, with

accuracy of the order of a few metres. This is important both for the safe deployment of the mechanical structures and for the determination of the absolute position and pointing direction of the telescope. During the operation phase, the positioning system must give the positions of the optical modules with the necessary accuracy for the muon tracking. For this requirement the DOMs must be monitored every ~30 s, in a local reference system, with an accuracy of better than 20 cm in order to correct for the motion of the detection units due to the sea currents. The positioning system consists of four elements: acoustic transceivers, anchored on the seabed in known positions constituting the Long Base-Line (LBL); acoustic receivers (hydrophones) rigidly connected to the telescope's mechanical structures holding the DOMs; devices (compasses-tiltmeters) to measure the orientation of each storey; computers on-shore for data analysis. The reconstruction of the shape of the DU is extracted by the mechanical models which predict the behavior of the DU due to the sea current velocity and considering the mechanical parameters of the DU. The input for this reconstruction is given by the orientations measured by the compass-tiltmeter system and the positions of hydrophones given by the APS. This is done by measuring the acoustic travel time between the transceiver signal emission and the reception in the hydrophones of the DUs. For each receiver, having a set of at least three acoustic travel times of different transceivers, the positions of the hydrophone are determined by triangulation with respect to the long base-line system [TDR11]. The scheme of the acoustic positioning system is shown in Figure 2.11. The emission frequency range of the transceivers will be between 25-45 kHz. Hydrophones will be sampled continuously at a rate of about 200 kHz, with at least 16 bits resolution, and the continuous stream of data will be sent to shore.
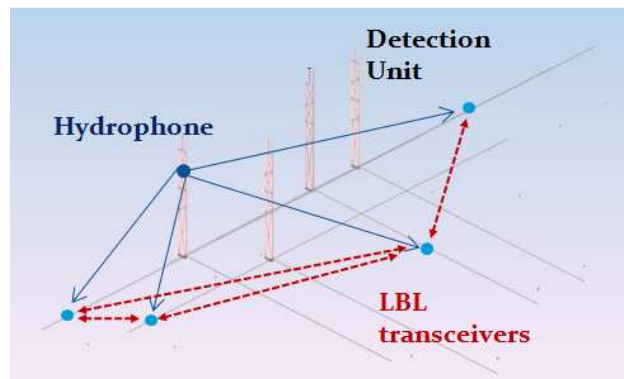
Figure 2.11: Scheme of the acoustic positioning system. The LBL is a geo-referenced system to identify the positions of acoustic receivers on the DU. The system is based on measurements of acoustic time of flight between transceivers and hydrophones.

The KM3NeT positioning system design is based on the experience of the systems developed for ANTARES and NEMO, but with a better accuracy in the time synchronization between transceivers and receivers and the implementation of all data to shore approach, that is all acquired data will be sent to shore for next analysis. It is fully integrated with the detector electronics. The components are commercially available and have been tested to 3500 m depth by the pilot projects [TDR11]. Test on the transceivers and hydrophones are currently conducted. The transceiver in use are the free flooded ring ceramic transducer (FFR) model SX30 from Sensortech Ltd, Canada connected to a *Sound Emission Board* used when it acts as a beacon. They permit to obtain both optimal transmission and reception voltage response to build efficient LBL transceivers [LAR12] and will be described in detail in the next chapters. Acoustic receivers will be installed on each storey of the DU, as mentioned above, and promising options are the use of the SMID hydrophones, the FFR transducers acting as receivers and/or a piezoelectric sensor directly glued inside the glass sphere of the DOM. These different options will be investigated on the KM3NeT Pre-Production Model test.

Both the acoustic receivers of the DUs and the LBL transceivers are synchronous and phased with respect to the master clock time signal transmitted from shore. This set-up allows also for the use of acoustic data for studies of acoustic neutrino detection and searches for acoustic and optical coincidences. It will also allow for monitoring of the environment around the detector and studies of Earth and Sea Science: biology, geophysics and oceanography.

The absolute azimuth measurement of the LBL system is made by a surface boat equipped with an acoustic emitter, with a position known from differential GPS, moving around the detector while periodically its distance to each of the long-base-line transceivers is measured. The geodetic positions of these transceivers are then determined with an accuracy of ~1 m radius by triangulation and minimisation method [TDR11].

Chapter 3

3.1 Transceiver for the KM3NeT Acoustic Positioning System

The Acoustic Positioning System (APS) for the future KM3NeT neutrino telescope, as described in chapter 2, consists of a series of acoustic transceivers distributed on the sea floor at known positions (constituting the Long Base Line system) and acoustic receivers rigidly connected to the detection unit holding the optical modules. The transceivers that are being evaluated for the final implementation of this facility are composed of a transducer and an electronic board named S*ound Emission Board (SEB)* to manage it. Moreover, these transceivers have been integrated in the ANTARES and NEMO detector to be tested in situ. In the next section these two components of the system and the performed tests on them will be presented. The integration in ANTARES and NEMO detector will be described in chapter 4.

3.1.1 The Acoustic Sensors

The acoustic sensors have been selected to attend to the specifications required for the KM3NeT positioning which are: withstand high pressure, a good receiving sensitivity and transmitting power capability, nearly omnidirectional, low electronic noise, a high reliability, and also affordable for the units needed in a cubic kilometer. Among different options we have selected the Free Flooded Ring (FFR) transducers SX30 model (FFR-SX30) manufactured by Sensor Technology Ltd, Canada [SENSw]. FFR transducers have ring geometrical form and therefore maintain the same hydrostatic pressure inside and outside of the ring. This characteristic shape reduces the change of the properties of piezoelectric ceramic under high hydrostatic pressure. For this reasons they are a good solution to the deep submergence problem [SHE07]. FFR-SX30s are efficient transducers that provide reasonable power levels over a wide range of frequencies, and deep ocean capability. They work in the 20–40 kHz frequency range and have dimensions of a 4.4 cm outer diameter, a 2 cm inner diameter and a 2.5 cm height.

They can be operated in the deep sea and have a transmitting and receiving voltage response at 30 kHz of 133 dB re 1µPa/V at 1m and -193 dB re 1V/µPa, respectively. The maximum input power is 300 W with 2% duty cycle (with signals of a few ms). These transducers are simple radiators and have an omnidirectional directivity pattern in the plan perpendicular to the axis of the ring (xy-plane), whilst the aperture angle in the other planes depends on the length of the cylinder (xz-plane), and is 60º for the SX30 model [SENSw]. Table 3.1 summarizes the main characteristics of the FFR-SX30 transducers. The directivity pattern and the curves of the sensitivity measured by the manufacturer are shown in Figures 3.1 and 3.2, respectively.

Resonance Frequency	30 kHz
Transmit Voltage Response, TVR	133 dB re µPa/V @ 1m
Receive Voltage Response, RVR	-193 dB re V/µPa
Useable Frequency range	20 kHz – 40 kHz
Beam pattern	Radial: Omni Axial: Toroidal (60°)
Efficiency	50%
Input Power	300 W (2% duty cycle)
Operating Depth (Meters)	Unlimited
Cable	1N2
Weight in grams (with cable)	112
Dimension	4.4 cm outer diameter, 2 cm inner diameter 2.5 cm height

Table 3.1: Characteristics of the SX30 FFR transducers [SENSw].
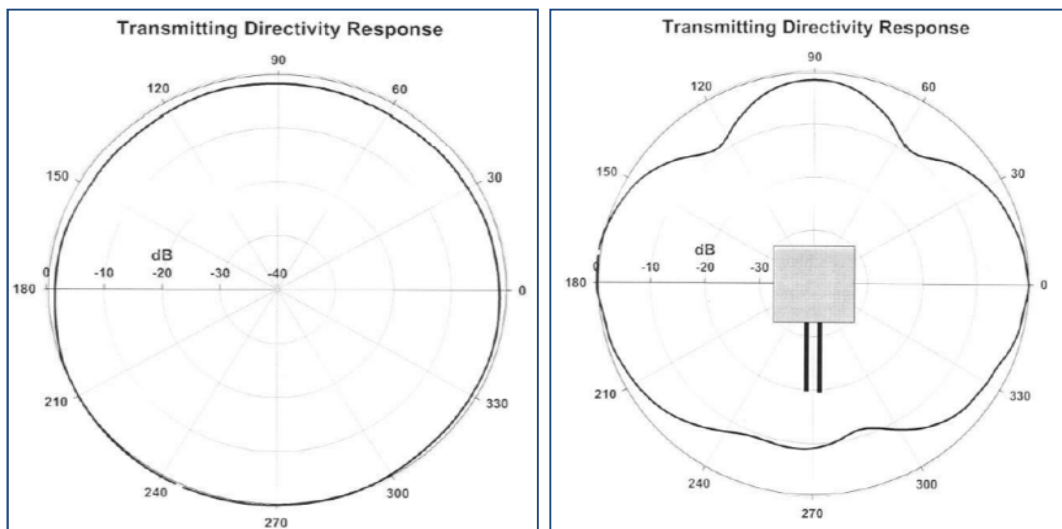
Figure 3.1: Directivity Pattern in the plane perpendicular to the axis of the ring (plane XY) (left) and the aperture angle in the other plane depends on the length of the cylinder (plane XZ) (right) measured at a depth of 0.6 meters and a temperature of 20ºC [SENSw].
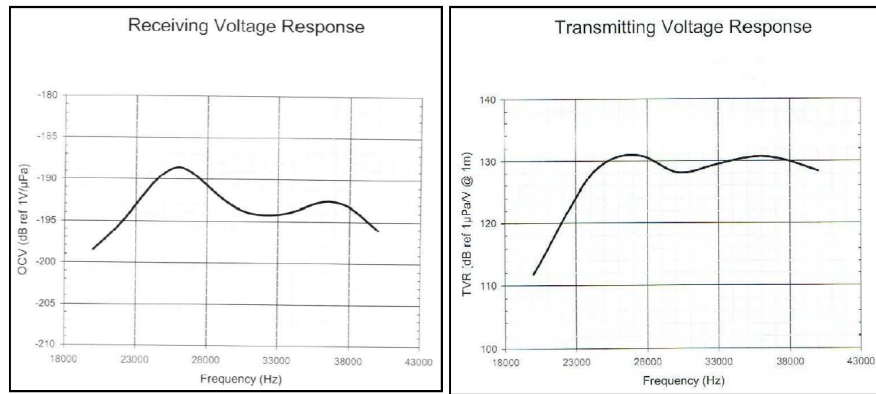
Figure 3.2: Receiving Voltage Response (left) and Transmitting Voltage Response (right) of the FFR-SX30 transducer measured at a depth 0.6 meters and a temperature of 20ºC [SENSw].

The cable on the free-flooded rings is a 20 AWG, which is TPE (Thermoplastic elastomer) insulated. The cable is affixed directly to the ceramic crystal. The whole assembly is then directly coated with epoxy resin. Both the epoxy resin and the cable are resistant to the salt water, oils, mild acids and bases. But the cables are not totally water blocking (fluid penetration into the cable may cause irreversible damage to the transducer). For this reason and following KM3NeT technology standards, the FFR-SX30 transducer have been over-moulded with polyurethane material to block water and to facilitate its fixing and integration on mechanical structures. The moulding of the transducer has been made by McArtney-EurOceanique SAS [McArw]. Moreover, to facilitate the connection of the cable for deep-sea a10 meter cable type 4021 with one connector type OM2M with locking sleeves type DLSA-M/Fhas been assembled. The connector body is of neoprene material and the locking sleeve is of plastic material. Figure 3.3 shows the pictures of the FFR-SX30 transducer with and without over-molding.

Figure 3.3: View of the Free Flooded Ring transducer with (right) and without (left) over-moulding.

3.1.2 The Sound Emission Board

Dedicated electronics, named Sound Emission Board (SEB) [LLO12], have been developed in order to enable communication and configuration of the transceiver, and furthermore, to control the emission and reception. The solution adopted is specially adapted to the FFR-SX30 transducers. With respect to the emission, it is able to store the needed energy in order to have enough acoustic power and to set the signals for positioning and amplify them, so being able to feed the transducer with high amplitude of short signals (a few ms) with arbitrary waveform that can be detected from acoustic receivers at 1-1.5 km distance from the emitter. Moreover, it is also able to switch between emission and reception modes. The board prototype diagram is shown in Figure 3.4. It consists of three parts: the communication and control which contains the micro-controller dsPIC (blue part) [MICRw], the emission part constituted by the digital amplification plus the transducer impedance matching (red part), and the reception part (green part). In the reception part a relay controlled by the dsPIC switches the mode and drives the signal from the transducer to the receiving board of the positioning system.
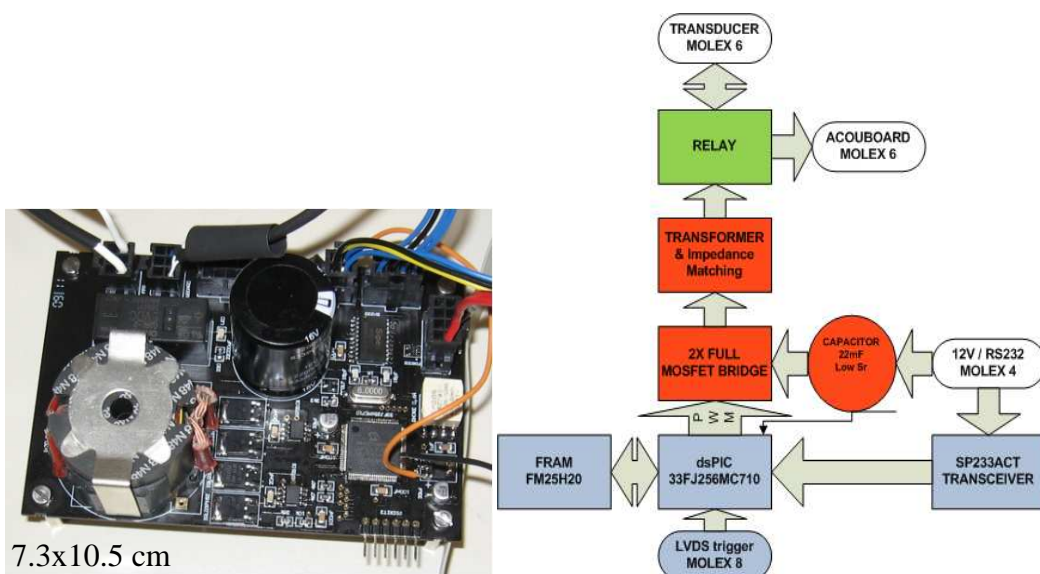
Figure 3.4: View and diagram of the Sound Emission Board.

The SEB has been designed for low-power consumption and it is adapted to the neutrino telescope infrastructure using power supplies of 12 V (control part) and 5 V (power part) with a consumption of 1 mA and 100 mA respectively, furnished by the power lines of the neutrino telescope infrastructure. To avoid initial high currents when

the capacitor starts to charge, there is a current limit of 15 mA. Few seconds later the current stabilizes at 1 mA. As the instantaneous power available through the telescope 12 V DC distribution system is less than that needed to excite the transducer to cover long distances, it has been necessary to implement an energy storage block. For this reason, a capacitor of 22 mF @ 16 V from Panasonic with a very low equivalent series resistance has been selected. It is able to charge and store the energy needed for the emission. This solution allows for fast charging, and correspondingly short time delays between successive emissions (the usual mode of operation is a high-power emission of a few ms duration every few seconds). The charge of this capacitor is monitored using the input of the ADC of the micro-controller. Moreover, the output of the micro-controller is connected through 2x Full MOSFET Driver and a MOSFET full bridge constituting the power amplifier. The main characteristics for the MOSFETs are the low R_{on} (transistor ON resistance) of 11 mΩ, the fast switching (13 ns rise and 4.7 ns fall) and low gate charge (QG =7.2 nC). Other important characteristics are the high drain current (Id = 200 A, 0.1 ms signal) and the maximum drain to source voltage (20 V). The latter is successively connected to the transformer with a frequency and duty cycle programmed through the micro-controller which also plays the main role of impedance matching for the transducer. The transformer is able to increase the voltage of the input signal to an output signal from ~35 V_{pp} to ~400 V_{pp} depending on the input values.

Besides, concerning the reception part of the board, it also has the possibility to directly apply an anti-aliasing filter and return the signal to an ADC of the microcontroller. This functionality may be very interesting not only in the context of neutrino telescopes, but also to have the receiver implemented in different underwater applications, such as affordable sonar systems or echo-sounds.

The micro-controller drives the power amplifier and has two inputs, one for the low bitrate communication port and one for the trigger signal. Moreover, it contains the program for the emission of the signals. The signal modulation is done with Pulse-Width Modulation (PWM) technique which permits the emission of arbitrary intense short signals [BAR01]. The PWM carry frequency of the emission signal is 400 kHz and has been tested up to 1.25MHz. The basic idea of this technique is to modulate the signal digitally at a higher frequency using different width of pulses and the lower frequency signal is recovered using a low-pass filter (it will be described in the next section). In addition, it will have an increase in the amplitude of the signal using a full

H-Bridge. The communication of the board with the control PC for its configuration is established through the standard RS232 protocol using an SP233 adapter in the board. In order to provide a very good timing synchronization the emission is triggered using a LVDS signal. The delay between the arrived trigger and the emission time depends slightly on the emitted signals, but the differences between the different signals are small, about 100 ns.

In summary, the board, designed for an easy integration into a neutrino telescope infrastructures, can be configured from shore and can emit arbitrary intense short signals, or act as receiver with very good timing precision (the measured latency is 7 µs with a stability better than 1 µs), as shown in the KM3NeT APS joint tests [SIM12].

3.1.2.1   Microcontroller and Signal generator block

A microcontroller is composed of a single integrated circuit containing a processor core, memory, and programmable input/output peripherals. For the signal generator the Microchip "Motor Control" function inside most of the dsPic microcontroller series has been chosen. PIC is a family of modified microcontrollers and is used in industrial developers and hobbyists due to their low cost and wide availability. The dsPic selected is the dsPic33FJ256MC710 at 16 bit [MICRw]. This microcontroller has 40 MIPS of processing power for signal processing specific instructions, enough FLASH and RAM memories for our purposes and a 10 bits @1MSps ADC converter. The "Motor Control" function is basically a digital counter that works with the main frequency of the microcontroller (40 MHz). This device has all the necessary components to work with full MOSFET bridges (symmetric outputs, dead time generators, etc.), and for this reason matches perfectly for our purposes. Having chosen the full bridge power amplifier, it must be fed with square signals. This is not a problem if we want to send square signals like a MLS (Maximum Length Sequence) signal, which is a very useful signal extensively used in electro-acoustic measurements. The main characteristics of this signal are the flat spectrum and the non-correlation with any other signal. It can be used to obtain the impulse response of the entire system and for time of flight measurements. Moreover, if we wish to send standard sinusoidal or arbitrary signals we can take advantage of the fact that the transducer and the transformer are good band pass filters in our band of interest: we can emit a square signal in the band and all the

highest frequencies that are out of the working band will be removed. Therefore, we can also use square signals and obtain sinusoidal signals in the emission, although the best technique—should we wish to send arbitrary signals by generating squared signals—is using PWM (Pulse Width Modulation) with a modulation frequency outside the main band. To implement PWM we must vary the width of the square signal in direct relation to the voltage of the desired signal (0–100% Pulse width). The classic way to do this is to compare the desired signal with a triangular or saw tooth signal in order to obtain a square signal at the output of the comparator. After the amplification, the desired signal is integrated (filtered by the transformer and the transducer) and the median value of the square signal is obtained. This median value is the desired signal. In particular, in order to generate the signal two of the function modes of the motor control are used. The first is the "free run" mode; in this mode we can obtain a pulse with modulation similar to the classic one that compares the modulation signal with a saw tooth. Using this mode when the counter arrives to the PxTPER[1] (maximum) value it is reset and starts again from zero. The device has also other comparators in order to establish the width of the pulse. The second mode is the "up/down" mode. The only difference between this and the previous mode is that when the counter arrives to PxTPER it starts counting down instead of resetting. This mode is similar to the classic PWM modulation that compares the signal with a triangular wave. With this mode we obtain a more symmetric square signal with fewer harmonics [LLO12].

3.1.2.2 The firmware

Different firmware versions have been developed in order to adapt the SEB to the communication prerequisites of the different test installations at the ANTARES and NEMO neutrino telescope sites (in ANTARES: with MODBUS[2] over RS485; in NEMO: console over RS232). In Figure 3.5 the basic working process is described. The basic firmware has three main parts. The first is the processing of commands that arrive at the low bitrate communication port: these commands usually are used to configure the board or define the signal to be emitted. The second block is in the main part of the program and is aware of the trigger port in order to start the emission when a trigger

---

[1] PxTPER is the PWM time base period register. It sets the maximum value of the counter.
[2] MODBUS is a communication protocol used in industrial environments.

signal arrives. The third block is an interrupt code that works when the "Motor Control" counter arrives to the PxTPER register. This code changes the registers of the "Motor Control" device in order to obtain the next cycle of the desired square signal (frequency, pulse width, etc.) [LLO12].
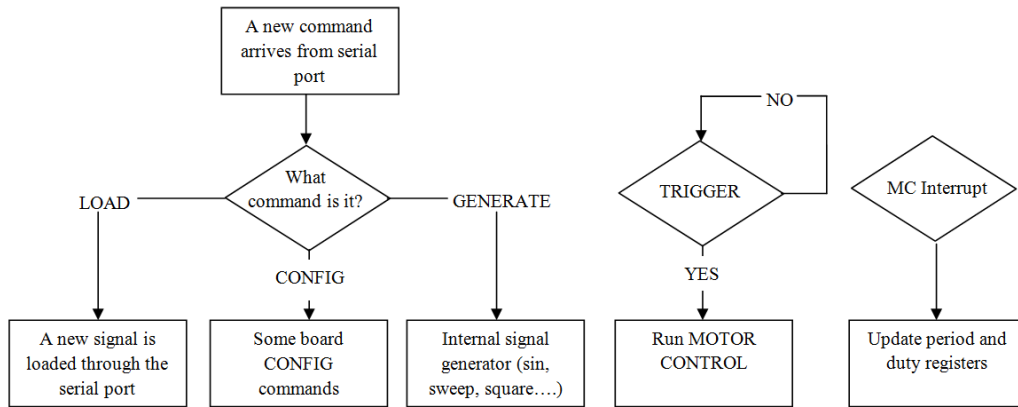
Figure 3.5: Diagram of the firmware working process.

3.2 Sensitivity tests of the FFR-SX30

With the objective to study the possibility of using the FFR transducers as emitters and receiver in the APS of KM3NeT neutrino telescope several studies have been done.

The first tests were done in the laboratory of Gandia in order to characterize the transducers in terms of the transmitting and receiving voltage responses (TVR, RVR) as a function of the frequency and as a function of the angle (directivity pattern). The tests have been performed in a fresh-water tank with dimension of 87.5 x 113 x 56.5 cm^3. For the tests omnidirectional calibrated transducers, model ITC-1042 [ITCw] (with transmitting voltage response 148 dB ref. 1µPa/V @ 1 m) and RESON-TC4014 [RESOw] (with receiving voltage response -186 dB ± 3 dB re 1V/µPa) have been used as reference emitter and receiver, respectively. The FFR-SX30 transducers were used as emitters and receivers in order to calculate their TVR and RVR, respectively. Figure 3.6 shows the used position for the study of the sensitivity of the FFR-SX30 transducers which will be named position 1 and 2. In the position 1 the sensitivity is omnidirectional for the horizontal plane, whereas in the position 2 the sensitivity changes as function of the angle. The FFR-SX30 transducer was placed at 10 cm from the reference transducers with the aim to study their sensitivity as a function of the frequency and as a function angle (directivity pattern) in the position 1 and position 2 (Fig.3.7-3.8).

Besides, different tone bursts signals with 5 Vp and 10 Vp of amplitude and 5 cycle length in the frequency range 18-42 kHz were generated through a NI PCI-5412 board [NATIw] controlled with a control PC. A LabVIEW program was used for the emission, reception and recording of the data. The received signals were amplified from a RESON CCA100 (1nF = Input Capacitance, 10kΩ = Input Resistance, X dB = output gain used) and RESON EC6073 preamplifier for the FFR-SX30 and Reson-TC4014 receiver hydrophones respectively. A positioning motor made by ISEL automation and PI micos, Germany [ISELw, MICOw], have been used to position the hydrophone in the tank. It is able to move in the three dimension x, y and z and has an accuracy of 0.01mm. The signal length was chosen according to the dimensions of the tank to avoid the interference of the reflected signals from the walls and water surface with the direct signal.
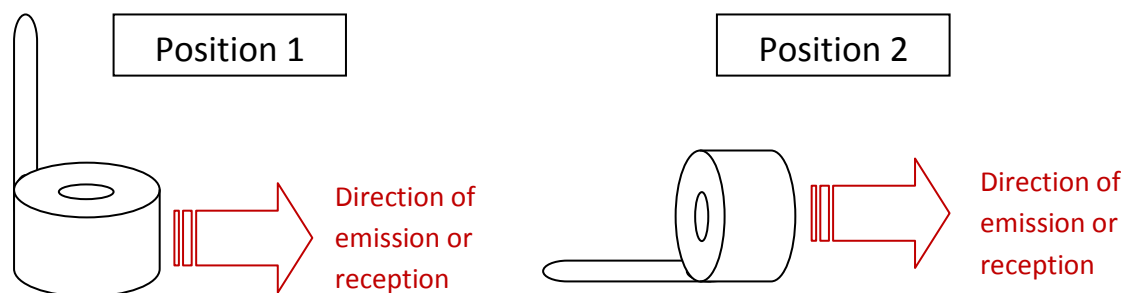
Figure 3.6: Scheme of the used position (orientation) for the measurements of sensitivity for the FFR-SX30 transducers.
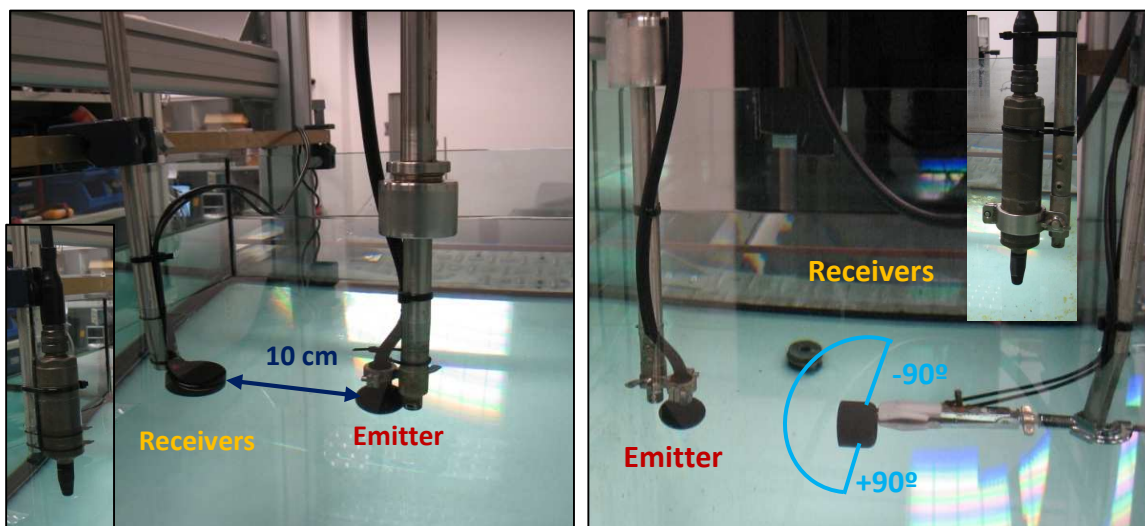
Figure 3.7: Configuration used to calculate RVR of the FFR-SX30 as a function of the frequency and as a function of the angle (directivity pattern) in position 1 (left) and position 2 (right).
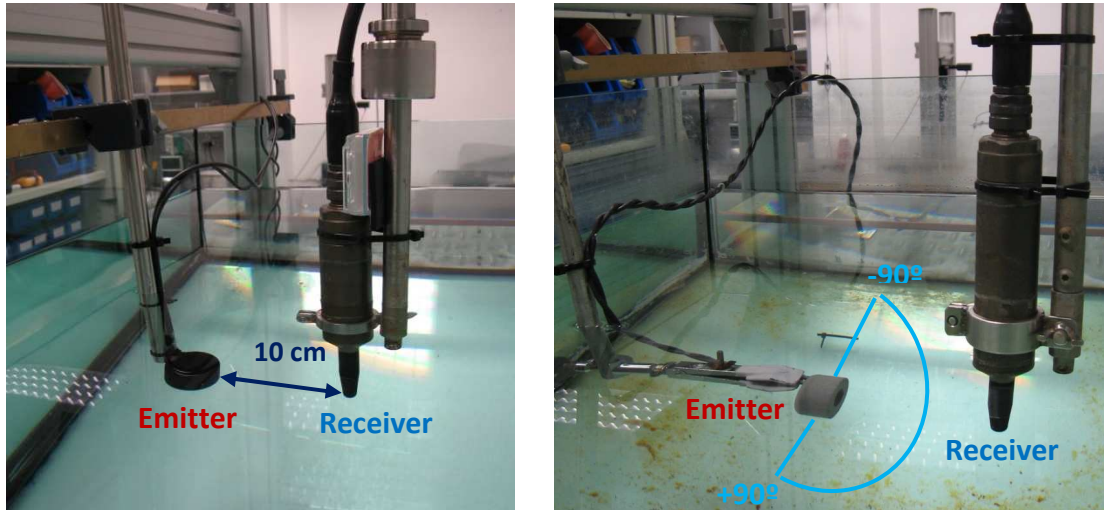
Figure 3.8: Configuration used to calculate TVR of the FFR-SX30 as a function of the frequency and as a function of the angle (directivity pattern) in the position 1 (left) and position 2 (right).

Furthermore measurements in the anechoic chamber of the Campus de Gandia were done in order to acquire the electronic noise of the FFR-SX30 hydrophones as receivers. Figure 3.9 shows the power spectrum density of some FFR hydrophones. The level of the noise is below -120 dB re V^2/Hz (~ ≤Sea State[3] 1, that is of the sea ambient noise in the state 1).
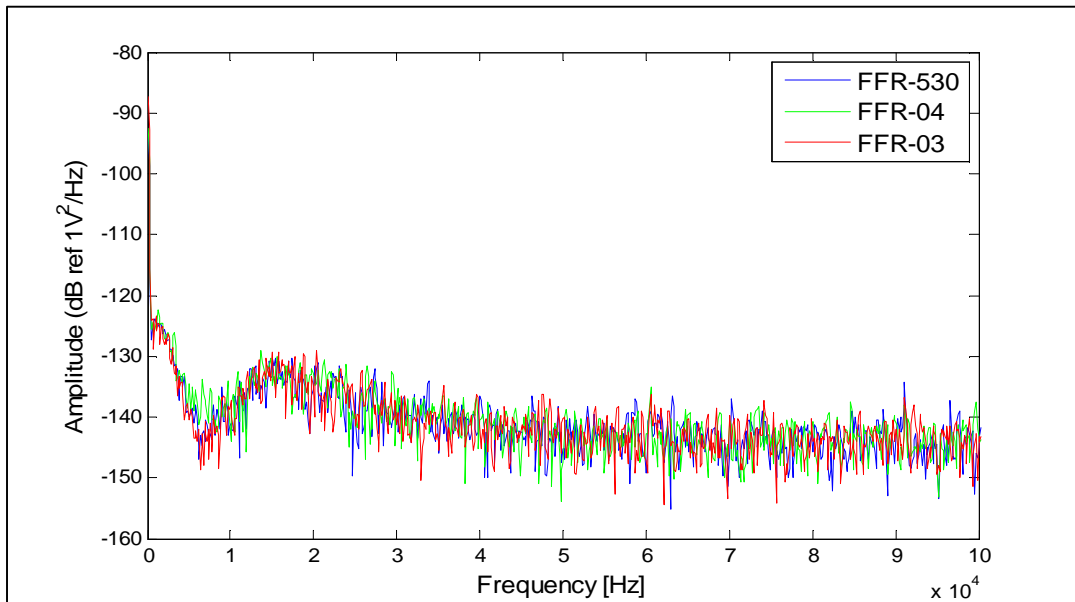
Figure 3.9: Power density spectrum of some FFR-SX30 hydrophone. The level noise is below - 120 dB re V^2/Hz (~ ≤Sea State 1).

---

[3] The Sea State is the general condition of the free surface on a large body of water and depends of wind speed and wave height. Sea Sate 0 is the calm sea.

The equation used to calculate the receiving voltage response is:

$$S_{FFR}(dB) = S_{Reson}(dB) + 20 \cdot log_{10}\left(\frac{V_{FFR}(V)}{V_{Reson}(V)}\right) - X(dB); \quad [dB \ re \ 1V/\mu Pa]$$

(3.1)

where:

$S_{FFR}(dB)$ is the sensitivity in dB of the FFR-SX30 (unknown).

$S_{Reson}(dB)$ is the sensitivity in dB of the calibrated Reson hydrophone (known) .

$V_{FFR}(V)$ is the amplitude of the signal in V received by FFR-SX30 hydrophone.

$V_{Reson}(V)$ is the amplitude of the signal in V received by calibrated Reson hydrophone.

$X(dB)$ are the different gains selected in the preamplifier connected to the FFR-SX30 receiver hydrophones.

The equation used to calculate   the Transmitting Voltage Response of the FFR hydrophones is the following:

$$T_R(dB) = 20 \cdot log_{10}\left(\frac{P(Pa @ 1m) \cdot 10^6 \cdot \mu Pa/Pa}{V_{in}(V)}\right); \quad [dB \ re \ 1\mu Pa/V]$$

(3.2)

where:

$T_R(dB)$ is the Transmitting Voltage Response in dB of the transducer (unknown).

$V_{in}(V)$ is the value of the amplitude of the emitted signal by the FFR-SX30 transducer.

$P(Pa @ 1m)$ is the pressure measured at the distance of 1 m by the emitter transducer. It is calculated by the following equation:

$$P(Pa @ 1m) = \frac{V_{receiver}(V)}{S_{linear}(V/Pa)} \frac{d(m)}{1 \ m} \ [Pa]$$

where $V_{receiver}(V)$ is the value of the amplitude of the received signal in V by the calibrated Reson TC4014 hydrophone when the FFR-SX30 transducer emits, $S_{linear}(V/$

Pa) is the value of the Received Sensitivity in *V/Pa* of the calibrated Reson-TC4014 hydrophone, which is known, and $d(m)$ is the distance between transducers in m.

In order to determine the voltage amplitude of the emitted and received signals recorded an algorithm in MATLAB software has been implemented. It finds all the maximum values of each signal recorded collecting them in histograms and calculates the mean value (of the histograms) through fitting the data to a Gaussian distribution. This method has been compared with other possible procedures, such as using the Hilbert function to obtain the envelope of the signal and averaging the value in the stable region. Similar results have been obtained for both methods. Once the voltage amplitude of the emitted and received signals have been obtained, the Receiving Voltage Response and Transmitting Voltage Response of the different FFR-SX30 hydrophones have been calculated (in this case, for twelve FFR-SX30 transducers). The uncertainties on the measurements are about 2 dB.

Figure 3.10 shows the calculated sensitivity of reception and emission (Receiving Voltage Response and Transmitting Voltage Response) for the four [4] FFR-SX30 transducers, with serial numbers 788, 530, 566 and 774, as function of the frequency in the position 1 (the lines connecting the measured values are only to guide the eye). Figures 3.11- 3.15 show the calculated sensitivity of reception and emission (Receiving Voltage Response and Transmitting Voltage Response) for the remaining[5] FFR-SX30 transducers with serial number from 01 to 08 as function of the frequency and of the angle in the position 1 and 2, respectively (the lines are only to guide the eye).
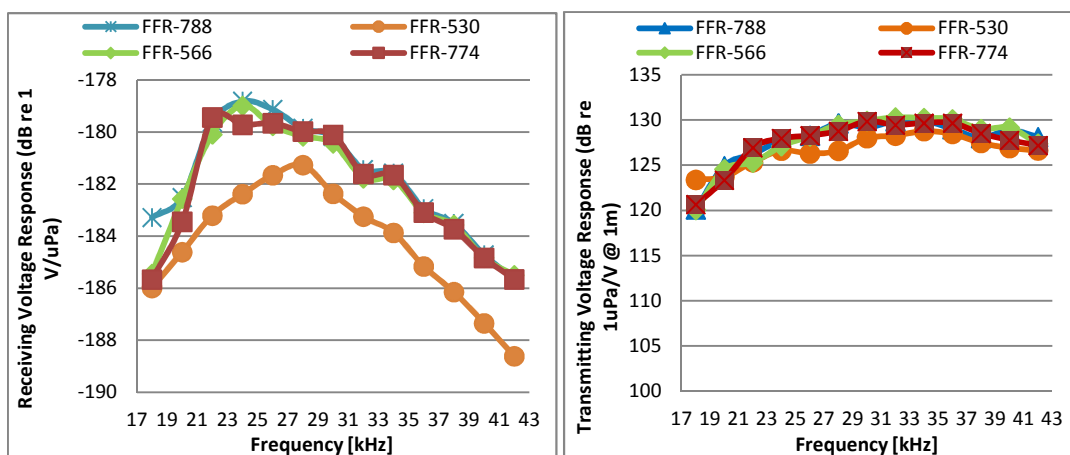
Figure 3.10: Receiving Voltage Response and Transmitting Voltage Response of the FFR-SX30, serial numbers 788, 530, 566 and 774 calculated in the position 1 as a function of the frequency.

---

[4] Transducers bought in 2008.
[5] Transducers were bought in 2010.
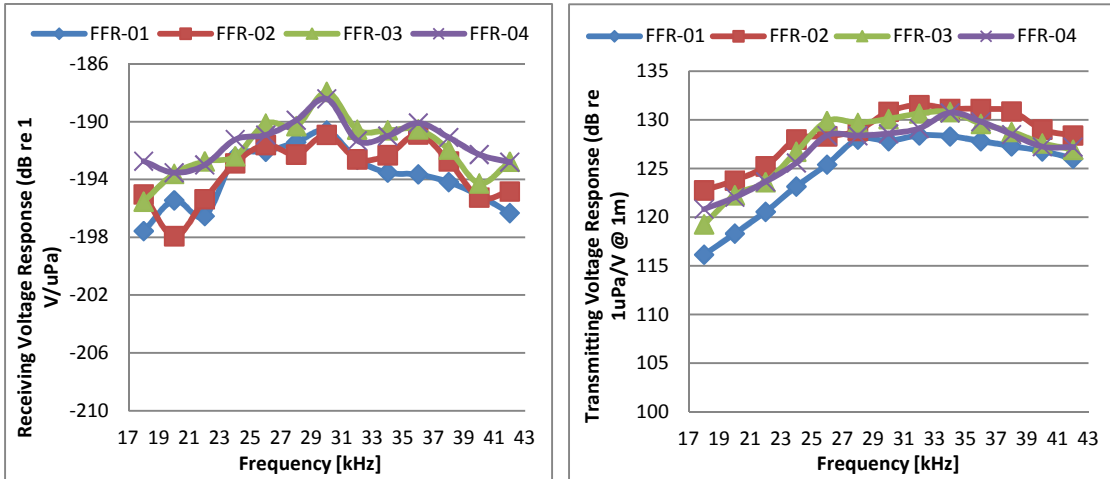
Figure 3.11: Receiving Voltage Response and Transmitting Voltage Response of the FFR-SX30 serial number from 01 to 04 calculated in the position 1 as a function of the frequency.
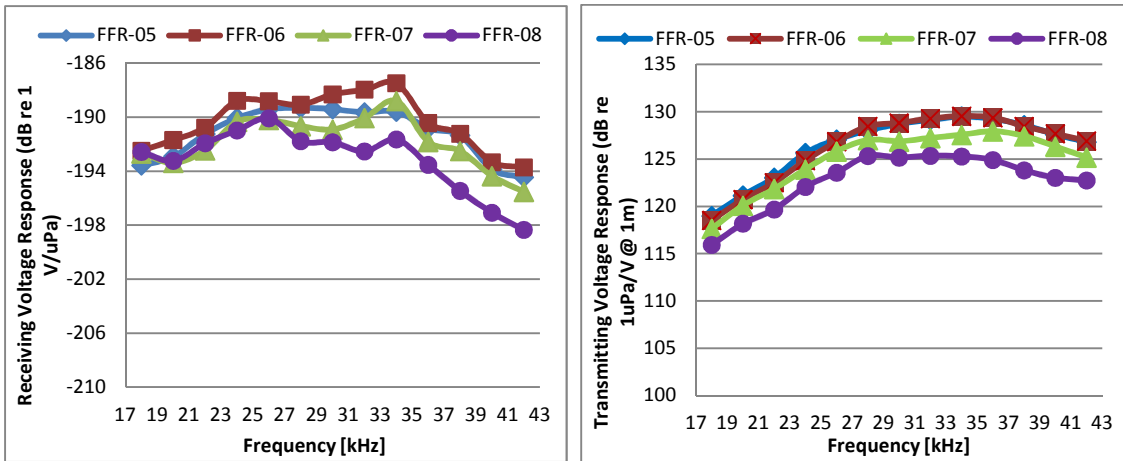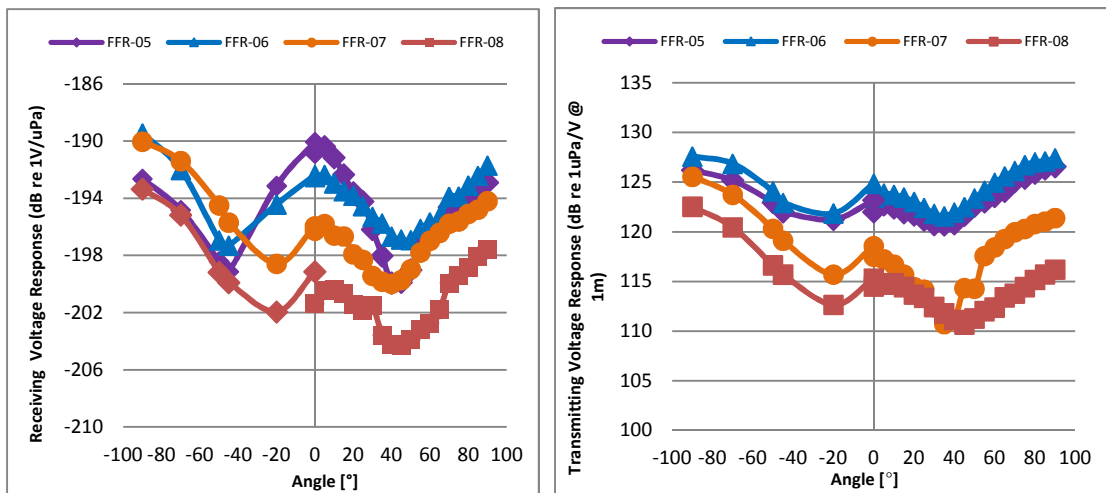

Figure 3.12: Receiving Voltage Response and Transmitting Voltage Response of the FFR-SX30 serial number from 05 to 08 calculated in the position 1 as a function of the frequency.
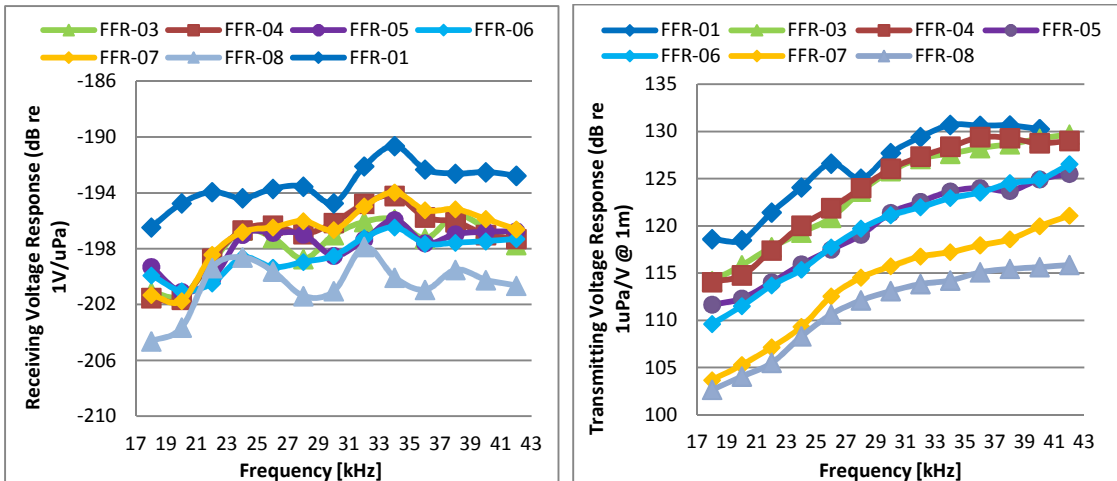
Figure 3.13: Receiving Voltage Response and Transmitting Voltage Response of the FFR-SX30 serial number 01 and from 03 to 08 calculated in the position 2 as a function of the frequency.
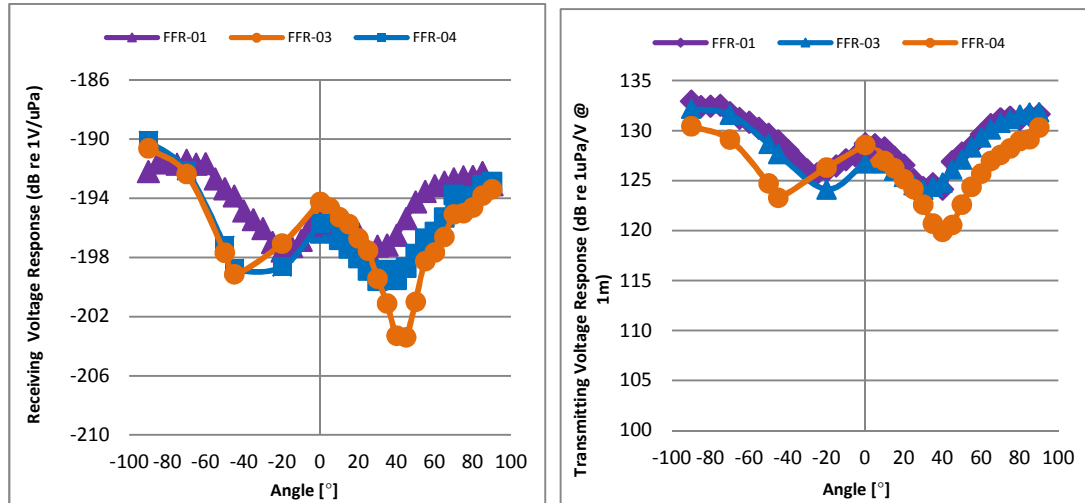
Figure 3.14: Receiving Voltage Response and Transmitting Voltage Response of the FFR-SX30 serial number 01, 03 and 04 calculated in the position 2 as a function of the angle.

Figure 3.15: Receiving Voltage Response and Transmitting Voltage Response of the FFR-SX30 serial number from 05 to 08 calculated in the position 2 as a function of the angle.

Comparing the different figures, we can realise that the transducers, with serial numbers 788, 530, 566 and 774, have a higher sensitivity in reception than the transducers with serial numbers 01-08. This is in agreement with the sensitivity produced on the manufacturer's web page in 2008, which was -183dB re dB re V/µPa. In 2010 the receiving voltage response produced by the manufacturer was changed and it was -193dB re dB re V/µPa.

The results of the measurements to the transducers with serial number from 01 to 08 confirm the values produced by the manufacturer and show that the differences in the 20-40 kHz frequency range are moderate, and they can be handled for the application as transceivers for the KM3NeT APS. Moreover, the Figures 3.14 and 3.15 show the Receiving Voltage Response and Transmitting Voltage Response of the FFR-SX30

64

transducers as a function of the angle using a 30 kHz tone burst signal (measured in the position 2 where 0º corresponds to the direction opposite to the cables). As expected, a minimum of sensitivity appears at about 30º due to the shape of the transducer. These latter variations of sensitivity are about 5 dB (almost 50%) to each one transducer, which is a noticeable value, but, again these variations in sensitivity can be handled without major problems for the use as transceiver for the KM3NeT APS application. In case the FFR-SX30 will be used as receiver hydrophones for the KM3NeT APS, a good parameterisation of the sensitivity as a function of the frequency and angle for each transducer will be needed, especially for the potential use of these hydrophones for deep-sea acoustic monitoring studies or for the acoustic detection of Ultra-High-Energy neutrinos. For this application, it would be good to have precise measurements of the sensitivities at larger distances between both transducers, and some work is going on within the research group in that respect.

3.3 Pressure tests

One of the most important requirements for the KM3NeT detector is the possibility of using the selected transducers under high pressure [ARD10]. For this reason, a measurement campaign using a large hyperbaric tank at *IFREMER* (*Institut Francais de Recherche pour L'exploitation de la Mer*) research facilities at Plouzane (near Brest, France) was performed in 2009. The aim of these measurements was to study the behaviour of four FFR-SX30 transducers under different values of pressure, in the frequency range of interest 21 kHz – 42 kHz, recording the emitted and received signals and then, observing the relative acoustic power variations. Two hydrophones and a sound velocimeter used in the ANTARES submarine neutrino detector were also tested (the study of these devices has not been part of this thesis). Figure 3.16 shows the fresh-water hyperbaric tank used to simulate the pressure in large water depth and a table with its main characteristics.

CHARACTERISTICS	
Box beam	1000 bar ACB
Max pressure	1000 bar
Useful height	2 m
Useful diameter	1 m
Pressure cycle	Yes
Temperature Controlled	2ºC
Connection - Electric - hydraulic	 Yes Yes
Fluid of compression	Fresh water

Figure 3.16: View of the hyperbaric tank at IFREMER research facilities, Plouzane (near Brest - France) (right) and its main characteristics (left) [IFREw].

The used measurement set-up was chosen to avoid interference effects between the hydrophones. For this reason a metallic plate was used in order to separate the FFR-SX30 transducers, mounted on the top part of the tank, and the sound velocimeter and the ANTARES hydrophones mounted on the bottom part of the tank (Fig. 3.17 (left)). During the measurements, electric signals coupling problems were found, due to the physical housing of the cables in the same cable holder. They were solved using separated cable holders. The inner electrical connections between the hydrophones (and the velocimeter) and the tank were achieved with special connectors watertight up to 600 bars [IFREw]. Figure 3.17 shows the assemblage and the connections used for the measurements and the special connectors watertight.

Figure 3.17: Views of the assemblage and the electrical connections used for the measurement (left and top right) and of the special connectors watertight up to 600 bars (bottom right).

The pressure dependence on the transceivers in both conditions of rising and decreasing pressures in the range from 1 to 440 bars was investigated. For each pressure value, different tone bursts signals with 10 Vp of amplitude and 10 cycle length in the frequency range 18-42 kHz were emitted. The latter were generated through a signal generator and sent to a pair of emitter-receiver FFR-SX30 transducer. Successively, the received signals were amplified through a CCA100 amplifier RESON (1n = Input Capacitance, 10k = Input Resistance, 12 = dB output gain) and recorded with a NI USB-5132 board by National Instrument [NATIw] managed with a control PC through USB port. The signals are recorded as a text file containing a matrix which columns hold the time and the emitted and received signal wave form.

In order to test the transducers at high pressure for a long time, the transducers and the sound velocimeter were left at the pressure of 440 bars for all the night.

In Figure 3.18 an example of the emitted and received signal at 30 kHz and 440 bars of pressure for the pair of emitter-receiver FFR-SX30 transducer are shown.
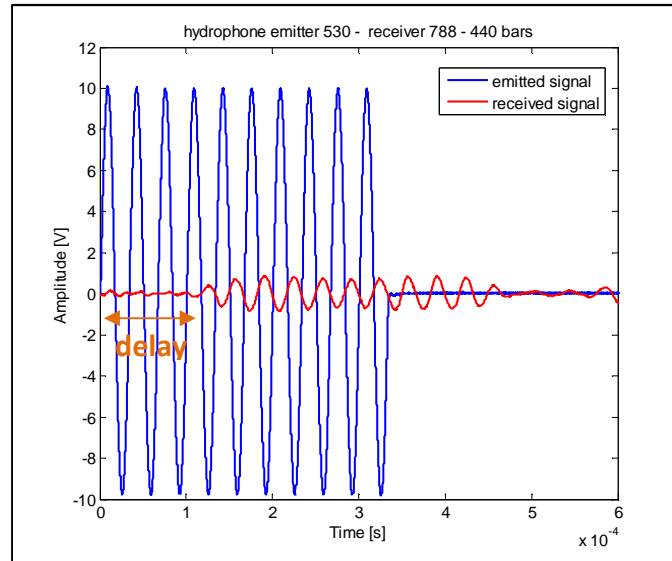
Figure 3.18: Emitted (blue line) and received signal (red line) to the pair of emitter-receiver FFR-SX30 530 and FFR-SX30 788 at 440 bar of pressure.

In order to calculate the acoustic power variation as a function of the pressure only the recorded files in the conditions of decreasing pressures (440, 300, 200, 50, 1 bar) was analyzed. A problem was found during the measurements in the conditions of rising pressures (at the pressure of 1, 50, 200, 300 bar), some hydrophones did not work due to bad connections and the data could not be used in the analysis.

The variation of the amplitude in the frequency spectrum at different pressure and frequency was analyzed, considering only the received direct signal without taking into account the reflections. In this way, for each frequency and pressure, the maximum amplitude of the Power Spectral Density (PSD) using Welch's method of MATLAB was calculated. Figure 3.19 shows an example of the results obtained from these measurements for the acoustic transmission between two FFR-SX30 transducers as a function of the frequency and pressure. The uncertainties of the measurement are about 1.0 dB. Moreover, only the frequencies range 24-40 kHz is shown due to the bad signal to noise ratio measured for other frequencies.
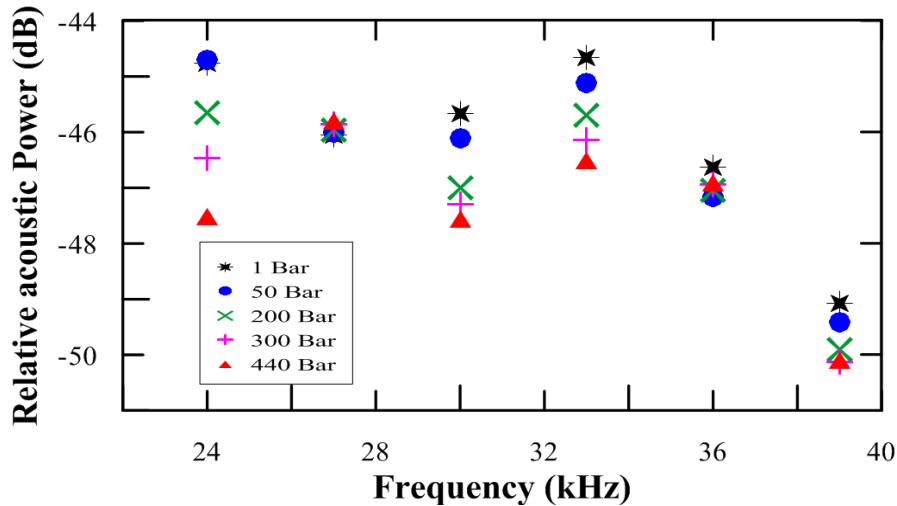
Figure 3.19: Pressure dependence of the FFR-SX30 hydrophones as a function of the frequency. The uncertainties of the measurements are about 1.0 dB.

Furthermore in the IFREMER research facilities at *Plouzane* the electrical resistance and capacity of the transceivers were measured through a HP4284A LCM meter from Agilent[6] with basic accuracy of 0.05% [AGILw]. Figure 3.20 shows the resistance and capacity values measured for the FFR-SX30 774 transducer (similar values are obtained for the others transducers).

From the measurements we can conclude that these transducers are quite stable with depth. The little variations observed are not problematic for the KM3NeT APS application.
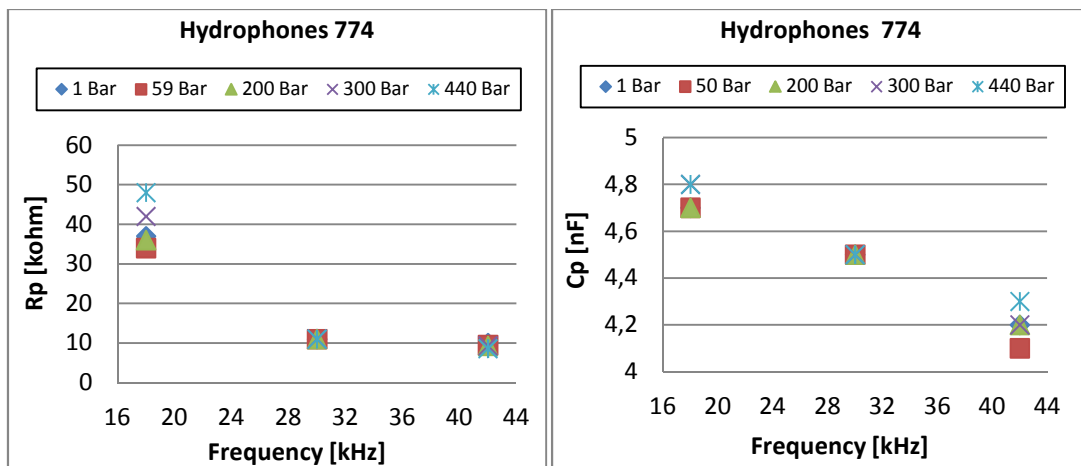
Figure 3.20: Resistance and Capacity values to the FFR-SX30 774 transceiver at the different pressure measured in IFREMER research facilities at Plouzane.

---

[6] This model was from Hewlett Packard Company before.

3.4 Tests on the Transceiver

The transceiver has been tested in a fresh-water tank in the laboratory, in a pool and in shallow sea water in order to be integrated in the instrumentation line of the ANTARES neutrino telescope and in the NEMO Phase II tower for the in situ tests in the deep sea. For simplicity and due to limitations applying for the integration in both experiments, it was decided to test the transceiver only as an emitter. The receiver functionality will be tested in other in situ KM3NeT tests.

To test the system, the transceiver has been used with different emission configurations in combination with the omnidirectional transducer RESON-TC4014, which was used as receiver. Different signals have been used (tone bursts, sine sweeps, maximum length sequence MLS signals, *etc.*) to study the performance of the transducer in different situations. In order to study with accuracy the performance of the system the positioning system mounted on the tank has been used to position the hydrophone in it. It allows the motion in three dimension x, y and z with an accuracy of 0.01 mm. Figures 3.21 and 3.22 show the configuration of the transceiver (named position 1 and 2, as explained above) and the set up used for the measurements. In the next section, the activities and results of these tests are described.
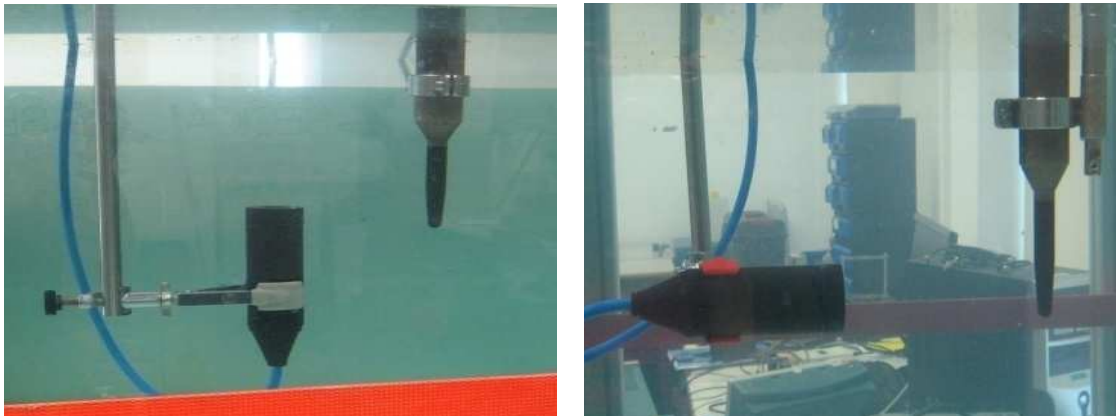
Figure 3.21: Configuration used to test the system as a function of the frequency (position 1, left) and as a function angle (position 2, right).
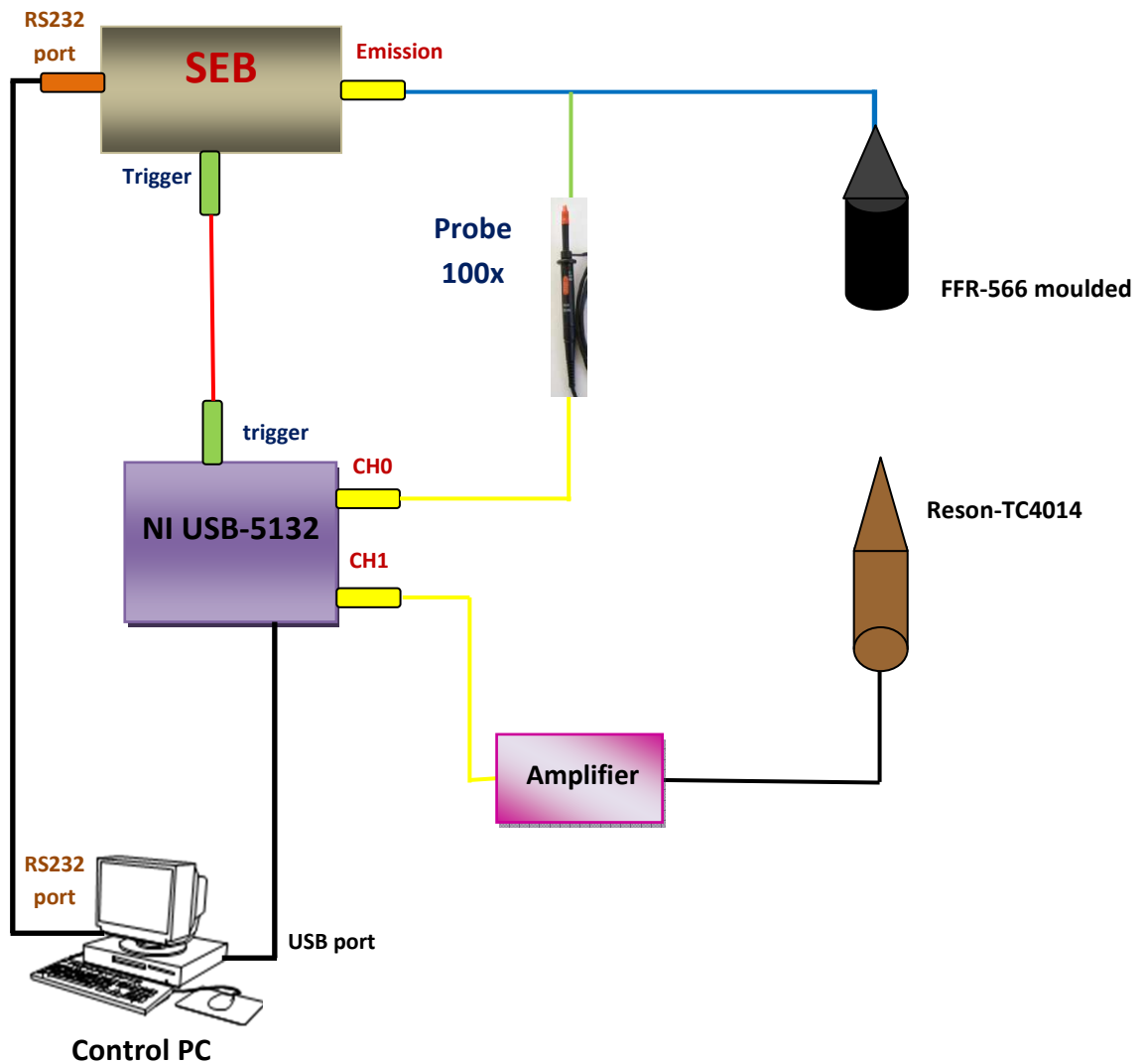
Figure 3.22: Set up used to test the system. The signal was generated through the SEB and sent to the FFR emitter. The received signal was collected from the RESON-TC4014 receiver, amplified with RESON amplifier and recorded through NI USB-5132 board managed with a control PC through USB port.

3.4.1 Sensitivity tests of the system

In the first step, the sensitivity of the moulded FFR-SX30 transducer as a function of frequency has been measured in order to check the functionality after the transducer moulding. Different tone bursts signals with ~350-426 Vpp of amplitude, 250 µs length in the 18-50 kHz frequency range were generated through the SEB directly connected to the FFR-SX30 transducer. The emitted and received signals were recorded through a NI USB-5132 [NATIw] managed with a control PC and stored in the latter. The signal length was chosen according to the dimensions of the tank to avoid the reflections from

the walls and water surface. Figure 3.23 shows the emitted signals amplitude as a function of the frequency.
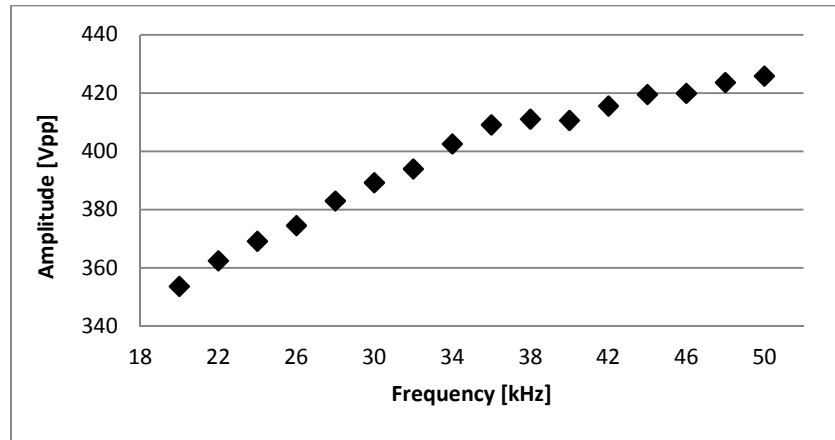
Figure 3.23: Emitted signals amplitude through the SEB as a function of the frequency.

The Transmitting Voltage Response (TVR) as a function of frequency was calculated using the formula (3.2) and is shown in Figure 3.24. The uncertainties on the measurements are 1.0 dB.
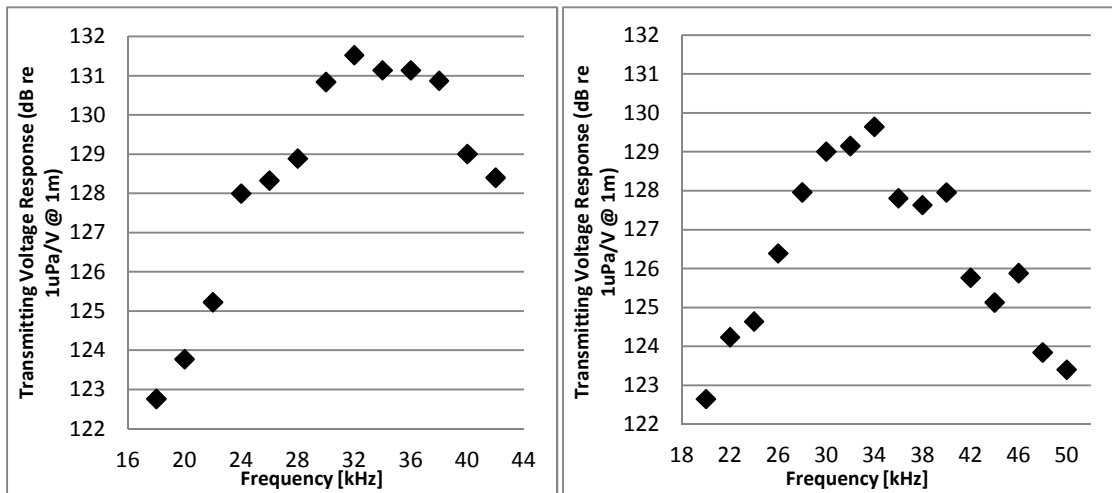
Figure 3.24: Transmitting Voltage Response as a function of the frequency for the nude FFR-SX30 (left) and moulded FFR-SX30 transducer (right).

Comparing the TVR of the FFR-SX30 with and without over-moulding, a loss of ~1-2 dB is observed for the over-moulded transducer.

In a second step, the Transmitting Acoustic Power of the transceiver has been calculated. Figure 3.25 shows the Transmitting Acoustic Power of the transceiver as a function of the frequency (measured in the position 1, that is, in direction perpendicular to the axis of the transducer). The Transmitting Acoustic Power of the transceiver as a

function of the angle (directivity pattern) using a 30 kHz short tone burst signal is also shown (measured in the position 2, 0º corresponds to the direction opposite to the cables) [LAR12]. The measurements have been done in similar conditions to those of Figure 3.24.
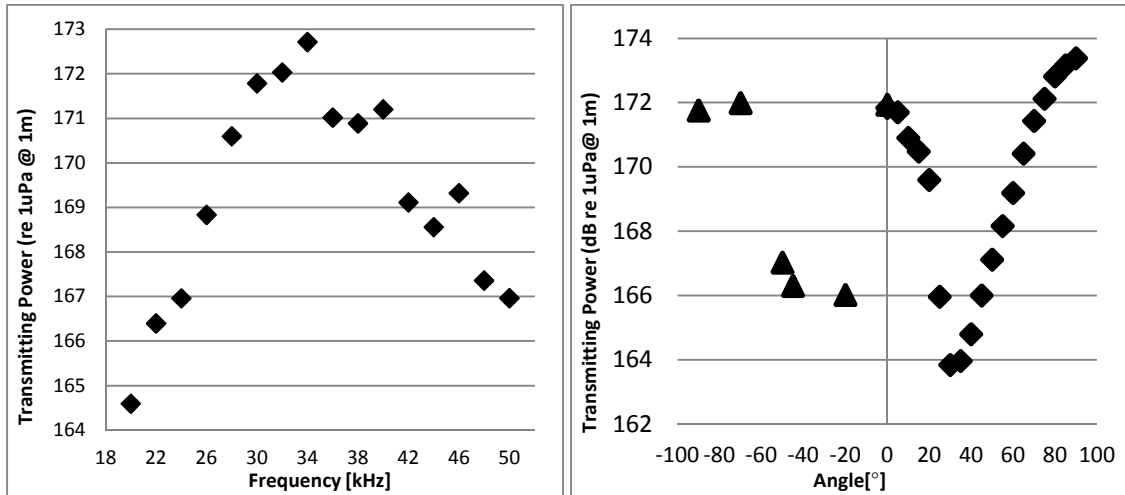
Figure 3.25: Transmitting Acoustic Power of the transceiver as a function of frequency and of angle, respectively.

Figures 3.25 shows that the results for the transmitting acoustic power in the 20-50 kHz frequency range is in the 165-173 dB re 1μPa @ 1 m range, in agreement with the electronics design and the specifications needed. Acoustic transmitting power may be considered low in comparison with the ones used in Long Base Line positioning systems, which usually reach values of 180 dB re 1μPa @ 1 m. Despite this, the use of longer signals in combination with a broadband frequency range and signal processing techniques will allow us to increase the signal-to-noise ratio, and to therefore allow the possibility of having an acoustic positioning system of the 1 μs accuracy (~ 1.5 mm) order over distances of about 1 km, using less acoustic power, that is, minimizing the acoustic pollution and reducing the power consumption of the KM3NeT detector. In the next section the tests to study this possibility of the system are described.

3.4.2 Functionality tests of the system

In order to study the transceiver over longer distances, the response in a noisy environment and also the possibilities of the signal processing techniques, tests were designed in a pool and in shallow sea water at the Gandia Harbour (Spain). Particularly,

we were interested in studying the use of different acoustic signals for positioning purposes. We were confident that the use of wideband signals, Maximum Length Sequence (MLS) signals and sine sweep signals, instead of pure sinusoidal signals may result in an improvement of the signal-to-noise ratio, and therefore resulting in an increase in the detection efficiency, as well as in the accuracy of the time of detection.

In the first step, the measurements in a fresh-water pool of a $3.60 \times 6.30 \times 1.30$ m^3 in Catadau near Valencia were performed using the transceiver (FFR-SX30 plus SEB) as emitter and the Reson as receiver hydrophone. In a second step, the measurements in Gandia Harbour were carried out using the transceiver (FFR-SX30 plus SEB) always as emitter and a second FFR-SX30 serial number 07 with a Reson preamplifier, model CCA100 as receiver hydrophone. The set up used was the same as represented in Figure 3.22 for short distance (from 10 cm to 4.50 m). In addition, for long distance (140 m) an external trigger synchronization system between the emitter and the receiver was used. This trigger signal arrives with a delay of 8.25 ± 0.03 ms in the acquisition system of the receiver channel. MLS signals, sine sweep signals and pure sinusoidal signals were emitted with different amplitude and length. In the pool different distances between the transducer were chosen and located at 57 cm depth. On the other hand, in the harbour the study was done at 4.50 m and 140 m and the transceivers were located at 1 m depth. Figure 3.26 shows the configuration used for the tests made at 10 cm of distance in the pool, at 4.50 m and 140 m of distance in the harbour, respectively.
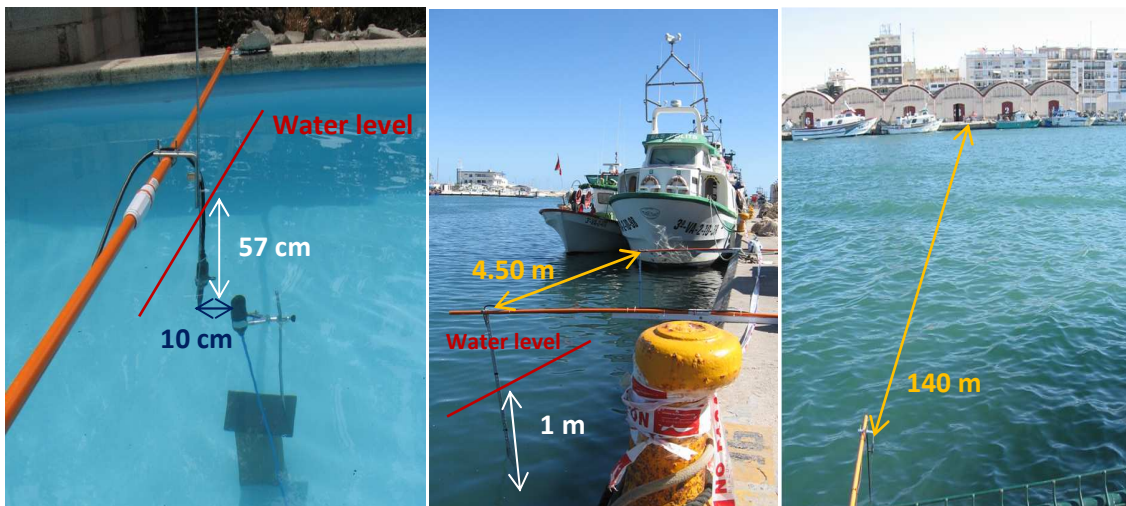
Figure 3.26: Configuration used for the measurements in the pool and in the Gandia Harbour.

Figure 3.27-3.30 show the received signals using a MLS signal (order: 11, sampling frequency: 200 kHz), a linear sine sweep signal (frequency range: 20-48 kHz, length: 1

ms or 4 ms), and a pure sinusoidal signal (frequency: 30 kHz, length: 0.25 ms, 1 ms or 4 ms) and the correlation between the receiving and emitted signals, for the tests in pool and in harbour respectively. The time when the signal appears is clearly observed. The SEB emission is produced with a delay of 0.0054 ms which has been taken into consideration. The direct signal arrives at about 0.075 ms (for the 10cm of distance) and 0.69 ms (for 1 m of distance) in pool; at about 2.9 ms and 85 ms in harbour for the distance of 4.50 m and 140 m respectively. The other peaks are due either to reflections or to the ambient noise (in the case of the Gandia harbour). In particular, in the Figure 3.28 a second peak is well-visible, mainly in the case of the MLS signal, due to reflections on the surface expected at 1.01 ms. Moreover, in the same Figure 3.28 is clearly observed the electromagnetic signals before the received acoustic signals for the three kinds of signals visible near 0 seconds for the cross-correlation plots. For the case of the MLS and sine sweep signals, a clear thin peak is observed, and therefore it is easy to determine the time of detection. The measurements were performed three times obtaining times of detection shown in Table 3.2 for the different signals (MLS and sweep signals) corresponding to distance uncertainties from 0.1 cm to 4.5 cm.

	Time arrival of the direct signal			
Signals	In pool: D=10 cm	In pool: D=1 m	In harbour: D=4.50 m	In harbour: D=140 m
MLS	0.074±0.001 ms	0.691±0.004 ms	2.981±0.003 ms	85.08±0.03 ms
Sweep	0.070 ±0.002 ms	0.695 ±0.003 ms	2.932±0.008 ms	85.08±0.02 ms

Table 3.2: Time arrival of the direct signal for the different signals and distances of the different tests.

The case of the pure sinusoidal signal is quite different since a very broad peak is observed due to the cross-correlation method. Moreover, in the harbour at the long distance the noise was quite high (~Pa), and reflections were detected resulting in a not easy identification of the signals. The time of the maximum was quite sensitive to noise or reflections.

Following the previous approach, an uncertainty of the order of ~2 ms is obtained, and therefore this method is not the best one for this kind of signals. Usually, a band-pass frequency filter is applied, and the detection time is determined by reaching a threshold level [ARD09, AGU11a]. Doing this properly requires a very accurate calibration in order to determine the inertial delay of the hydrophone, and even so, it can give bad

results in case of high noise, or intense reflections nearby that can be added to the waves constructively, as it happened during our measurement in the harbour. In contrast, the cross-correlation of broadband signals is less sensitive to these effects. The inertial delay, which affects mainly to the start and end of the signal, is rendered less important by considering the whole duration of the signal. The effect of the reflections is reduced by distinguishing between different peaks of the cross-correlated signal, the first main peak being the one to consider [LAR12a].

Figure 3.31 and 3.32 show a zoom of the receiving signals and of the cross-correlation peak for the three signals of Figure 3.30. It is clearly observed that the cross-correlation method is better for the MLS signals than for the other kinds of the signals and in particular it does not work well for a pure sinusoidal signal.
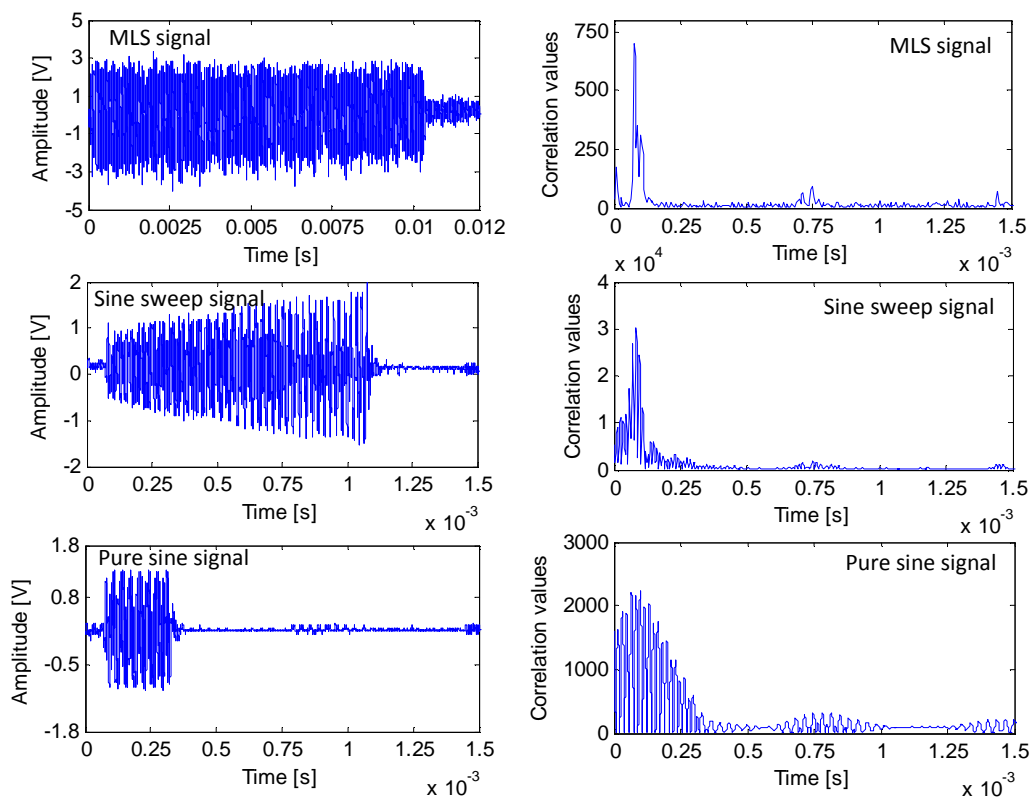
Figure 3.27: Receiving signal using three different kinds of signals (left) and correlation between emitted and received signals (right). The measurements have been done in pool and the transducers are located at 10 cm distance.
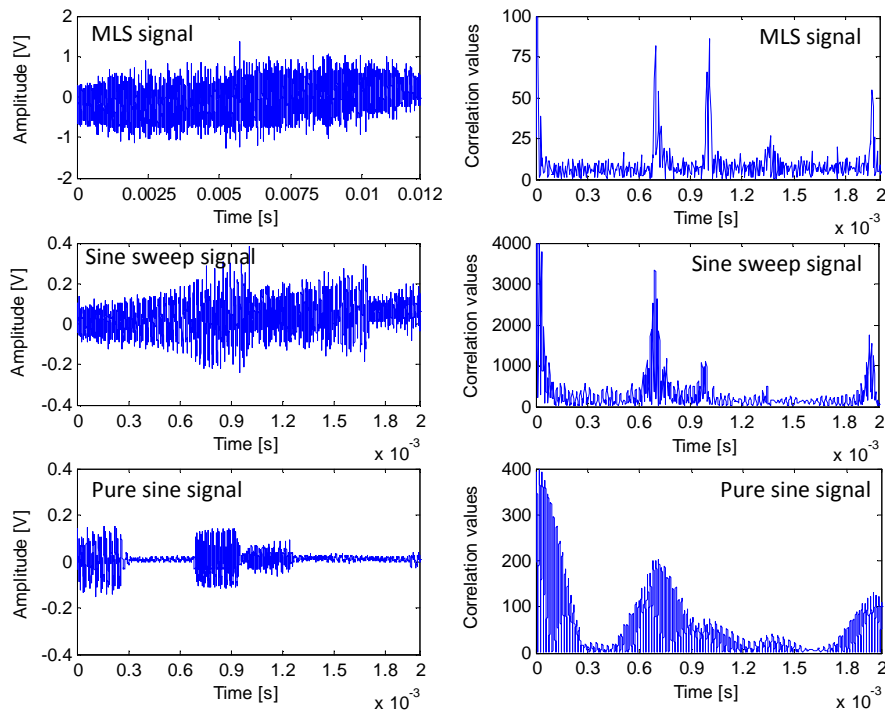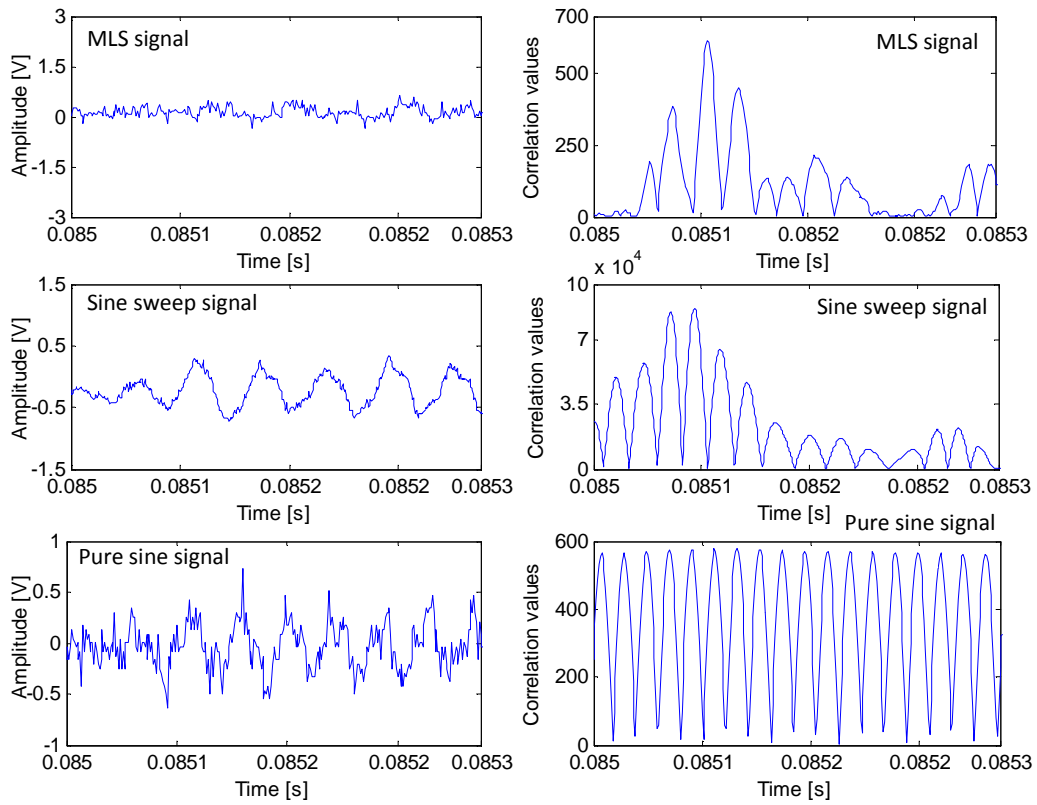
Figure 3.28: Receiving signal using three different kinds of signals (left) and correlation between emitted and received signals (right). The measurements have been done in pool and the transducers are located at 1 m distance.
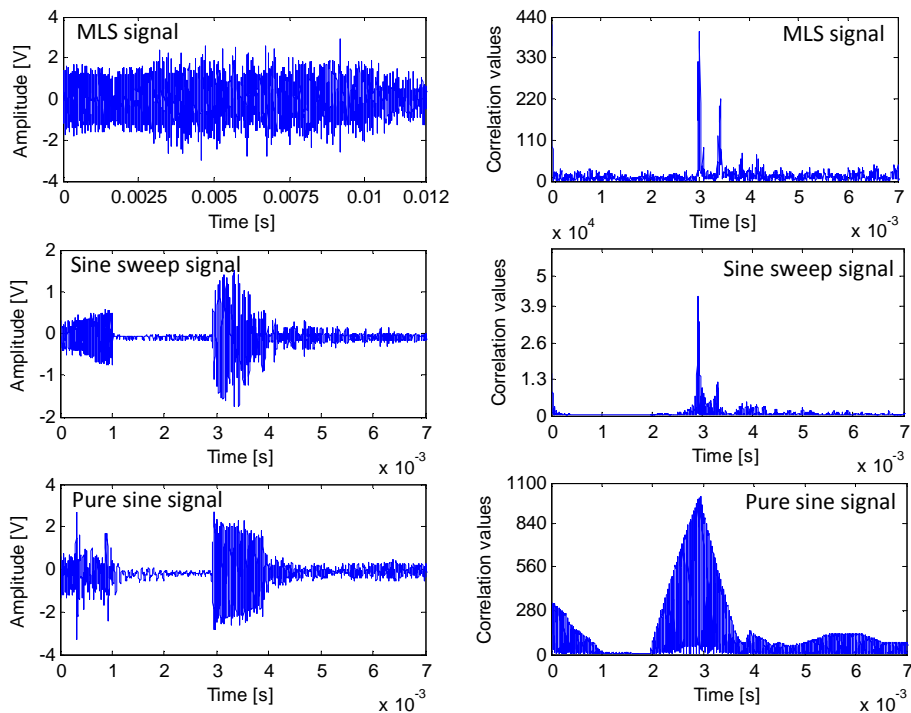
Figure 3.29: Receiving signal using three different kinds of signals (left) and correlation between emitted and received signals (right). The measurements have been done in harbour in Gandia and the transducers are located at 4.50 m distance.
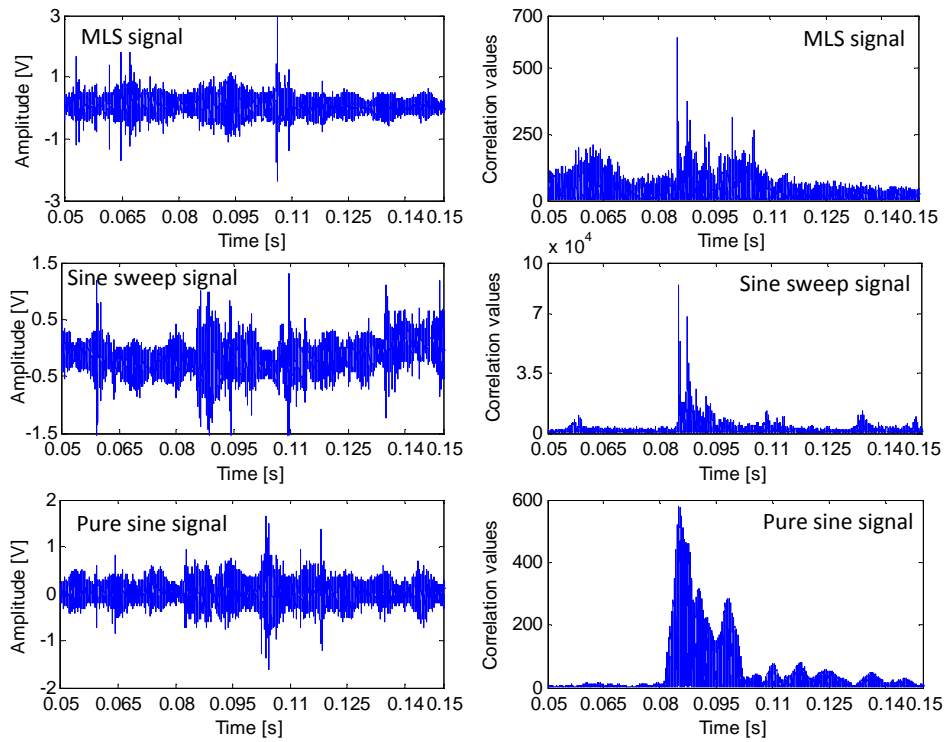
Figure 3.30: Receiving signal using three different kinds of signals (left) and correlation between emitted and received signals (right). The measurements have been done in harbor in Gandia and the transducers are located at 140 m distance.
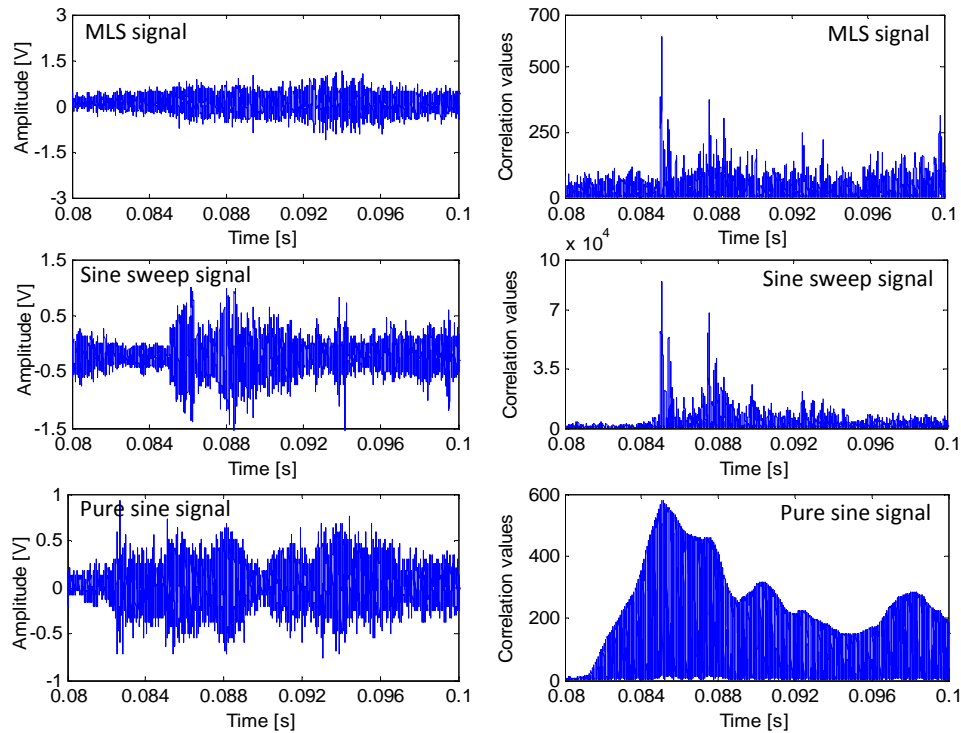
Figure 3.31: Zoom of the Receiving signal using three different kinds of signals (left) and zoom of the correlation between emitted and received signals (right). The measurements have been done in harbor in Gandia and the transducers are located at 140 m distance.

78

Figure 3.32: Zoom of the Receiving signal using three different kinds of signals (left) and zoom of the correlation between emitted and received signals (right). The measurements have been done in harbor in Gandia and the transducers are located at 140 m distance.

Chapter 4

Integration of the acoustic transceiver in Underwater Neutrino Telescopes

In this chapter the different activities and tests performed towards the integration of the acoustic transceivers in neutrino telescopes infrastructures are presented. This will allow for testing the acoustic transceiver in real conditions and studying their behaviour in situ. Two different initiatives are presented: the integration in the instrumentation line of ANTARES and the integration in the NEMO-Phase II tower.

4.1 Integration in ANTARES Neutrino Telescope

The acoustic transceiver presented in the previous chapter, already tested in the laboratory, the pool and in Gandia Harbour, has been finally integrated in the active anchor of the Instrumentation Line 07 (IL07), renamed IL11, of the ANTARES detector on 3rd June 2011. The SEB was installed in a titanium container named Laser Container holding also other electronic parts and the Laser Beacon system (LB) used for timing calibration purposes. The Laser Container consists of a cylinder of 542 mm length and with a diameter of 142 mm made of titanium grade 5 (Ti6AI4V). It is composed of three different pieces: the cylindrical tube, the low cap (connector cap) and the upper cap with the anti-biofouling system (described below). The inner aluminium mechanics provides the structure where the different devices of the laser beacon are integrated. It consists of two aluminium rings joined together by two aluminium beams. One of the rings is screwed to the lower titanium end-cap. The drawings of this piece are shown in Figure 4.1. The anti-biofouling system is made by a diffuser disk and a quartz cylinder rod which spreads light out following a cosine distribution over a half sphere (Figure 4.2). The laser is needed for the timing calibration of a neutrino telescope and a new laser will be tested in the IL.

The LB and the transducer were fixed on the active anchor through supports of polyethylene designed and produced at the *Instituto de Física Corpuscular*, Valencia

(Spain). Figures 4.3, 4.4 and 4.5 show the drawings of all the pieces composing the supports of the LB and of the acoustic transducer.
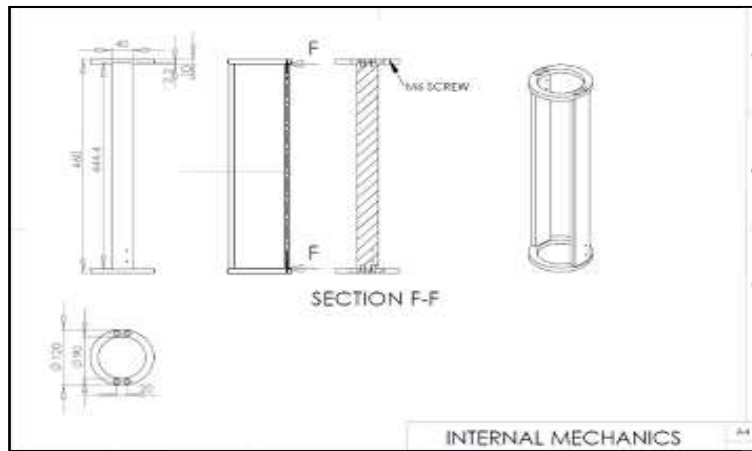

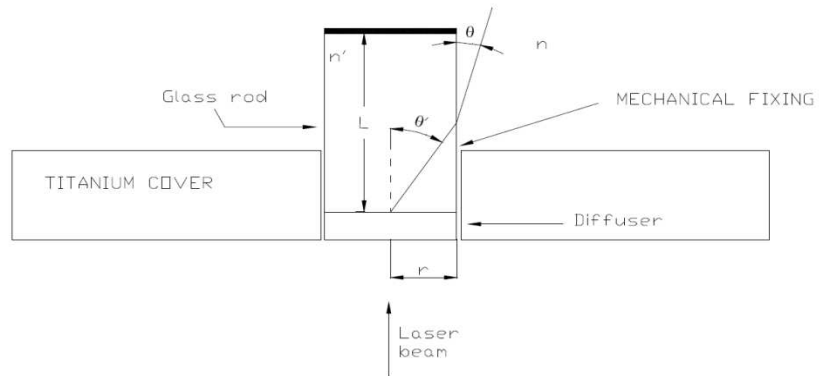*Figure 4.1: Drawings of the internal mechanics of the container.*

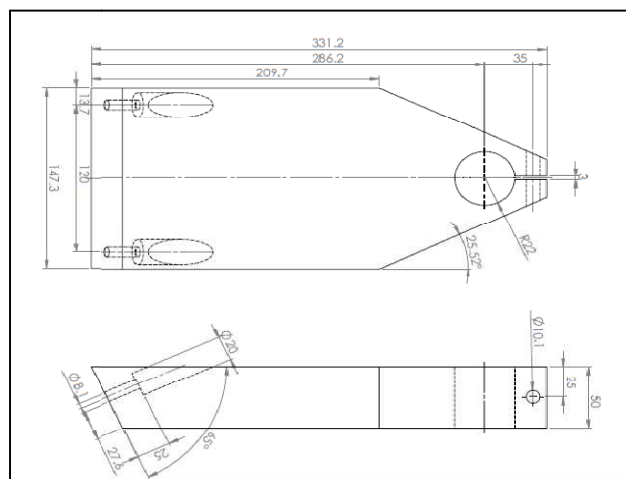*Figure 4.2: Diagram of the rod insertion.*

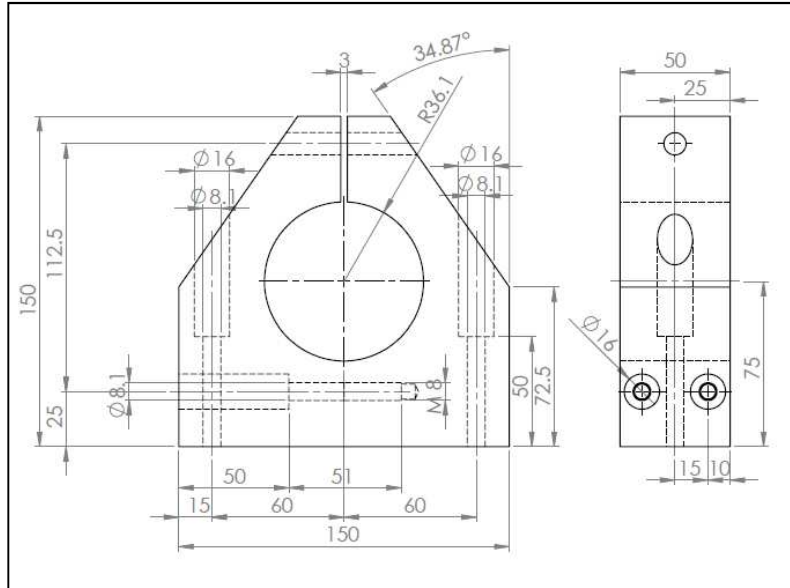*Figure 4.3: Drawings of the supports for holding the acoustic transducer.*

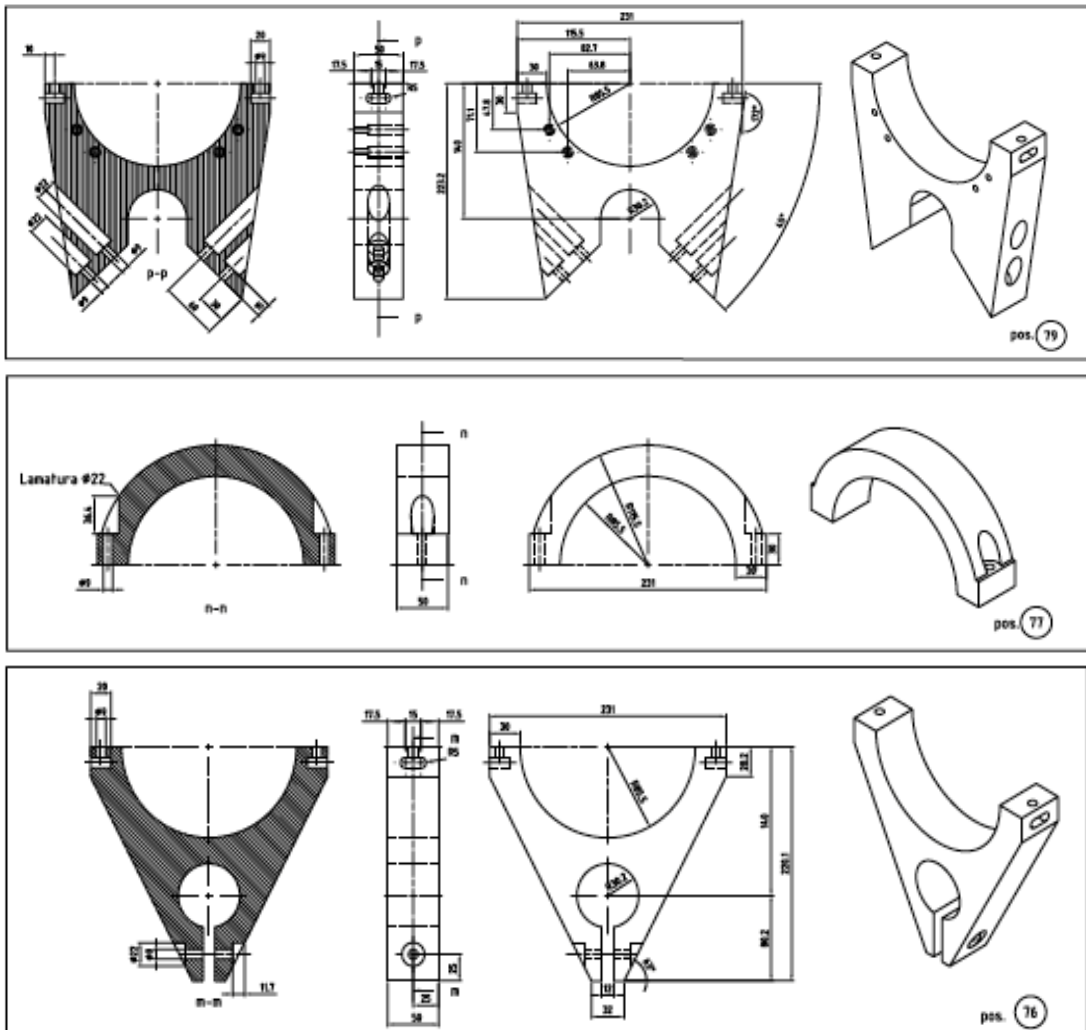*Figure 4.4: Drawings of the transducer supports to fix it to the bar of the IL11 anchor.*

Figure 4.5: drawings of the LB supports.

The FFR-SX30 serial number 02 transducer was fixed in the base of the line at 2.87 m from the bottom of the anchor and at 50 cm from the standard emitter transducer of the ANTARES positioning system with the area opposite to the moulding and the cable of the transducer pointing upwards. The anchor with all the integrated instrumentation has a mass of 804 kg weigh. Figures 4.6 and 4.7 show some pictures of the final integration of the system in the anchor of the Instrumentation Line of the ANTARES detector. Finally, the Instrumentation Line was successfully deployed at 2475 m depth on 7th June 2011 at the nominal target position. However, due to a faulty connector and cable, the line could not be connected to shore. Depending on the availability of the ROV, a new attempt to connect the Line will be made in the second half of 2012. Afterwards, the transceiver can be tested, as emitter, under real conditions.
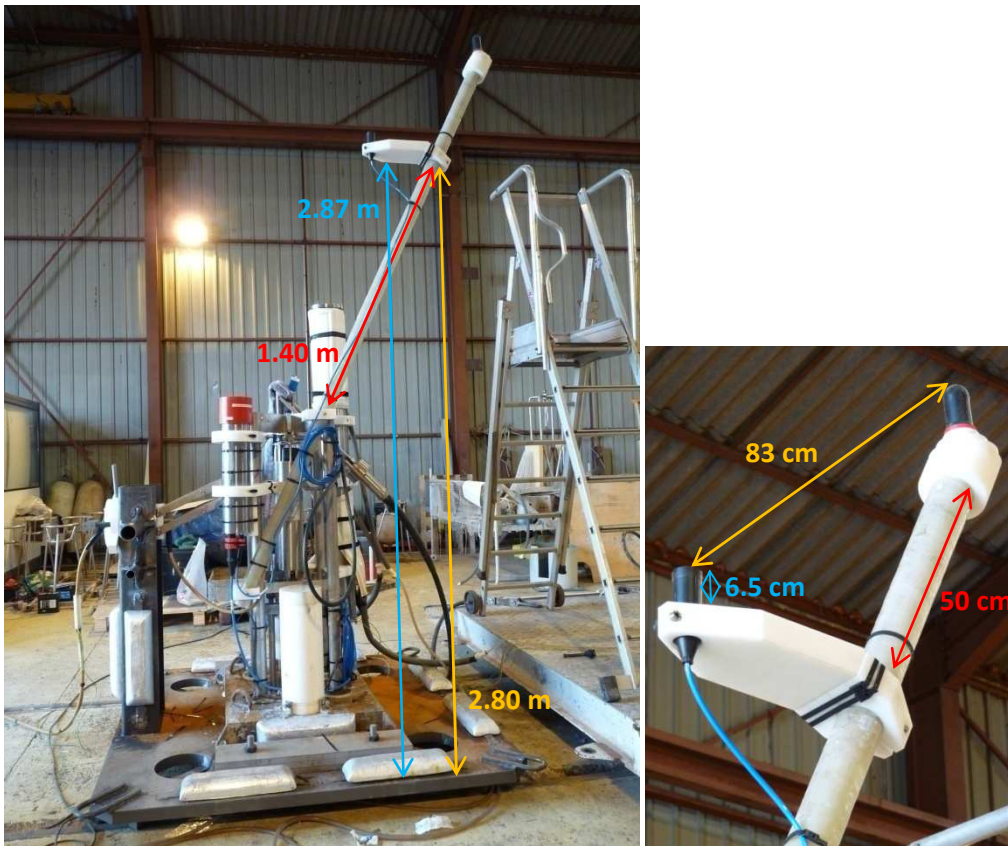
Figure 4.6: Anchor of the IL11 of the ANTARES detector (left) and details of the FFR transducer with the support in polyethylene (right).
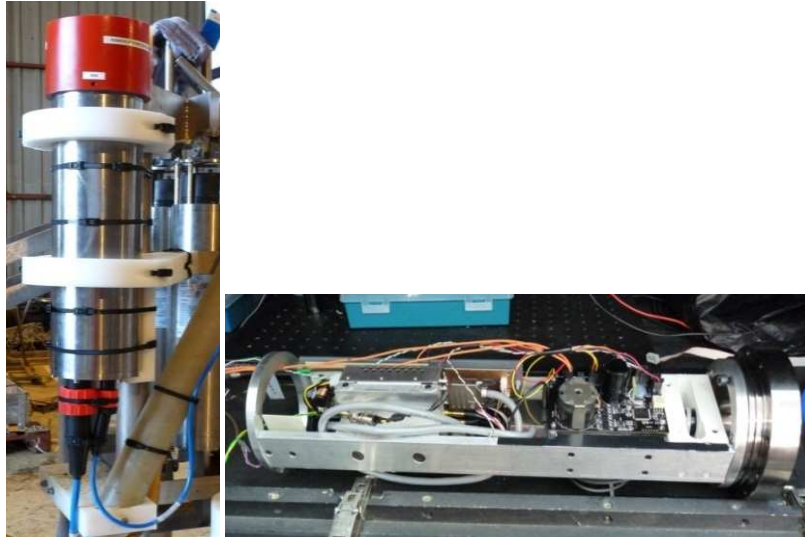
Figure 4.7: View of the LB integrated in the IL11 anchor (left), and inner view of the Laser Container including the SEB integrated inside of the titanium vessel (right). The red cap on the LB is needed to screen the quartz cylinder. It is removed before the deployment.

4.1.1 SEB for the integration in ANTARES detector

In order to integrate the system in the ANTARES detector and to test the system in situ at 2475 m depth some changes in the SEB were done. The reasons for the changes were to simplify the system and to deal with the particular limitations of the ANTARES instrumentation line infrastructure. For ANTARES, it was decided to test the transceiver only as emitter, the functionality as receiver will be tested in other in situ KM3NeT tests. The changes done in the SEB are the following: the reception part was eliminated, the standard RS232 was adapted to standard RS485, a new functionality for the microcontroller to control the laser emission and the instructions to select the kind of signals to emit matching the procedures of the ANTARES DAQ system through the MODBUS communication protocol were implemented. The acoustic transceiver operation mode will be tagged as APS (Acoustic Positioning System) in order to distinguish this functionality from that of the Laser Beacon mode.

A picture and a diagram of the SEB integrated in IL11 are shown in figure 4.8. The use of the RS485 connection and adapter is shown and it can be noticed that the relay, related to the reception, was removed.
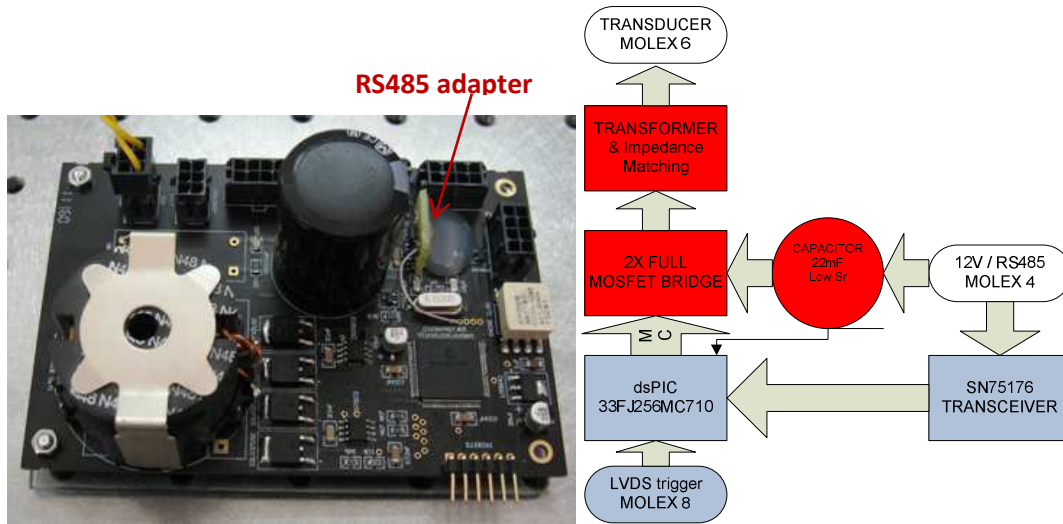
Figure 4.8: View and diagram of the SEB integrated in the IL11 of the ANTARES detector.

The MODBUS is a communication protocol used in industrial environment and it is amongst the most common means of connecting industrial electronic devices. There are many variants of MODBUS protocols: MODBUS RTU, MODBUS ASCII, MODBUS TCP/IP etc. Here only the MODBUS RTU will be explained since it is the communication protocol used. It is used in serial communication and makes use of a compact, binary representation of data for protocol communication. The RTU format follows the commands/data with a cyclic redundancy check (CRC) checksum as an error check mechanism to ensure the reliability of the data. Each device intended to communicate using MODBUS is given a unique address. A MODBUS command contains the MODBUS address of the device it is intended for. Only the intended device will react to the command, even though other devices might receive it. All MODBUS commands contain checking information, ensuring that a command arrives undamaged [MODBw]. In our case, the MODBUS commands are sent by the run control application. The commands sent by run control are summarized in table 4.1:

1	070F002000080100 + CRC	COMMAND NOT NEEDED
2	070F0040000801A0 + CRC	COMMAND NOT NEEDED
3	070F00000008012A + CRC OR 070F000000080100 +CRC	ACTIVATE LASER OR APS (Depend on ACTIVELASER) DESACTIVATE LASER OR APS
4	07 06 00 0**Y** 0**X XX** + CRC	LASERKIND TO BE USED IN ORDER TO CHOOSE BETWEEN LB AND APS **Y = 2** (LASER) **Y = 3** (APS)

Table 4.1: MODBUS commands sent to control the LB and the APS.

The XXX value represents the acoustic signal to emit or the light attenuation value for the laser, and the Y represents the choice between the devices. The microcontroller receives them and acts according to the specified protocol, activating either the Laser Beacon, fixing in this case the polarization value of the attenuator, or the APS.

In order to simplify the instruction for the choice of the different devices in the MODBUS communication protocol a program with graphic interface was created. Figure 4.9 shows the graphics interface to send the MODBUS commands.
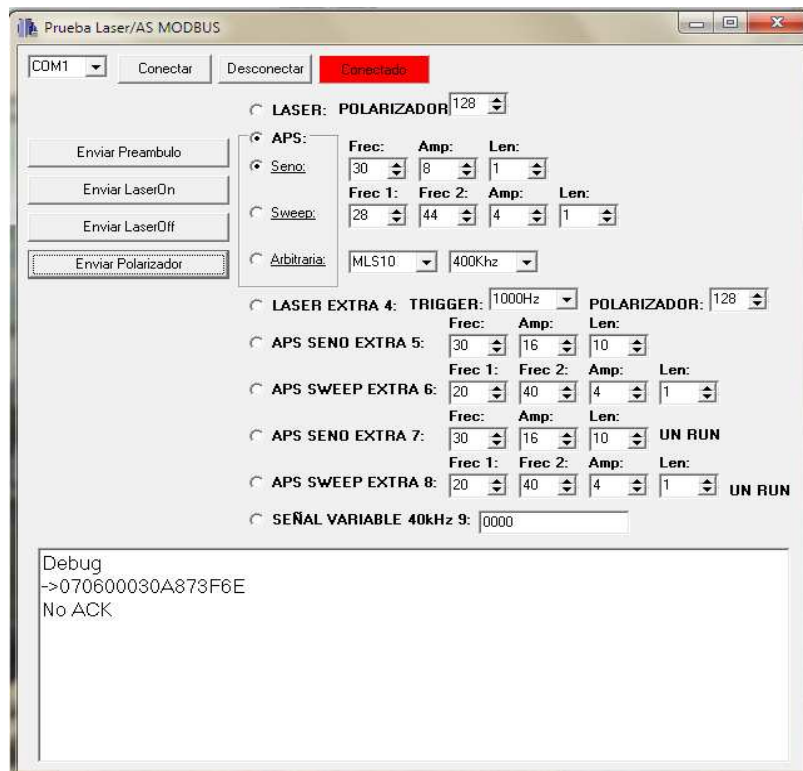
Figure 4.9: Graphic interface for the MODBUS commands.

This interface application permits to select the different devices (LB or APS) and to choose the light attenuation value for the laser (with the POLARIZZADOR command), and to select the kind of signals to emit (pure sinusoidal signals, MLS signals, sweep signals etc.). In Figure 4.9 the graphics interface for MODBUS option is shown.

4.1.2 Transmitting Power of the system for the ANTARES detector

Before the integration of the transceiver in the instrumentation line of the ANTARES neutrino telescope, it has been tested in a fresh-water tank in the laboratory, in a pool and in shallow sea water, as explained in chapter 3. Figure 4.10 shows the Transmitting Acoustic Power of the transceiver as a function of the frequency, measured in the positions (orientations) 1 and 2, see section 3.2 for details. The Transmitting Acoustic Power of the transceiver as a function of the angle (directivity pattern) using a 30 kHz short tone burst signal is shown in Figure 4.11 (measured in position 2, 0° corresponds to the direction opposite to cables) [LAR12].
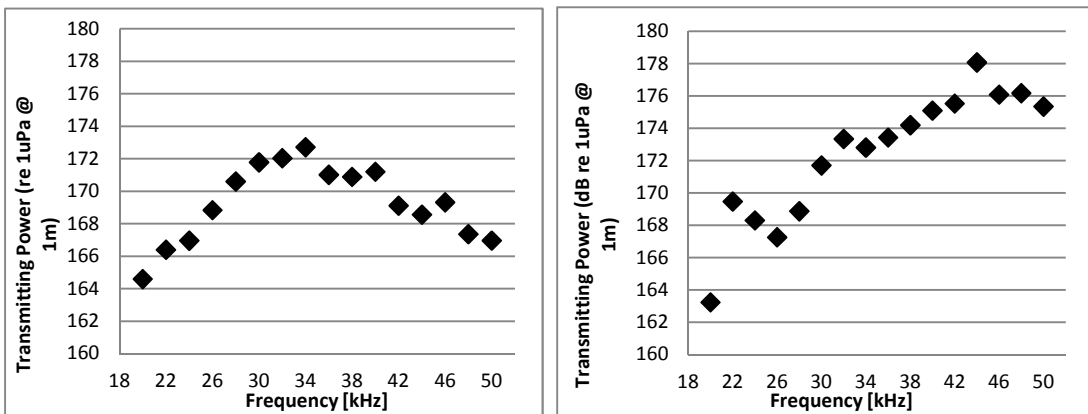
Figure 4.10: Transmitting Acoustic Power of the transceiver as function of frequency measured in position 1 (left) and position, 2 (right), respectively.
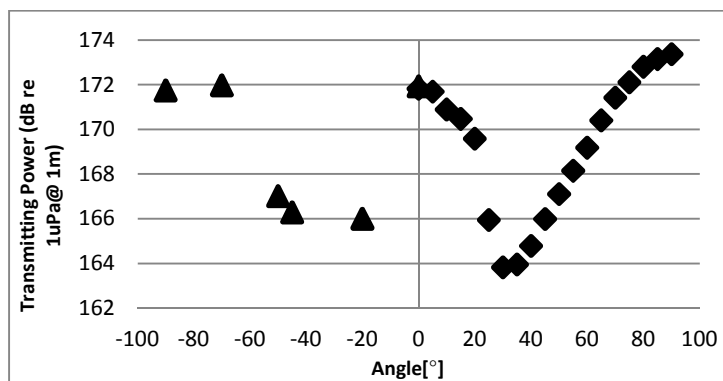
Figure 4.11: Transmitting Acoustic Power of the transceiver as function of angle measured in position 2.

The transmitting acoustic power in the 20-50 kHz frequency range is in the 165-173 dB re 1µPa @ 1 m range for the position (orientation) 1 and in the 165-178 dB re 1µPa @ 1 m for the position (orientation) 2, in agreement with the electronics design and fulfilling the specifications needed for this test. Since it may be considered low in comparison with the ones used in Long Base Line positioning systems, which usually reach values of 180 dB re 1µPa @ 1 m, the received pressure variation as a function of the distances at 30 kHz and 44 kHz have been calculated for the vertical direction (along the IL11). The equation used is the following:

$$P_r = \frac{P_0}{r} \cdot e^{-\alpha r} \quad [\mu Pa], \quad (4.1)$$

where P_r is the pressure calculated at distance r, P_0 is the received pressure at 1 m from the RESON hydrophone in the measurement with orientation at 0° in position 2 and α is the absorption coefficient calculated by using the parameterisation of François et Garrison [FRA82]:

$$\alpha = \frac{A_1 P_1 f_1 f^2}{f_1^2 + f^2} + \frac{A_2 P_2 f_2 f^2}{f_2^2 + f^2} + A_3 P_3 f^2 \quad [Np/m], \quad (4.2)$$

Figure 4.12 shows the received pressure variation as a function of the distances for 30 kHz and 44 kHz short tone burst signals emitted with the transceiver.
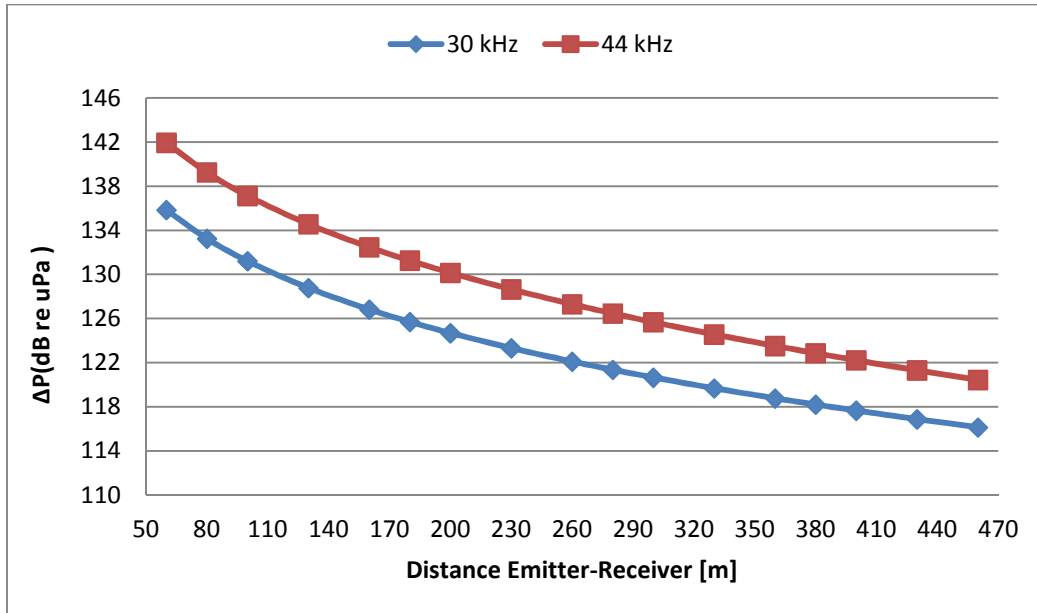

Figure 4.12: Received pressure variation as a function of the distances for 30 kHz and 44 kHz short tone burst signals emitted.

The results show clearly that the pressure decreases with distance until 116 dB re µPa and 120 dB re µPa at 460 m for 30 kHz and 44 kHz tone burst signals respectively. Successively, these data have been used to calculate the received electric signal amplitude that would be measured the AMADEUS and ANTARES hydrophones, knowing that the sensitivity for the AMADEUS hydrophone is -145.5 dB re 1V/µPa at 30 kHz and for the ANTARES hydrophone is -196 dB re 1V/µPa at 44kHz. Figures 4.13 and 4.14 show the received amplitude calculated for the AMADEUS and ANTARES hydrophones, respectively.
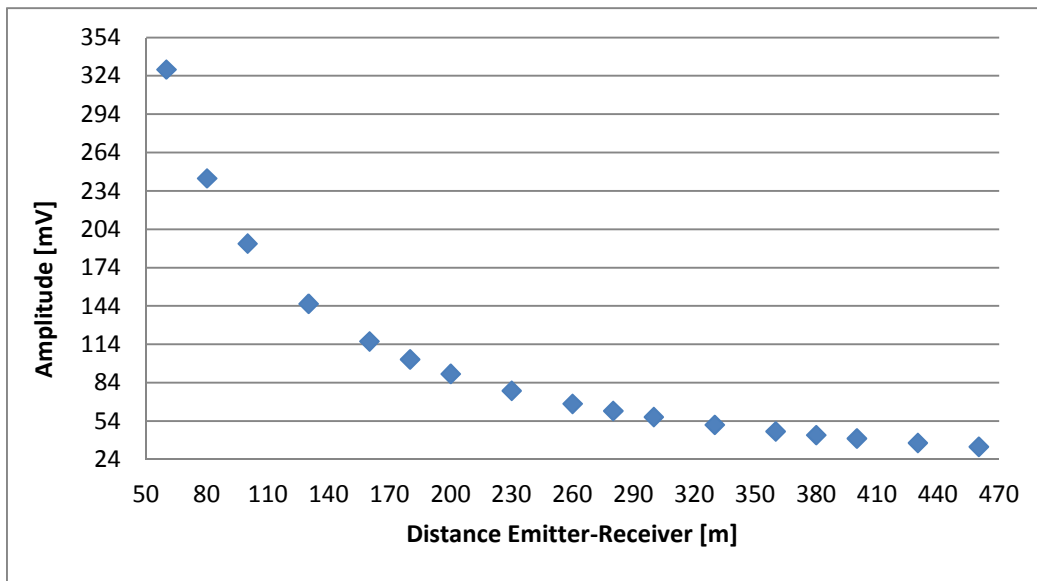
Figure 4.13: Received amplitude with the AMADEUS hydrophones at 30 kHz frequency. In the IL07 (IL11), the AMADEUS hydrophones are located at distances of 180 m, 195 m and 305 m.
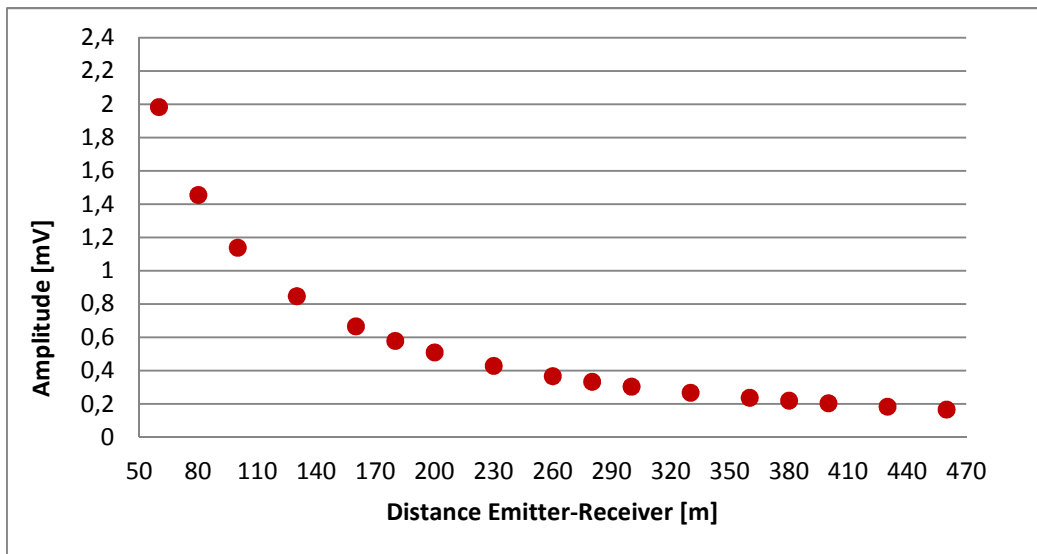
Figure 4.14: Received amplitude with the ANTARES hydrophone at 44 kHz frequency.

The results show that at 460 m signals with amplitudes of about 34 mV and 0.2 mV for the AMADEUS and ANTARES hydrophone, respectively, are expected. Considering that the last storey in the IL with AMADEUS hydrophones is located at 305 m above the sea floor, the signal measured will be of about 57 mV amplitude, enough to be recorded above the ambient noise. Whereas for the ANTARES hydrophones the results show that the signal amplitude is weak and difficult to be useful for long distances.

Moreover, the received pressure variation and the electric signal amplitude expected for the AMADEUS hydrophones on the Line 12 for a 30 kHz short tone burst signal emitted with the transceiver have also been calculated and shown in figure 4.15. The orientation of the emitter and receivers has been taken into account (it corresponds to an angle of ~60º with position 2). Here, again the expected electric signal is enough to be recorded above the noise.
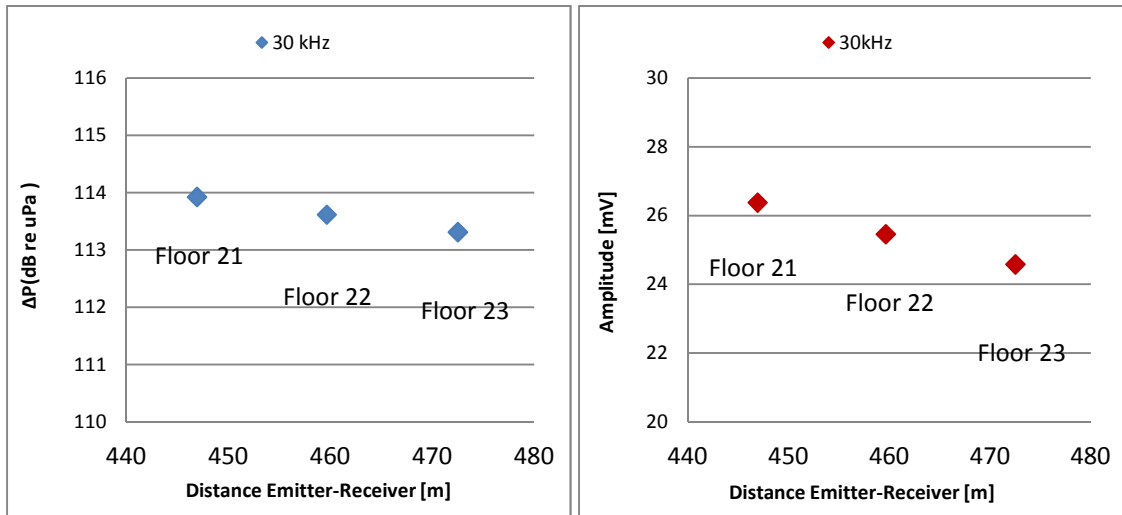

Figure 4.15: Pressure variation (left) and expected electric signal amplitude (right) for the AMADEUS hydrophones of Line12 floor 21-23 using 30 kHz tone burst signals.

Following these results, we can consider that the integration of the emitter in the IL of ANTARES is very important in order to test it in situ and validate it for deep sea conditions. The use of the transceiver in combination with the AMADEUS hydrophones makes the test very complete since it allows studying the transceiver emission for different conditions of distances and orientation. Moreover, it is possible to study in situ different kind of signals (tone bursts at different frequencies, but also broadband frequency signals such as MLS or sine sweeps) and conclude about the possibility of

improving the signal to noise ratio (and therefore being able to cover longer distances) by using broadband frequency signals.

4.2 Integration in NEMO detector

The transceiver prototype system is also already available to be integrated in the base of the NEMO Phase II tower. The integration is estimated by July 2012. The system is composed of a moulded FFR-SX30 transducer, serial number 566, and a Sound Emission Board as described in sections 3.1.1 and 3.1.2, respectively. Furthermore, two other FFR transducers, with serial numbers 788 and 05, will be integrated as receiver in different floors of the tower. The latter were connected to a SMID AM-401 preamplifier [SMIDw] with 20 x 80 mm^2 of dimension and 38 dB gain and the whole receiver moulded by SEACON (europe) Ltd [SEACw]. The moulding and the cable are both in polyurethane. Figure 4.16 shows the FFR-SX30 moulded from by SEACON together with the SMID preamplifier. Tests performed at INFN-LNS have demonstrated the full compatibility of the sensors with the SMID AM-401 preamplifier [VIO12]. These sensors together with 2 piezo-sensors developed by ECAP, 14 further high sensitivity and broadband SMID hydrophones and the transceiver prototype will constitute the APS prototype to be tested in NEMO-Phase II.

Figure 4.16: A picture of the two hydrophones (FFR-SX30 with SMID preamplifier) moulded by SEACON.

As in the case of the integration in the ANTARES detector (Figures 4.1 and 4.2), the transceiver here will be tested only as emitter and in connection with the Laser Beacon

used for timing calibration purposes. Some changes in the SEB were needed in order to adapt it to the particularities and specifications of NEMO-Phase II. The changes in the SEB have been: to eliminate the reception part and to implement a new functionality for the microcontroller to control the laser emission. A picture and the diagram of the SEB are shown in Figure 4.17 and an inner view of the laser container is shown in figure 4.18.
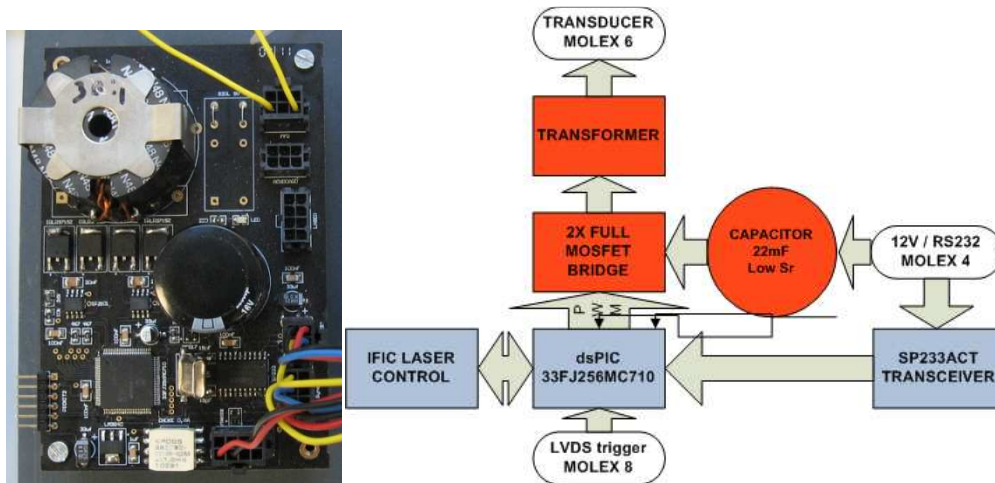

Figure 4.17: View and diagram of the SEB that will be integrated in the NEMO Phase II tower.

Figure 4.18: Inner view of the Laser Container. The laser and the integrated SEB can be seen.

The Laser Beacon will be installed in the anchor of the tower base by means of supports of polyethylene designed and produced at the *Instituto de Física Corpuscular*, Valencia (Spain). The transceiver will also be installed in a bar attached to the anchor of the tower near the Laser Beacon. Figures 4.19 and 4.20 show the anchor of the NEMO tower and a drawing of the installation of the Laser Beacon and of the transducer.
The tests done on the transceiver alone and together with the receiver hydrophones will be described in next sections.

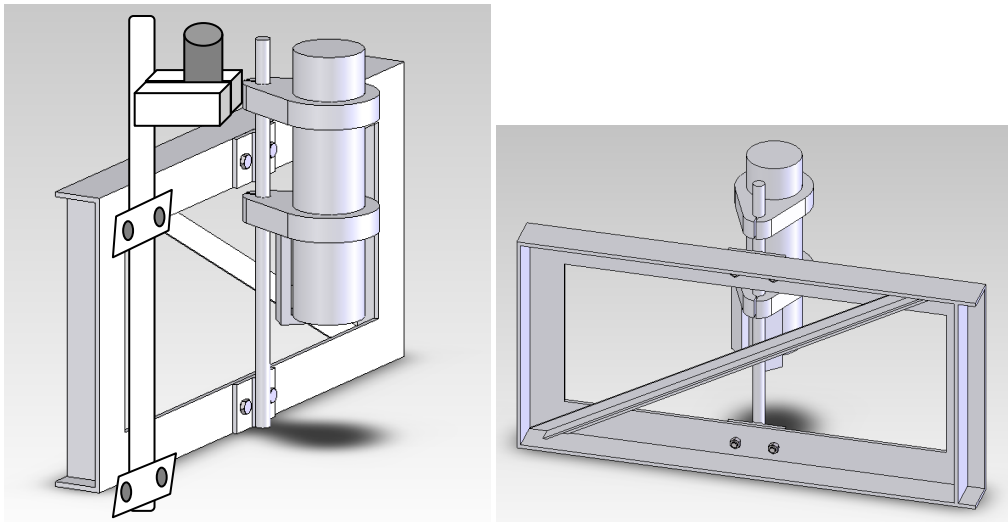*Figure 4.19: The NEMO-Phase II tower and the anchor.*

Figure 4.20: Drawings of the installation of the Laser Beacon and of the acoustic transducer.

4.2.1 Transmitting Power of the system for NEMO detector

The sensitivity of the system has been calculated as described in section 3.4.1. In the first step, the sensitivity of the moulded FFR-SX30 serial number 566 transducer as function of frequency has been measured in order to check that it works correctly after the moulding. Figure 4.21 shows the emitted signal amplitude as a function of frequency. The Transmitting Voltage Response (TVR) as a function of frequency of the FFR-SX30 with and without moulding calculated using the formula (3.2) are shown in Figure 4.22. The uncertainties on the measurements of the TVR are 1.0 dB.

94
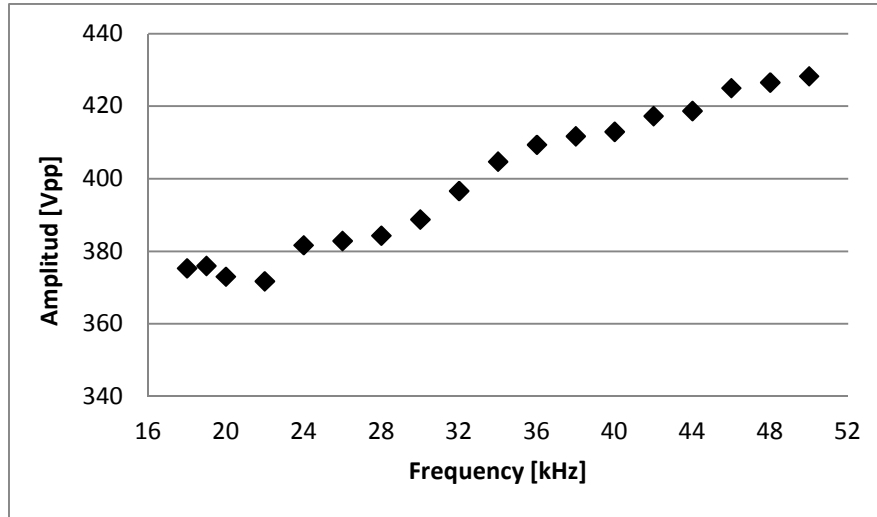
Figure 4.21: Emitted signal amplitude through the SEB as a function of the frequency.
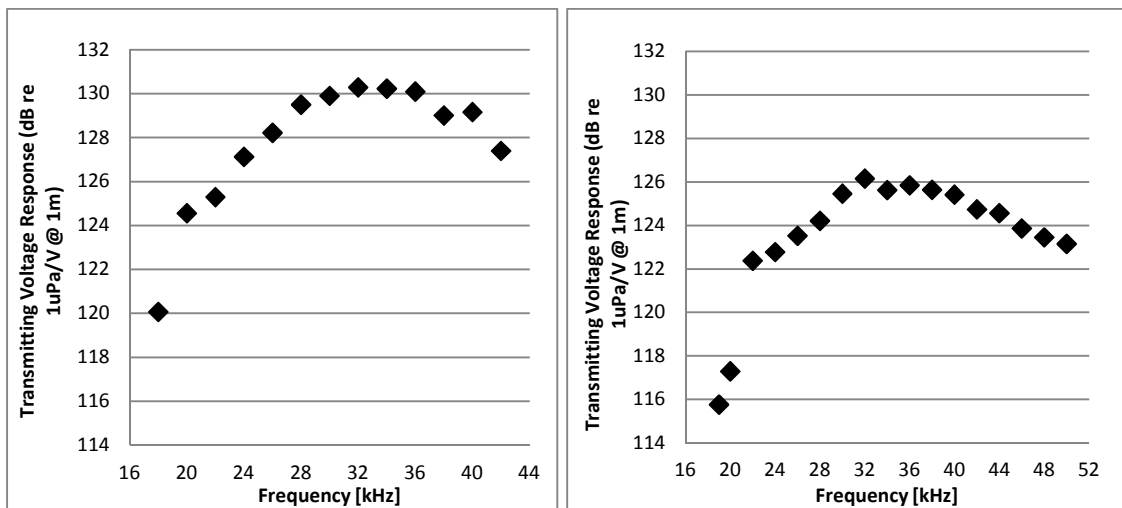

Figure 4.22: Transmitting Voltage Response as a function of the frequency for the nude FFR-SX30 (left) and moulded FFR-SX30 transducer (right).

Comparing the TVR of the FFR-SX30 with and without over-moulding, a loss of ~4 dB is observed for the over-moulded transducer.

In the second step, the Transmitting Acoustic Power of the transceiver has been calculated in the positions 1 and 2, which are with the orientations explained in chapter 3. Figure 4.23 shows the Transmitting Acoustic Power of the transceiver as a function of the frequency (measured in the positions 1 and 2). The Transmitting Acoustic Power of the transceiver as a function of the angle (directivity pattern) using a 30 kHz short tone burst signal is shown in Figure 4.24 (measured in the position 2, 0º corresponds to the direction opposite to cables). The uncertainties on the measurements are 1.0 dB.

Comparing the Transmitting Acoustic Power measured in position 1 and 2 an increase of about 1-2 dB in the frequency range 30-50 kHz is observed for the position 2.
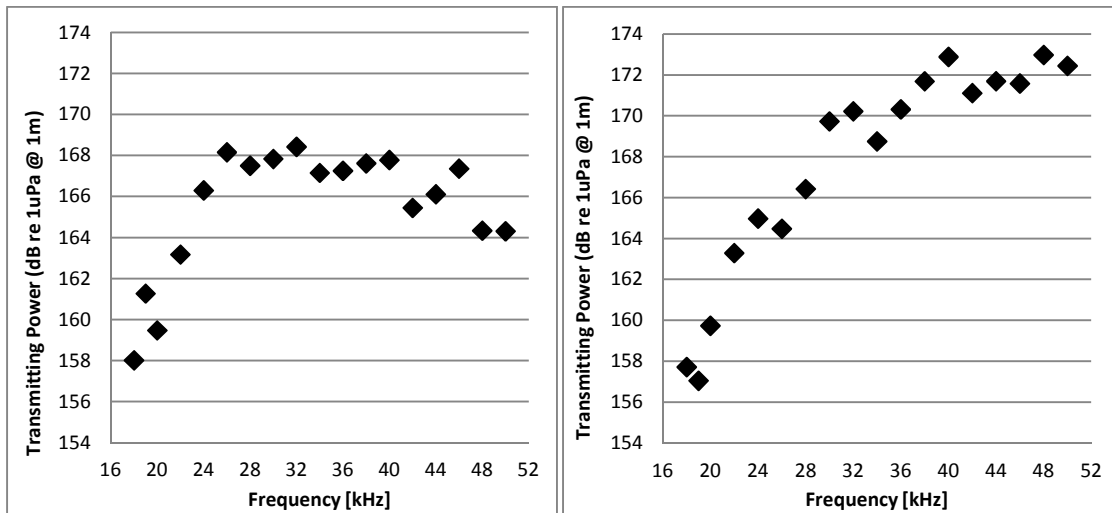

Figure 4.23: Transmitting Acoustic Power of the transceiver as a function of frequency measured in position 1 (right) and in position 2 (left), respectively.
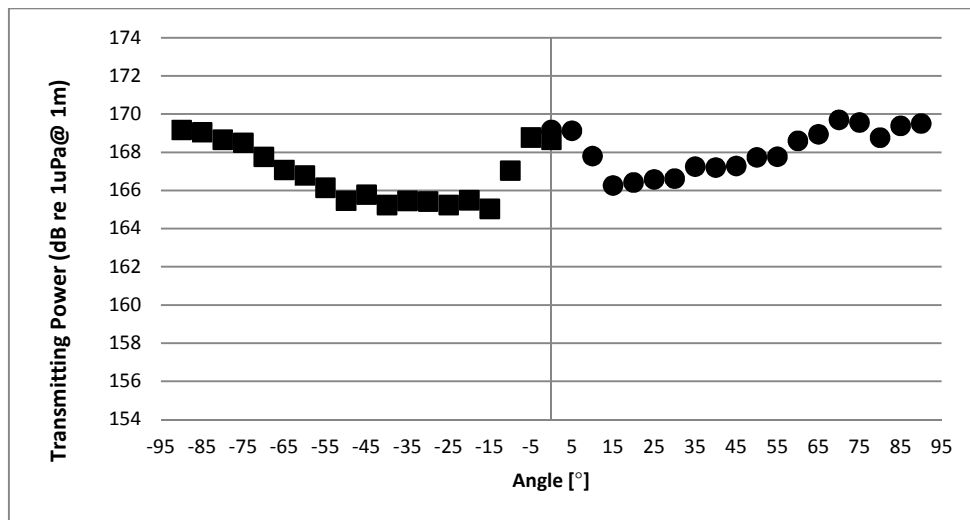

Figure 4.24: Transmitting Acoustic Power of the transceiver as a function of the angle, measured in position 2.

The results of Figure 4.23 show that the Transmitting Acoustic Power in the 20-50 kHz frequency range is in the 156-173 dB re 1μPa @ 1 m range, roughly in agreement with combined effect of the specified emission power of the FFR and the electronics. This complies with the requirements for the system.

Also in this case the received pressure variation as a function of the distances for a 30 kHz short tone burst emitted signal have been calculated using the equations (4.1) and (4.2) (in the direction of the tower, that is the vertical, which coincides with the more

powerful direction of emission according to Figure 4.24). The results are shown in Figure 4.25.
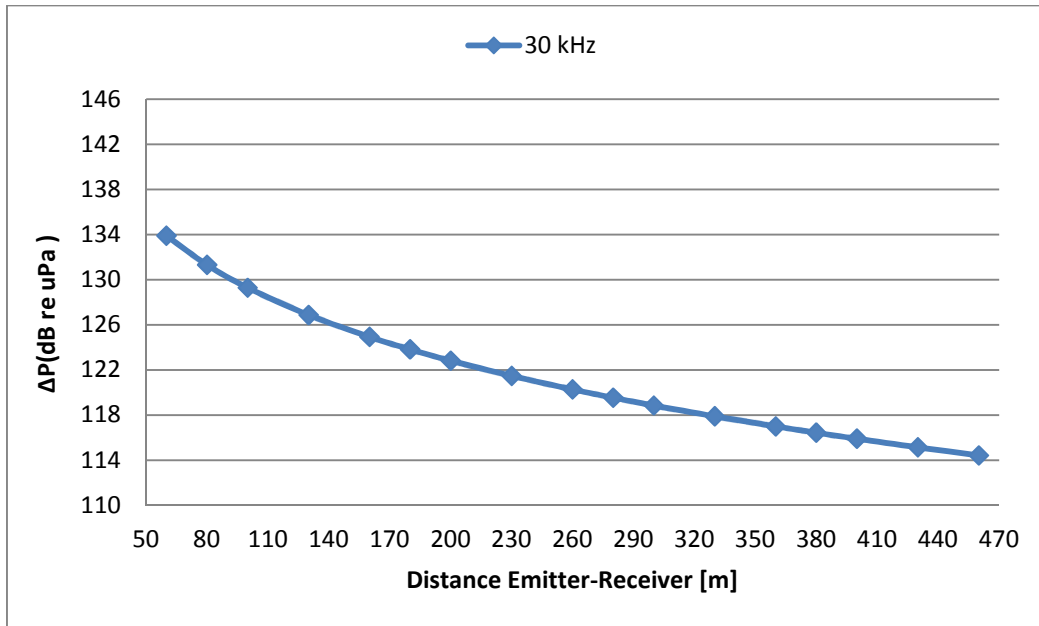

Figure 4.25: Received pressure variation as a function of distance for a 30 kHz short tone burst emitted signal.

Based on these calculations, the received amplitude that would be recorded by a NEMO hydrophone with its typical sensitivity of -172 dB re 1V/µPa has been calculated and is shown in Figures 4.26.
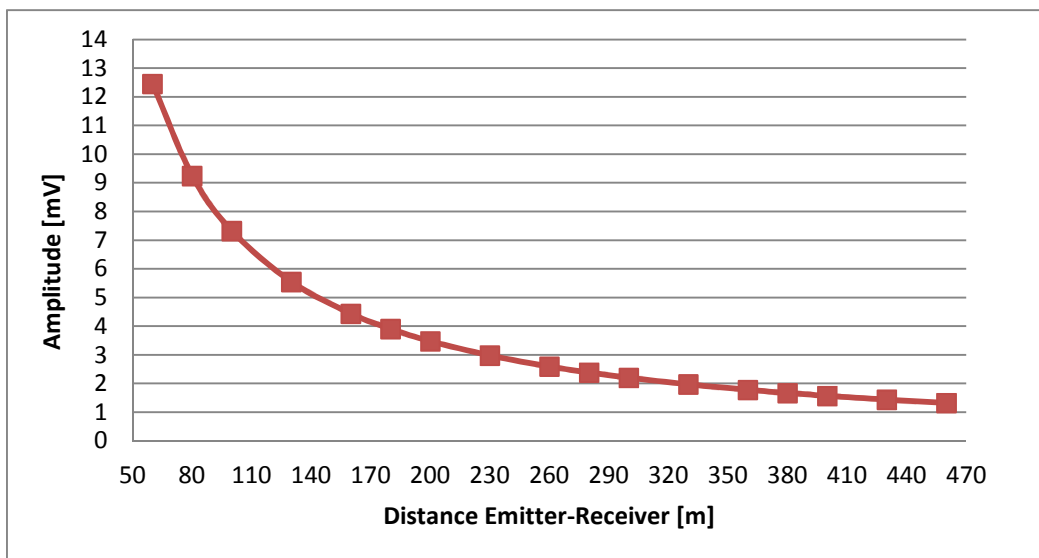

Figure 4.26: Received amplitude with the NEMO hydrophone at 30 kHz frequency.

The results show that at 460 m the expected signal has an amplitude of about 1.3 mV for the NEMO hydrophones. Considering that the last storey in the NEMO Phase II is located at 420 m above the sea floor, the expected signal will have amplitude of about 1.6 mV, enough to be recorded above the ambient noise.

4.2.2 NEMO Phase II joint acoustic tests

The compatibility and functionality of different hardware and software for the NEMO Phase II test (developed by INFN-Italy, CPPM-France, ECAP-Germany and UPV-Spain towards an innovative APS within the KM3NeT Consortium) were performed in a joint acoustic test in the laboratory in Gandia in May 2010. In these tests the compatibility and functionality between the acquisition electronic chains NEMO and the transceiver (FFR-SX30 plus SEB) were successfully tested. Details about the joint acoustic tests can be found in [SIM12].

In order to evaluate and compare the performances in water of the two SMID and FFR-SX30 hydrophones and of the transceiver for the integration in NEMO Phase II tower, tests in a fresh water pool of dimensions 4 x 6 x 5.30 m have been performed at IDASC (Istituto di Acustica e Sensoristica "Orso Mario Corbino") [IDASw] in Rome (Figure 4.27).
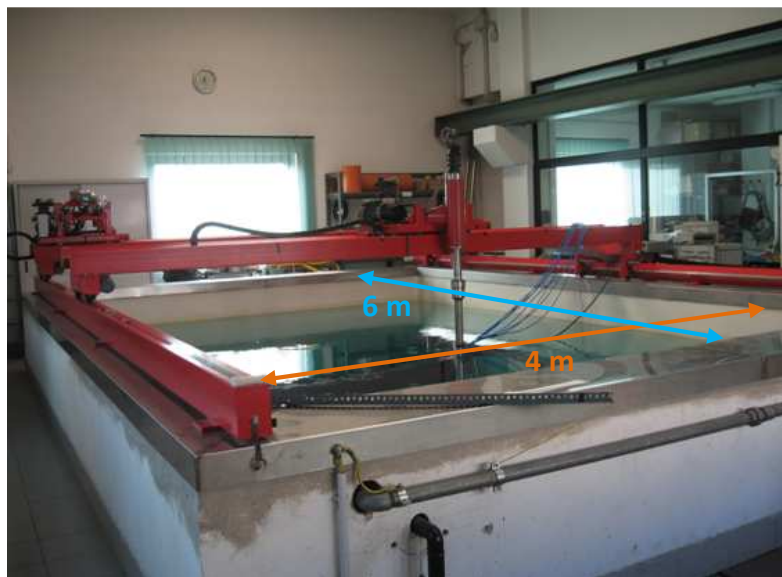

Figure 4.27: Fresh water pool at IDASC (Istituto di Acustica e Sensoristica "Orso Mario Corbino") with dimension of 4 x 6 x 5.30 m.

The transducers have been placed in the water pool at different positions and known distances from the acoustic sources by means of carbon fibre bars provided by IDASC and mechanical supports of polyethylene designed and produced at the INFN *(Istituto Nazionale di Fisica Nucleare),* Catania (Italy). Maintaining a similar notation to that of chapter 3, the different configurations of the measurements have been named position 1 and 2 as shown in Figure 4.28. The receiver hydrophones were connected to the data acquisition system of the NEMO detector. The set up used for the emission, reception and acquisition of data is shown in Figure 4.29.
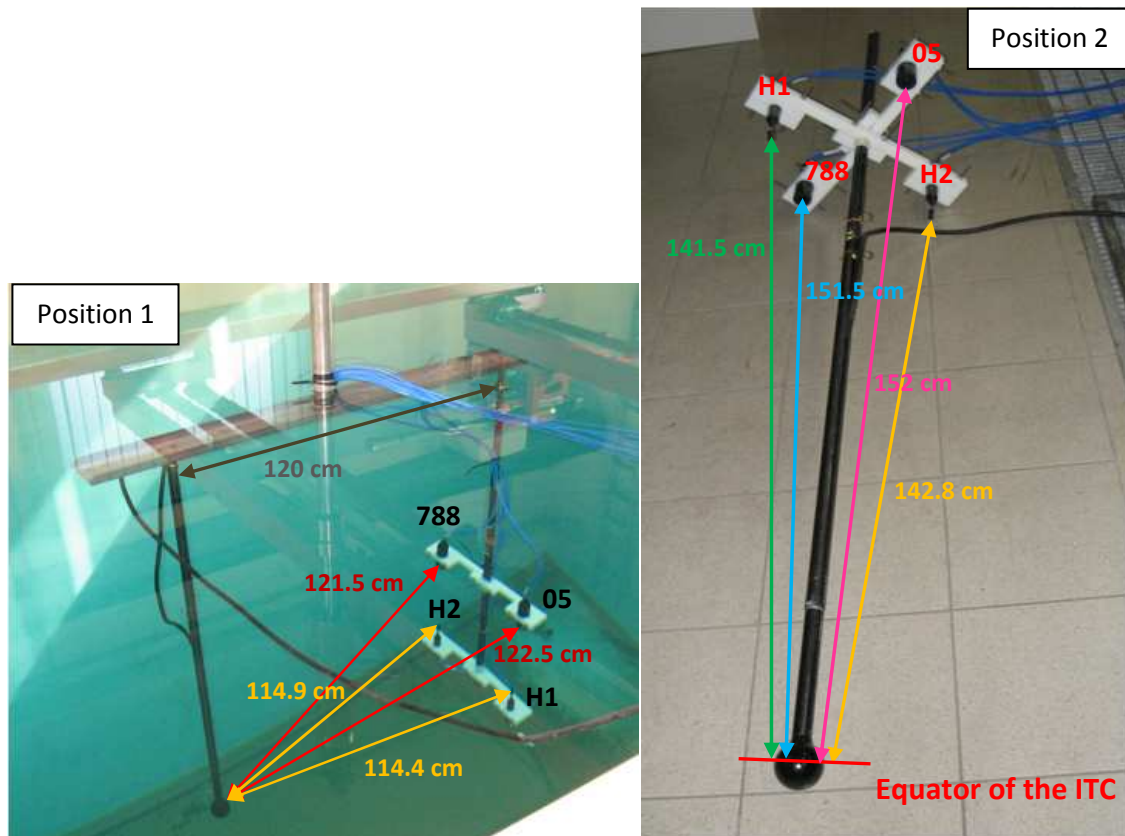

Figure 4.28: Experimental setup for the acoustic measurements in water pool at IDASC. Position 1 on left and position 2 on right. Emitter ITC 1032 and Receivers FFR-SX30 788 and 05, and SMID H1 and H2.

The emitted signal was generated through a signal generator and sent to the transducer (ITC 1032) for the emission. The trigger of the signal generator was managed from GPS with a signal named PPS (Pulse Per Second). The latter provide in output two channel one for the clock and another for the IRIG code data (year, month, day, etc.). Furthermore, it was connected to the Fan Time board in order to distribute the master clock (that is, the clock at 10MHz of the receiver GPS) and GPS time to electronic

chain: EFCM (Ethernet Floor Control Module, on-shore), FCM (Floor Control Module, off-shore) and ACOU (Acoustic Board ADC, off-shore). The EFCM and FCM, on-shore and off-shore modules for the electronic control of the floor in the detector, are connected through the optical fiber. The ACOU was connected at the receiver hydrophones and contains the electronics to acquire and digitalize the received signal.

In order to perform the measurement under the same conditions the temperature of the water pool and the ambient temperature were monitored and checked, in order to verify that the water conditions during the measurements were stable (~0.05 ºC).
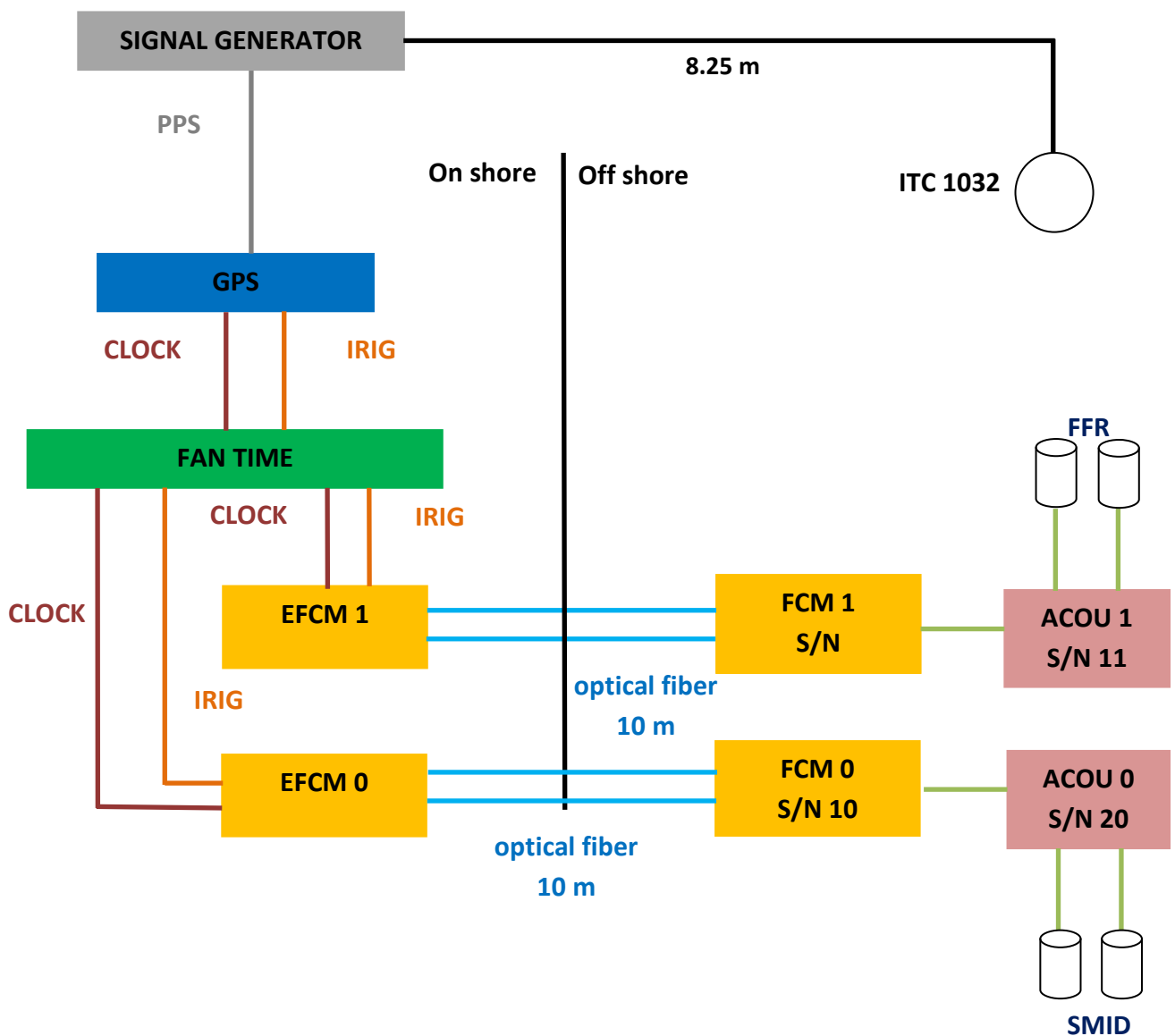

Figure 4.29: Set up used in the emission, reception and acquisition of data.

In the first step, the ambient noise was acquired for the two pairs of SMID and FFR-SX30 hydrophones without emission in order to monitor the intrinsic electronic noise and environmental noise. Figure 4.30 shows the power spectrum density of the acquired data calculated applying the function "periodogram" of the MATLAB software. The level of noise spectrum is about -120 dB re V^2/Hz and -100 dB re V^2/Hz for the pair of FFR-SX30 and SMID hydrophones, respectively. Notice that this level of noise was due to the intrinsic electronic noise but also to the environmental noise (acoustic and electromagnetic).
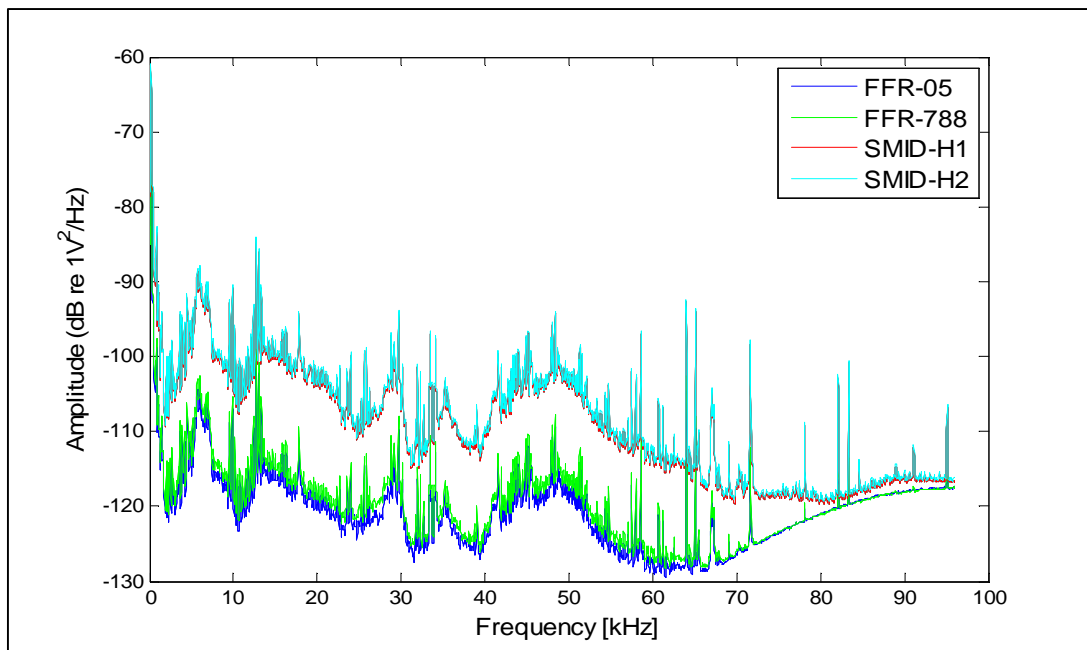

Figure 4.30: Ambient noise for the SMID and FFR-SX30 hydrophones.

In the second step, the hydrophones (FFR-SX30 and SMID) have been characterized using a calibrated emitter ITC 1032 [ITCw] provided by IDASC. Different tone burst signals with different amplitudes and frequencies with 5 and 10 cycles length were generated through a signal generator from AGILENT [AGILw]. Successively, they were amplified by a factor 50 through an amplifier of the FALCO SYSTEM model WMA-300 [FALCw]. The trigger was provided by the GPS (1 PPS), as described previously, and the acquisition time was ~5 minutes. Figure 4.31 shows the calibrated transmitting voltage and current response levels of the ITC 1032 transducer. The sensitivity of this transducer has been used to calculate the receiving voltage response of the SMID and FFR-SX30 receiver hydrophones for both positions, 1 and 2, using the

equation (3.1). The results are shown in Figure 4.32, it includes the 38 dB gain of the SMID AM-401 preamplifier. The uncertainties on the measurements are about 1 dB. The receiving voltage response at 32 kHz is about -168 dB re V/µPa and -184 dB re V/µPa for the FFR-SX30 and SMID hydrophones, respectively.
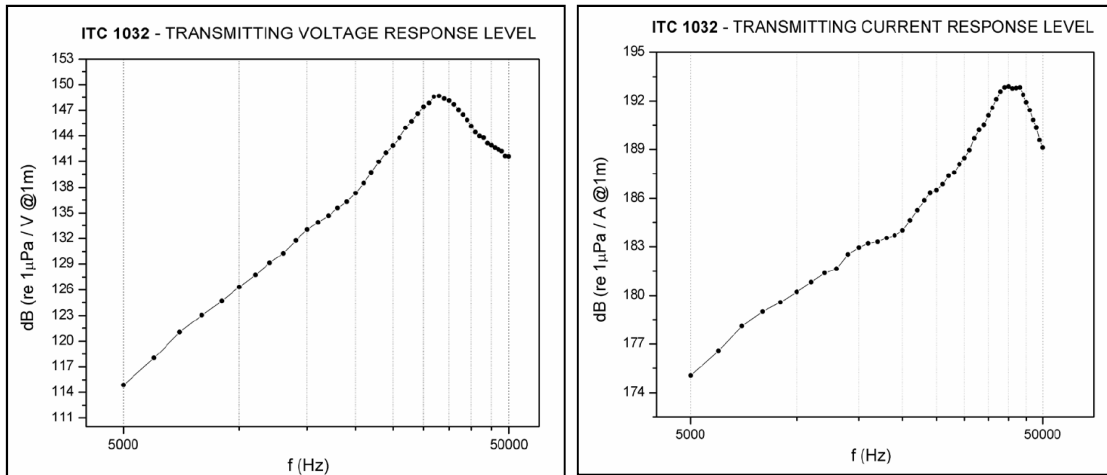

Figure 4.31: Transmitting voltage (left) and current (right) response level of the ITC 1032 transducer respectively [IDASw].
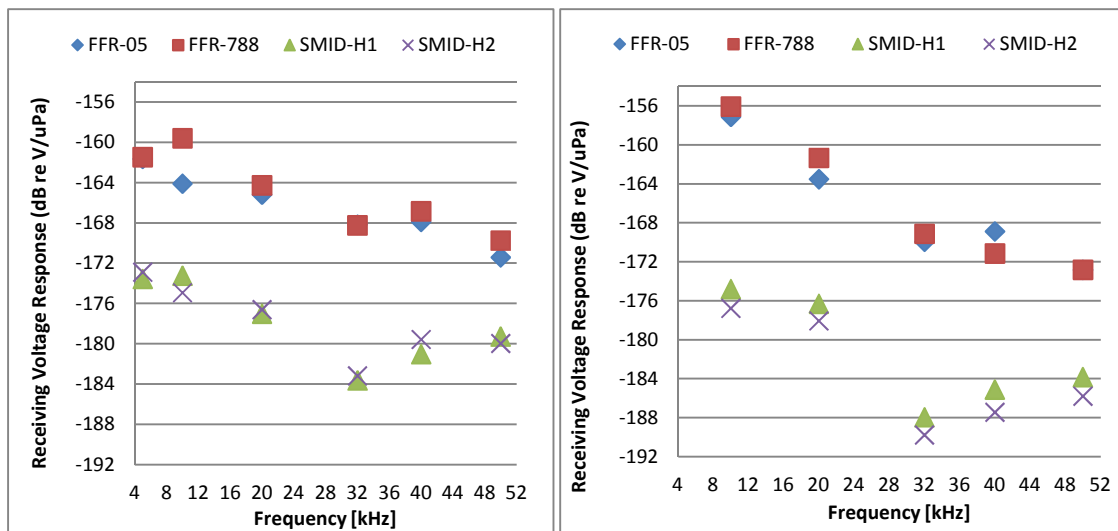

Figure 4.32: Receiving Voltage Response of the SMID and FFR-SX30 hydrophones in position 1 (left) and position 2 (right), respectively.

In the third step, joint tests of the transceiver prototype and receiver hydrophones (SMID and FFR-SX30) have been done. The emitter hydrophone ITC 1032 has been substituted by FFR-SX30 serial number 566 fed by the SEB. Again the transducers have been placed at known distances using the same bars and mechanical structure described previously. Different tone burst signals with different amplitude in the 20-40 kHz frequency range and 5 cycles length, and linear sine sweep signals (frequency range: 20-

40 kHz and 10-50 kHz, length: 1 ms) were generated through the SEB and sent to the transducer FFR-SX30 for synchronized emission with the GPS signal. The set up used for the reception and acquisition data was the same as shown in Figure 4.29. Figure 4.33 shows the configuration used in this case for the measurements.
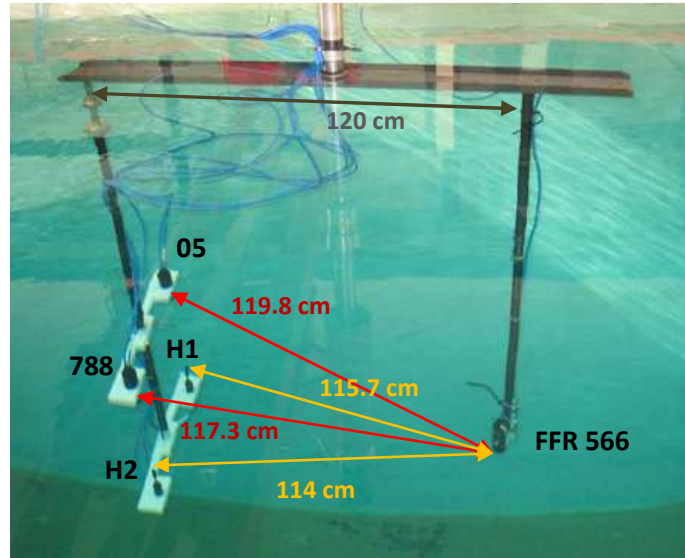

Figure 4.33: Experimental setup for the acoustic measurements in water pool at IDASC. Emitter FFR-SX30 566, receivers FFR-SX30 788 and 05, and SMID H1 and H2.

The Transmitting Power of the transceiver (FFR-SX30 566 plus SEB) has been also calculated using the sensitivity of the receiver hydrophones in position 1 calculated previously (Fig. 4.32 (left)) and is shown in Figure 4.34. The statistical uncertainties on the measurements are about 1 dB. The Transmitting Power of the transceiver at 32 kHz is about 178 dB re µPa @ 1 m.
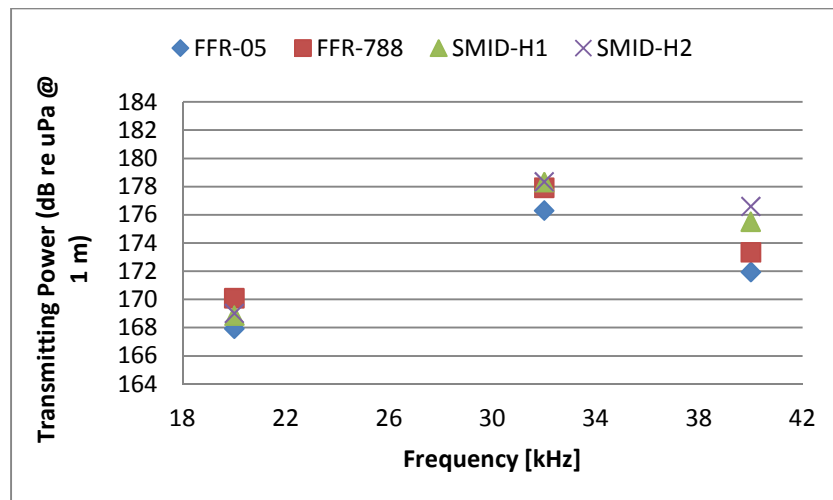

Figure 4.34: Transmitting Power for the transceiver (FFR-SX30 566 plus SEB) calculated using the sensitivities of the receiver hydrophones (FFR-SX30 and SMID) measured previously.

Finally, in order to determine the distance between emitted and received hydrophones, as described in the section 3.4.2, the correlations between different emitted and received linear sine sweep signals and tone burst signals at 32 kHz (of about 100 recorded signals) have been calculated. Due to the lack of knowledge of the exact time for the emission in the data acquisition system, synchronization between the emitted signal (acquired though the NI USB-5132) and received signal (acquired through the data acquisition system of NEMO detector) is not possible. However, it is possible to study the difference of detection times between different hydrophones (that is, the difference between the distances of the different hydrophones). The difference between the different distances, measured experimentally in situ, between the FFR-SX30 566 emitter and FFR-SX30 receivers (05 and 788) is 0.025±0.005 m. In order to not be limited by the 192 kHz sampling frequency, we have interpolated the signals up to 9.6 MHz. Notice that this process can produce some offsets on time due to the filters applied for the interpolation that should be checked and calibrated for absolute timing. Nevertheless, since we are here just interested on time differences, this should not have any effect on our analysis. The average time differences obtained between FFR hydrophones are 19.98 ± 0.03 µs, 19.58 ± 0.02 µs and 19.99 ± 0.02 µs for the 20-40 kHz sine sweep signal, 10-50 kHz sine sweep signal and 32 kHz tone burst signal, respectively. It is remarkably the low statistical deviation of different measurements, which is due to the fact that the time difference appears just in two bins, anyway it can be considered as a prove of the stability of the measurements. The fact that there is a small difference between the values of the sine sweep signal could be an indication of a small systematic uncertainty which depends on the frequency. Anyway, it seems it seems not to be very important, as it is smaller than 1 µs. Considering the velocity of the sound in water as 1450 ± 50 m/s, the measured difference of distances between FFR hydrophones is 0.029 ± 0.001 m. From these results we can conclude that the method used is stable and the time accuracy of the whole system is better than 1 µs, in good agreement with previous measurements described in [SIM12].

Conclusions

The main aim of the thesis has been the design, development and test of the acoustic transceiver for the APS in underwater neutrino telescopes, particularly KM3NeT. The APS in an underwater neutrino telescope has a double objective: during the deployment phase, the APS must provide the position of telescope's mechanical structures, in a geo-referenced coordinate system, with an accuracy of about 1 m; during the telescope operation phase, the APS data are used to recover the positions of OMs, which can have some motion due to the sea currents. Their positions are monitored during the time with an accuracy of about 10 cm. Then, the R&D activity described in this thesis has been carried out in order to satisfy these requirements about the acoustic transceiver and APS in the frame of the KM3NeT Consortium.

The studies realized in order to use the FFR-SX30 transducers as emitters and receivers in the APS of KM3NeT neutrino telescope (Chapter 3), demonstrated that sensors can be handled without major problems for the application as transceivers for the KM3NeT APS, although the variations in power transmission and sensitivity to different frequencies and angles have to be considered. The intrinsic electronic noise of the FFR-SX30 hydrophones as receivers is low, but, in case of willing to use the FFR-SX30 as receiver hydrophones of the KM3NeT APS, a good parameterisation of the sensitivity as a function of the frequency and angle for each transducer will be needed, especially if willing to use these hydrophones for deep-sea acoustic monitoring studies or for the acoustic detection of Ultra-High-Energy neutrinos. For this application, it would be good to have precise measurements of the sensitivities at larger distances between both transducers. In fact, some work is going on in this sense within the research group. Tests in hyperbaric tank have permitted us to conclude that these transducers are quite stable with depth and the little variations observed are not problematic for the application.

In order to integrate the transceiver prototype (FFR-SX30 plus SEB) in the instrumentation line of the ANTARES neutrino telescope and in the NEMO Phase II tower for the in situ tests in deep-sea, it has been tested in a fresh-water tank in the laboratory, in a pool and in shallow sea water. For simplicity and due to limitations to both infrastructures, it was decided to test the transceiver only as emitter. The receiver

functionality will be tested in other in situ KM3NeT tests. The changes performed in the transceiver, particularly in the SEB, show the capacity to adapt the electronic parts to the situation and available conditions.

The transceiver prototype, with low power consumption, is able to have a transmitting power above 170 dB re 1μPa @ 1 m in agreement with the electronics design and the specifications needed. It may be considered low in comparison with the ones used in Long Base Line positioning systems, which usually reach values of 180 dB re 1μPa @ 1 m. Despite this, the use of wideband signals, Maximum Length Sequence (MLS) signals and sine sweep signals, instead of pure sinusoidal signals result to be in an improvement of the signal-to-noise ratio, and therefore resulting in an increase in the detection efficiency, as well as in the accuracy of the time of detection. In this way, tests in fresh-water pool and in Gandia Harbour have permitted us to say that the accuracy is better than 30 μs and compatible with uncertainties on the order of a microsecond measured previously in the laboratory.

The system tested has been finally integrated in the active anchor of the Instrumentation Line of ANTARES together with the Laser Beacon used for timing calibration purposes. The expected pressure level and the expected electric signal for the AMADEUS and some ANTARES hydrophones have been calculated. The use of the transceiver prototype in combination with the AMADEUS hydrophones makes the test very complete since it allows studying the transceiver emission for different conditions of distances and orientation. Moreover, it is possible to study in situ different kinds of signals and their performance for positioning purposes.

The system for the NEMO Phase II tower base is already available and will be integrated in May this year. Tests in a water pool at IDASC in Rome have allowed us to evaluate and compare the performances of the two hydrophone models, SMID and FFR-SX30 for the integration in NEMO tower. The intrinsic electronic noise and the receiving voltage response have been measured. Moreover, tests on the prototype transceiver (FFR-SX30 plus SEB) with the whole data acquisition system of the NEMO detector have been done showing the compatibility and functionality of both system and a time of accuracy for the detection better than 1 μs. Also in this case the expected pressure and electric signal on the receiver hydrophones for an emitted signal of 30 kHz have been calculated. The results show that the signal level is enough to be recorded.

Finally, we would like to remark that the acoustic system proposed is compatible with the different options for the receiver hydrophones proposed for KM3NeT and it is versatile, so in addition to the positioning functionality, it can be used for acoustic detection of neutrinos studies or for acoustic monitoring studies in deep-sea. Moreover, the transceiver (with slight modifications) may be used in other marine positioning systems, alone or combined with other marine systems, or integrated in different Earth-Sea Observatories, where the localization of the sensors is an issue. In that sense, the experience gained from this research can be of great use for other possible applications.

Acronyms

ACOU: Acoustic Board ADC

ADCPs: Acoustic Doppler Current Profilers

ADC: Analog-to-Digital Converter

AMADEUS: Antares Modules for Acoustic DEtection Under the Sea

AMANDA: Antartic Muon And Neutrino Detector Array

AM: Acoustic Module

ANTARES: Astronomy with a Neutrino Telescope and Abyss environmental RESearch

ANTARES DAQ: ANTARES Data Acquisition

ASDIC: Allied Submarine Detection Investigation Committee

APS: Acoustic Positioning System

AWG: American Wire Gauge

BSS: Bottom string Socket

CDR: Conceptual Design Report

CNRS: Centre national de la recherche scientifique

CPPM: Centre de physique des particules de Marseille

CRC: Cyclic Redundancy Check

CTD: Conductivity – Temperature - Depth

DGPS: Differential GPS

DOM: Digital Optical Module

DU: Detection Unit

DWDM: Dense Wavelength Division Multiplexed

ECAP: Erlangen Centre for Astroparticle Physics

EFCM: Earth Floor Control Module

FFR: Free Flooded Ring

FCM: Floor Control Module

GPS: Global Positioning System

HFLBL: High Frequency Long Baseline positioning system

IceCube: Ice Cubic kilometer south pole neutrino observatory

IDASC: Istituto di Acustica e Sensoristica "Orso Mario Corbino"

IFREMER: *Institut Français de Recherche pour L'exploitation de la Mer*

IL: Instrumentation Line

INFN: Istituto Nazionale di Fisica Nucelare

JB: Junction Box

KM3NeT: km^3 Neutrino Telescope

LB: Laser Beacon

LBL: Long Base Line

LCM: Local Control Module

LFLBL: Low Frequency Long Baseline positioning system

LVDS: Low-Voltage Differential Signaling

MLS: Maximum Length Sequence

NEMO: Neutino Mediterranean Observatory

NESTOR: Neutrino Extendend Submarine Telescope with Oceanographic Research

OM: Optical Module

PMT: Photomultiplier

PPM: Pre-Production Model

PPS: Pulse Per Second

PVDF: polyvinylidene bifluoride

PWM: Pulse Width Modulation

PZT: Lead Zirconate Titanate *(piezoelectric ceramic material)*

R&D: Research and Development

ROV: Remotely Operating Vehicle

RVR: Receiving Voltage Response

Rx: Receiver

RxTx: Transceiver

SEB: Sound Emission Board

SBLs: Short-Baseline systems

SMID: Security Multi-Sensor Integrated Devices

SONAR: SOund NAvigation and Ranging

TCM2: Electronic Tilt-Compass sensor Module

TCS: Tiltmeter-Compass System

TDR: Technical Design Report

TDoA: Time Difference of Arrival

TOA: Time of Arrival

TOE: Time of Emission

TOF: Time of Flight

TPE: Thermoplastic elastomer

TSSC: Time Spectral Spread Codes

TVR: Transmitting Voltage Response

USBLs: Ultra-Short-Baseline systems

UPV: Universitat Politècnica de València

References

[ACSAw] ACSA homepage, available on: <http://www.underwater-gps.com>.

[ARD09] M. Ardid (for the ANTARES Collaboration), *Positioning system of the ANTARES neutrino telescope,* Nucl. Instr. and Meth. A 602 (2009) 174-176.

[ADR11] S. Adrian Martinez et al., ANTARES Collaboration, *First search for point sources of high energy cosmic neutrinos with the ANTARES neutrino telescope,* Astrophys. J. Lett. 743 (2011) L14-L19.

[ADR12] S. Adrian Martinez et al., ANTARES Collaboration, *The Positioning System of the ANTARES Neutrino Telescope*, arXiv:1202.3894v1 [astro-ph.IM].

[AGE11] M. Ageron et al., ANTARES Collaboration, *ANTARES: The first undersea neutrino telescope,* Nucl. Instr. and Meth. A 656 (2011) 11-38.

[AGILw] AGILENT Technologies homepage, available on: <http://www.home.agilent.com/>.

[AGU05] J. A. Aguilar et al., ANTARES Collaboration, *Study of large hemispherical photomultiplier tubes for the ANTARES neutrino telescope,* Nucl. Instr. and Meth. A 555 (2005) 132-141.

[AGU11] J. A. Aguilar et al., ANTARES Collaboration, *Time calibration of the ANTARES neutrino telescope,* Astroparticle Physics, 34 (2011), 539-549.

[AGU11a] J.A. Aguilar et al. (ANTARES Collaboration), *AMADEUS—The acoustic neutrino detection test system of the ANTARES deep-sea neutrino telescope,*Nucl. Instr. and Meth. A 626–627 (2011) 128.

[AGU11b] J.A. Aguilar et al., ANTARES Collaboration, *Search for a diffuse flux of high-energy vμ with the ANTARES neutrino telescope* Phys. Lett. B 696 (2011) 16-22.

[AMO08] I. Amore, Ph.D. thesis, University of Catania, 2008.

[AMO09] Isabella Amore, NEMO Collaboration, *First results from the NEMO Phase-1 experiment,* Nucl. Instr. and Meth. in Phys. Res. A 602 (2009) 68–71.

[ANTAw] ANTARES homepage, available on: <http://antares.in2p3.fr>.

[ARD09] M. Ardid, ANTARES Collaboration, *Positioning system of the ANTARES neutrino telescope,* Nucl. Instr. and Meth. A, Volume 602, (2009), pp. 174-176.

[ARD10] Ardid, M, M.Bou-Cabo, F.Camarena, V.Espinosa, G.Larosa, C.D.Llorens, J.A.Martínez-Mora, (For the KM3NeT Consortium), *A prototype for the acoustic triangulation system of the KM3NeT deep sea neutrino telescope.* Nucl. Instr. and Meth. A, 617 (2010) 459-461.

[AYN06] V. Aynutdinov et al., Baikal Collaboration, *The Baikal neutrino telescope,* Nucl. Instr. and Meth. in Phys. Res. A 567 (2006) 423.

[BAR01] M. Barr, *Introduction to Pulse Width Modulation, Embedded Systems Programming* 14 No. 10, 2001,p. 103.

[BIG09] Ciro Bigongiari, *The KM3NeT project for a Very Large Submarine Neutrino Telescope*, *Ad Hoc & Sensor Wireless Networks,* Old City Publishing, Inc, 00, (2009) 1–22.

[BRO09] A.M. Brown, ANTARES Collaboration, *Positioning system of the ANTARES Neutrino Telescope,* proceedings of the 31st ICRC, LÓDZ 2009, arXiv:0908.0814v1 [astro-ph.IM].

[BRU10] J. Brunner, ANTARES Collaboration , *The ANTARES neutrino telescope: status and first results*, Nucl. Instr. and Meth. A, 626-627 (2010) S19-S24.

[CDR08] KM3NeT Conceptual Design Report (2008) ISBN 978-90-6488-031-5, available on: <www.km3net.org>.

[CHE77] Chen and Millero, *Speed of sound in seawater at high pressures,* J. Acoust. Soc. Am., Vol. 62, No. 5, 1129-1135, Nov. 1977.

[DAV02] *Fundamentals and Applications of ULTRASONIC WAVES,* J. David N. Cheeke, CRC Press LLC, 2002.

[ECAw] ECA homepage, available on: < http://www.eca.fr>.

[FALCw] FALCO Systems homepage, available on: <http://www.falco-systems.com/>.

[FRA82] R. E. Francois and G. R. Garrison, *Sound absorption based on ocean measurements: Part I: Pure water and magnesium sulfate contributions*, J. Acoust. Soc. Am. Volume 72, Issue 3, (1982), pp. 896-907.

[HUL11] K. Hultqvist, IceCube Collaboration, *IceCube: physics, status and future*, Nucl. Instr. and Meth. A, 626-627 (2011) S6-S12.

[IDASw] Istituto di Acustica e Sensoristica "Orso Mario Corbino" homepage, available on: <http://www.idasc.cnr.it/>.

[IFREw] IFREMER homepage, available on: <http://www.ifremer.fr>.

[ISELw] ISEL automation homepage, available on: <http://www.isel-germany.de/>.

[ITCw] ITC-Transducers home page, available on: <http://www.itc-transducers.com>.

[IXSEw] IXSEA homepage, available on: < www.ixsea.com>.

[KEL07] P. Keller, *Acoustic Positioning System for the Deep-Sea ANTARES Neutrino Telescope*, Proc. SENSORCOMM Conf., 2007, 243-247 – ISBN: 0-7695-2988-7.

[KAL11] O. Kalekin, J.J.M.Steijger, H.P.Peek, (For the KM3NeT Collaboration), *Photomultipliers for the KM3NeT optical modules*, Nucl. Instr. and Meth. A in press, proceeding of the New Developments In Photodetection (NDIP) congress 2011, DOI: 10.1016/j.nima.2011.11.004.

[KAT11] U.F. Katz, (For the KM3NeT Collaboration), *The KM3NeT project,* Nucl. Instr. and Meth. A, 626-627 (2011) S57-S63.

[KM3Nw] KM3NeT homepage, available on: <http://www.km3net.org>.

[LAH12] R. Lahamann, (For the ANTARES Collaboration), *Status and recent results of the acoustic neutrino detection test system AMADEUS*, Nucl. Instr. and Meth. A 662 (2012) S216-S221.

[LAR12] G. Larosa, M. Ardid, C. D. Llorens, M. Bou-Cabo, J. A. Martínez-Mora, S. Adrían-Martínez, *Development of an Acoustic Transceiver for Positioning Systems in Underwater Neutrino Telescopes*, IARIA, proceeding of the GEOProcessing2012 congress, ISBN: 978-1-61208-178-6, 2012.

[LAR12a] Larosa, G; et al. *Development of an acoustic transceiver for the KM3NeT positioning system*, Nucl. Instr. Meth. A 2012, accepted.

[LLO12] C.D. Llorens et al., *The Sound Emission Board of the KM3NeT Acoustic Positioning System,* J. Instrum. (2012), *7*, C01001.

[LUR02] *An Introduction to Underwater Acoustics: Principles and Applications*, Xavier Lurton, Springer, Praxis Publishing Ltd, Chichester, UK, 2002.

[McArw] McArtney-EurOceanique SAS homepage, available on: <http://www.macartney.com>.

[MICOw] MICOS (Mechanische Instrumente Optische Systeme GMBH) homepage, available on: <www.micos.ws>.

[MICRw] Microchip homepage, available on: <http://www.microchip.com>.

[MIG06] E. Migneco, et al., *Status of NEMO*, Nucl. Instr. and Meth. A 567 (2006) 444-451.

[MODBw] MODBUS homepage, available on: <http://modbus.org/docs/Modbus_Application_Protocol_V1_1b.pdf>

[NATIw] National Instruments homepage, available on: <http://www.ni.com>.

[NEMOw] NEMO homepage, available on: <http://nemoweb.lns.infn.it>.

[NESTw] NESTOR homepage, available on: < http://www.nestor.org.gr>.

[MAR06] A. Margiotta, NEMO Collaboration, *Status report of the NEMO (Neutrino Mediterranean Observatory) project,* Phys. Scr. T127 (2006) 107–108.

[MED05] *Sounds in the sea: From Ocean Acoustics to Acoustical Oceanography,* Herman Medwin and colleagues, Cambridge University Press, 2005.

[PNICw] PNI Sensor Corporation homepage, available on: <http://www.pnicorp.com>.

[RESOw] RESON homepage available on: <http://www.reson.com>.

[RIC04] G. Riccobene, L. Cosentino, M. Musumeci, G. Pavan, F. Speziale, *Acoustic detection of UHE neutrinos: a station for measurement of the deep sea acoustic noise*, Nucl. Instr. and Meth. A, 518 (2004) 220–222.

[RIC09] G. Riccobene, NEMO Collaboration, *Long-term measurements of acoustic background noise in very deep sea,* Nucl. Instr. and Meth. A, 604 (2009) S149–S157.

[SEACw] SEACON homepage, available on: <http://seaconworldwide.com>.

[SENSw] Sensorthech homepage, available on: <http://www.sensortech.ca>.

[SHE07] C.H. Sherman and J.L. Butler, *Transducers and Array for Underwater Sound,* The Underwater Acoustic Series, Springer, 2007.

[SIM11] F. Simeone, S. Viola, *The SMO project: a submarine multidisciplinary observatory in deep-sea,* MASS, pp.898-903, 2011 IEEE Eighth International Conference on Mobile Ad-Hoc and Sensor Systems, (2011). ISBN: 978-076954469-4; DOI 10.1109/MASS.2011.107.

[SIM12] F. Simeone, F. Ameli, M. Ardid, V. Bertin, M. Bonori, M. Bou-Cabo, C. Calì, A. D'Amico, G. Giovanetti, M. Imbesi, P. Keller, G. Larosa, C.D. Llorens, R. Masullo, N. Randazzo, G. Riccobene, F. Speziale and S. Viola, KM3NeT consortium, *Design and first tests of an acoustic positioning and detection system for KM3NeT*, Nucl. Instr. and Meth. A, 662 (2012) S246-S248.

[SMIDw] SMID Technology homepage, available on: <http://www.smidtechnology.it>.

[SPI05] Ch. Spriering, *Neutrino Astrophysics in the Cold: Amanda, Baikal and IceCube,*Phys. Scripta T121 (2005) 112-118.

[TDR11] KM3NeT Technical Design Report (2011) ISBN 978-90-6488-033-9, available on: <www.km3net.org>.

[VIO12] S. Viola, NEMO and SMO Collaborations, M. Ardid, V. Bertin, A. Enzenhöfer, V. Espinosa, P. Keller, R. Lahmann, G. Larosa, C.D. Llorens, *NEMO-SMO acoustic array: a deep-sea test of a novel acoustic positioning system for a km3-scale underwater neutrino telescope,* Nucl. Instr. and Meth. A, (2012) accepted.

Acknowledgments